



**MODIFICATION OF GLASSY CARBON ELECTRODE USING
NICKEL-MAGNETITE NANOPARTICLES FOR
DEVELOPMENT OF GLUCOSE AND SULFITE CHEMICAL
SENSOR IN FOOD APPLICATIONS**



NONGYAO NONTAWONG

**A THESIS SUBMITTED IN PARTIAL FULFILLMENT OF THE
REQUIREMENTS FOR THE DEGREE OF MASTER OF SCIENCE**

MAJOR IN CHEMISTRY

FACULTY OF SCIENCE

UBON RATCHATHANI UNIVERSITY

ACADEMIC YEAR 2016

COPYRIGHT OF UBON RATCHATHANI UNIVERSITY



UBON RATCHATHANI UNIVERSITY
THESIS APPROVAL
MASTER OF SCIENCE
MAJOR IN CHEMISTRY FACULTY OF SCIENCE

TITLE MODIFICATION OF GLASSY CARBON ELECTRODE USING NICKEL-
MAGNETITE NANOPARTICLES FOR DEVELOPMENT OF GLUCOSE
AND SULFITE CHEMICAL SENSOR IN FOOD APPLICATIONS

AUTHOR MISS NONGYAO NONTAWONG

EXAMINATION COMMITTEE

ASST. PROF. DR. NATHAWUT CHOENGCHAN	CHAIRPERSON
ASST. PROF. DR. MALIWAN AMATATONGCHAI	MEMBER
ASST. PROF. DR. SANOE CHAIRAM	MEMBER

ADVISOR

..... *M. Amatongchai*
(ASST. PROF. DR. MALIWAN AMATATONGCHAI)

..... *Utith Inprasit* *A Pongrat*
(ASSOC. PROF. DR. UTITH INPRASIT) (ASSOC. PROF. DR. ARIYAPORN PONGRAT)
DEAN, FACULTY OF SCIENCE VICE PRESIDENT
FOR ACADEMIC AFFAIRS

COPYRIGHT OF UBON RATCHATHANI UNIVERSITY
ACADEMIC YEAR 2016

ACKNOWLEDGEMENT

I would like to thank my advisor, Asst. Prof. Dr. Maliwan Amatatongchai for her constant advice, guidance, insight, and sharing her extensive chemistry knowledge. I wish to thank Asst. Prof. Dr. Sanoë Chairam, Asst. Prof. Dr. Purim Jarujamrus for comments and suggestions and Asst. Prof. Dr. Nathawut Choengchan for his advice and criticism as the external examiner.

I also would like to thank the Science Achievement Scholarship of Thailand (SAST) and Ubon Ratchathani University for financial support. My gratitude is extended to Department of Chemistry, Faculty of Science, Ubon Ratchathani University for providing all laboratory facilities.

Above all, my deepest gratitude is given to my beloved parents for their eternal love and care throughout my life.

N. Nontawong
Nongyao Nontawong
Researcher

ABSTRACT

TITLE : MODIFICATION OF GLASSY CARBON ELECTRODE USING NICKEL-MAGNETITE NANOPARTICLES FOR DEVELOPMENT OF GLUCOSE AND SULFITE CHEMICAL SENSOR IN FOOD APPLICATIONS

AUTHOR : NONGYAO NONTAWONG

DEGREE : MASTER OF SCIENCE

MAJOR : CHEMISTRY

ADVISOR : ASST. PROF. MALIWAN AMATONGCHAI, Ph. D.

KEYWORDS: MAGNETITE, NICKLE NANOPARTICLES, CARBON NANOTUBES, GLUCOSE, SULFITE CHEMICAL SENSOR

This thesis presented the development of a high sensitive and selective chemical sensor for determination of glucose and sulfite with electrochemical method. The chemical sensor was developed based on modified glassy carbon electrode with magnetite (Fe_3O_4) and nickel nanoparticles decorated carbon nanotubes (Fe_3O_4 -CNTs-NiNPs). Fe_3O_4 nanoparticles were in situ loaded on the surface of carboxylated multi-walled carbon nanotubes (CNTs-COOH) by a chemical co-precipitation procedure. Nickel nanoparticles (NiNPs) were prepared through reducing nickel chloride by hydrazine hydrate and then decorated on Fe_3O_4 -CNTs using ultra-sonication. Chemical sensor was fabricated using glassy carbon (GC) coated with Fe_3O_4 -CNTs-NiNPs composites film. This developed chemical sensor (Fe_3O_4 -CNTs-NiNPs/GC) was applied to studied the electrochemical oxidation of two parts; (i) electrochemical oxidation of glucose, and (ii) electrochemical oxidation of sulfite. The electrochemical detection was investigated using Ag/AgCl and Pt wire as reference and counter electrode, respectively.

Glucose chemical sensor was developed based on electrochemical oxidation of glucose using amperometry on the modified electrode (Fe_3O_4 -CNTs-NiNPs/GC) in a supporting electrolyte of 0.1 M solution sodium hydroxide (pH 13.0). Results indicated that the Fe_3O_4 -CNTs-NiNPs/GC electrode exhibited excellent performance in the electrochemical oxidation of glucose at an applied potential of +0.55 V

(vs. Ag/AgCl). The developed electrode provided a linear dynamic range for glucose from 10 μM to 1.8 mM ($r^2 = 0.998$) with the sensitivity of 335.25 $\mu\text{A mM}^{-1}$; and a low detection limit of 6.7 μM (S/N = 3). The developed sensor provided good precision (%RSD = 4.18) was estimated from six amperometric measurements of 0.5 mM glucose. In addition, the fabricated sensor was successfully applied to determine glucose in honey and energy drinks with good results.

The development of sulfite chemical sensor using the modified electrode ($\text{Fe}_3\text{O}_4\text{-CNTs-NiNPs/GC}$) was also applied for determination of sulfite (SO_3^{2-}). Quantitative analysis of sulfite was studied at the modified electrode using linear sweep voltammetry in 0.1 M phosphate buffer pH 7.0 as supporting electrolyte. The oxidation of sulfite was found at +0.38 V. The sulfite oxidation currents varied linearly with the concentration of sulfite from was 0.1 – 10 mM ($r^2 = 0.995$) with the sensitivity of 12.748 $\mu\text{A.mM}^{-1}$. The limit of detection was 28 μM (S/N = 3). The application of this developed sensor in wine, pickled mustard green and garlic had also been successfully. The storage stability of $\text{Fe}_3\text{O}_4\text{-CNTs-NiNPs/GC}$ can be stored for up to 3 weeks at room temperature. Furthermore, the development chemical sensor provided a high sensitivity, acceptable selectivity and simples of preparation and low cost.

CONTENTS

	PAGE
ACKNOWLEDGEMENTS	I
THAI ABSTRACT	II
ENGLISH ABSTRACT	IV
CONTENTS	VI
LIST OF TABLES	VIII
LIST OF FIGURES	IX
LIST OF ABBREVIATIONS	XV
CHAPTER 1 INTRODUCTION	
1.1 The importance and the source of the research	1
1.2 Objectives	4
1.3 Expected outcomes	4
1.4 Scope of research	4
CHAPTER 2 LITERATURE REVIEWS	
2.1 Chemical sensor	6
2.2 Carbon nanotubes	7
2.3 Magnetite nanoparticles (Fe_3O_4)	9
2.4 Magnetite decorated carbon nanotubes (Fe_3O_4 -CNTs)	11
2.5 Nickel nanoparticles (NiNPs)	12
2.6 Reaction of glucose	13
2.7 Voltammetry	14
2.8 Amperometry	16
2.9 Related research	17
CHAPTER 3 EXPERIMENTAL	
3.1 Instrumentation	25
3.2 Reagent and Chemicals	26
3.3 Chemical preparation	27
3.4 Electrode preparation	28
3.5 Measurement procedures	29

CONTENTS (CONTINUED)

	PAGE
3.6 Sample preparation	30
3.7 Procedure	32
CHAPTER 4 RESULTS AND DISCUSSION	
4.1 Characterization of the synthesized nanocomposites	40
4.2 Development of glucose sensor based on Fe ₃ O ₄ -CNTs- NiNPs/GC	43
4.3 Development of sulfite sensor based on Fe ₃ O ₄ -CNTs- NiNPs/GC	58
CHAPTER 5 CONCLUSIONS	
REFERENCES	72
APPENDICES	84
A Characterization of nanocomposites	85
B Development of glucose sensor based on Fe ₃ O ₄ -CNTs- NiNPs/GC	87
C Development of sulfite sensor based on Fe ₃ O ₄ -CNTs- NiNPs/GC	96
D CONFERENCES	106
VITAE	125

LIST OF TABLES

TABLES		PAGE
3.1	Instrumentation used for cyclic voltammetric measurements.	25
3.2	List of reagents, grade and their suppliers.	26
3.3	Electrode codes for bare and modified glassy carbon electrodes.	34
3.4	Electrode codes for bare and modified glassy carbon electrodes.	36
4.1	Response characteristics of the Fe ₃ O ₄ -CNTs-NiNPs/GC electrode and other non-enzymatic glucose sensors.	52
4.2	Effect of foreign ions on the amperometric signals obtained from standard 1 mM glucose.	55
4.3	Glucose contents found in energy drinks (D-1 to D-3) and honey (H-1 to H-3), which were obtained by the developed method and comparative values from labeled value and glucose meter.	57
4.4	Anodic peak potentials ($E_{p,a}$) and current signals ($I_{p,a}$) of 4 mM sulfite using different modified electrodes.	60
4.5	Effect of foreign ions on the linear sweep voltametric signals obtained from standard 1 mM sulfite.	66
4.6	Sulfite contents found in wine (W-1 to W-3), pickled mustard green (M-1 to M-3) and pickled garlic (P-1 to P-3), which were obtained by the developed method and comparative values from iodometric method was carried out in triplicate for a sample.	68

LIST OF FIGURE

FIGURE		PAGE
2.1	Diagram of chemical sensor.	6
2.2	Schematic representation of the construction of a nanotube by rolling-up an infinite strip of graphene with different chirallities (Ba: armchair; Bb: zigzag and Bc: chiral).	8
2.3	Structure representation of multi-walled carbon nanotubes (MWCNTs).	9
2.4	Structure and unit cell of magnetite (Fe_3O_4).	10
2.5	Magnetizing CNTs by coprecipitation. When CNTs are treated with strong oxidizing acids, COOH , C=O , and C-OH groups are formed at defect sites. In the presence of Fe^{+2} , Fe^{+3} and a precipitating base serve as nucleation sites for (Fe_3O_4)	12
2.6	Schematic diagram showing the mechanism of glucose oxidation reactions occur during operation of the developed glucose chemical sensor.	14
2.7	Typical of a) cyclic voltammogram wave from: variation of the potential applied to the working electrode with time and b) cyclic voltammogram: resulting current-potential curves.	15
2.8	Linear sweep voltammetry of a) the variation of the potential applied to the working electrode with time and b) linear sweep voltammogram: resulting current-potential curves.	15
2.9	Amperometry of a) the potential-time profile for the stepped or staircase voltage applied to the working electrode. T_{step} , time interval of the voltage step ($=t_0$), ΔE_{step} , voltage step of the applied staircase wavefrom and b) typical amperometric i-t curve.	16
3.1	Schematic diagram of preparation steps for the chemical sensor modification ($\text{Fe}_3\text{O}_4\text{-CNTs-NiNPs/GC}$).	29

LIST OF FIGURE (CONTINUED)

FIGURE	PAGE	
3.2	Photograph of the set up for electrochemical measurements using a potentiostat (eDAQ) data processing and a voltammetric cell.	30
3.3	Sample of energy drinks (100 plus, Sponsor be fresh and Sponsor active) and honeys (Vejpong, Good.b and Floral longan honey).	30
3.4	Sample of wines (Boones pina colada, Boones cheek berry and Fresco berry red), pickled mustard green (Songheng, Songpueng and House wife) and pickled garlic (Ma jin, Big C and Vanusun), respectively.	31
3.5	Transmission electron microscope (JEM-1230; JEOL).	32
3.6	X-ray diffractometers (X' Pert MPD, Philip).	33
4.1	TEM images of a) CNTs, b) NiNPs, c) Fe ₃ O ₄ -CNTs and d) Fe ₃ O ₄ -CNTs-NiNPs.	41
4.2	XRD patterns of, a) NiNPs, b) Fe ₃ O ₄ -CNTs and c) Fe ₃ O ₄ -CNTs-NiNPs nanocomposites.	42
4.3	Cyclic voltammogram of a) bare glassy carbon electrode (GC), b) NiNPs/GC, c) Fe ₃ O ₄ /GC, d) Fe ₃ O ₄ -CNTs/GC, e) CNTs-NiNPs/GC and f) Fe ₃ O ₄ -CNTs-NiNPs/GC electrodes in 0.1 M NaOH, pH 13.0 (dashed line) and in 4 mM glucose (solid line), scan rate 0.05 V s ⁻¹ .	44
4.4	The effect of the concentration of Fe ₃ O ₄ -CNTs-NiNPs (mg mL ⁻¹) on the oxidation peak current of 4 mM glucose in 0.1 M sodium hydroxide solution (pH 13.0).	45
4.5	Cyclic voltammograms of Fe ₃ O ₄ -CNTs-NiNPs/GC electrode at various sodium hydroxide solution a) pH 10.0, b) pH 11.0, c) pH 12.0, d) pH 13.0 and e) pH 14.0 in the presence of 1 mM glucose (solid line), scan rate 0.05 V s ⁻¹	47

LIST OF FIGURE (CONTINUED)

FIGURE		PAGE
4.6	a) Cyclic voltammogram of Fe ₃ O ₄ -CNTs-NiNPs/GC electrode for 0.5 mM glucose in 0.1 M sodium hydroxide solution (pH 13.0) with the variation of scan rate ranging from 0.03 to 0.09 V s ⁻¹ . b) linear relationship is the plot of the anodic (I _{p,a}) and cathodic peak current (I _{p,c}) versus the square root of the scan rate.	48
4.7	a) Cyclic voltammogram of glucose in 0.1 M NaOH with the variation of glucose concentration from 0 to 6 mM and b) Calibration plot of anodic peak currents versus glucose concentration.	49
4.8	Anodic current of Fe ₃ O ₄ -CNTs-NiNPs/GC electrode at different potentials from 0.40 V to 0.70 V upon addition of 1 mM glucose to 0.1 M sodium hydroxide solution (pH 13.0).	50
4.9	a) Typical amperometric <i>i-t</i> curve of Fe ₃ O ₄ -CNTs-NiNPs/GC electrode to successive additions of glucose solution into a stirred system of 0.1 M sodium hydroxide solution (pH 13.0).at 0.55 V. b) The linear calibration plot of the corresponding oxidation peak current versus glucose concentration.	51
4.10	An amperometric response obtained from the developed glucose sensor for six replicates with the addition of 0.02 mM glucose in to 0.1 M sodium hydroxide solution (pH 13.0), applied potential at 0.55 V.	53
4.11	Amperometric response of glucose chemical sensor in 0.1 M NaOH (pH 13.0) upon the successive addition of 1 mM glucose, 0.5 mM uric acid (UA), 0.1 mM ascorbic acid (AA), 0.01 mM dopamine (DA) and 1 mM glucose, respectively.	54
4.12	Sensitivity of the calibration curves obtained from five electrodes fabricated independently, calibration curves were performed using the concentration of glucose from 0.5 to 2.0 mM.	56

LIST OF FIGURE (CONTINUED)

FIGURE		PAGE
4.13	Cyclic voltammogram of a) bare glassy carbon electrode (GC), b) NiNPs/GC, c) Fe ₃ O ₄ /GC, d) CNTs /GC e) NiNPs-CNTs /GC, f)Fe ₃ O ₄ -CNTs/GC and g) Fe ₃ O ₄ -CNTs-NiNPs/GC electrodes in 0.1 M phosphate buffer solution (pH 7.0) (dashed line) and in the presence of 4 mM glucose (solid line), scan rate 0.05 V s ⁻¹ .	59
4.14	The effect of the concentration of Fe ₃ O ₄ -CNTs-NiNPs mg mL ⁻¹ on the oxidation peak current of 4 mM sulfite in 0.1 M phosphate buffer solution, (pH 7.0).	61
4.15	a) Cyclic voltammetric responses of 4 mM sulfite at various buffer pHs and the dependence of buffer pH on the b) peak current and c) peak potential obtained from the chemical sensor, scan rate 0.05 mV s ⁻¹ .	62
4.16	a) Cyclic voltammograms, obtained at various scan rates for 4 mM sulfite in 0.1 M phosphate buffer solution, (pH 7.0) at modified sulfite sensor and b) linear relationship between oxidation peak currents and square root of the scan rate.	63
4.17	a) Cyclic voltammogram of sulfite in 0.1 M phosphate buffer solution, (pH 7.0) with the variation of sulfite concentration from 0 to 8 mM and b) calibration plot of anodic peak currents versus sulfite concentration.	64
4.18	a) Linear sweep voltammograms of the Fe ₃ O ₄ -CNTs-NiNPs/GC electrode to successive additions of sulfite standard into 0.1 M phosphate buffer solution, (pH 7.0) b) The linear calibration plot of the corresponding oxidation peak current versus sulfite concentration.	65
4.19	The storage stability of the developed sulfite sensor calculated from response of 1 mM sulfite in 0.1 M phosphate buffer solution, (pH 7.0).	67

LIST OF FIGURE (CONTINUED)

FIGURE	PAGE
A.1 XRD patterns of a) CNTs b) Fe_3O_4 c) NiNPs, d) Fe_3O_4 -CNTs and e) Fe_3O_4 -CNTs-NiNPs nanocomposites.	86
B.1 Cyclic voltammograms of concentration of Fe_3O_4 -CNTs-NiNPs (mg mL^{-1})	88
B.2 Amperograms of the applied potential on the glucose sensor response 0.1 mM glucose.	89
B.3 Amperograms of the interference on the glucose sensor.	92
B.4 a) Amperograms of the D-1 sample on the glucose sensor and b) linear calibration plot of anodic peak current versus glucose concentration and regression equation from standard addition method.	94
B.5 a) Amperograms of the H-2 sample on the glucose sensor and b) linear calibration plot of anodic peak current versus glucose concentration and regression equation from standard addition method.	95
C.1 Cyclic voltammograms of concentration of Fe_3O_4 -CNTs-NiNPs (mg mL^{-1}).	97
C.2 Linear sweep voltammograms of the interference on the Fe_3O_4 -CNTs-NiNPs/GC.	98
C.3 The storage stability of the developed sulfite sensor calculated from response of 1 mM sulfite in 0.1 M phosphate buffer solution, (pH 7.0).	101
C.4 a) Linear sweep voltammogram of the W-2 sample on the sulfite sensor and b) linear calibration plot of anodic peak current versus sulfite concentration and regression equation from standard addition method.	104

LIST OF FIGURE (CONTINUED)

FIGURE		PAGE
C.5	a) Linear sweep voltammogram of the M-1 sample on the sulfite sensor and b) linear calibration plot of anodic peak current versus sulfite concentration and regression equation from standard addition method.	105

LIST OF ABBREVIATION

ABBREVIATION	DEFINITION
GC	Glassy carbon
CNTs-COOH	COOH-functionalized multi walled carbon nanotubes
Fe ₃ O ₄	Magnetite
NiNPs	Nickel nanoparticles
DMF	<i>N,N</i> Dimethylformamide
g	Gram
mL	Milliliter
μA	Microampere
μL	Microliter
CV	Cyclic voltammetry
LSV	Linear sweep voltammetry
DI	Deionization
mM	Millimolar
M	Molar
E	Potential
I	Current
V	Volt
LOD	Limit of detection
°C	Degree Celsius
MW	Molecular weigh

CHAPTER 1

INTRODUCTION

1.1 The importance and the source of the research

Recently, methods for monitoring glucose levels in body fluids for clinical applications and in pharmaceutical products and beverages for industrial quality control have been received considerable attention. In the previous reports, efforts to develop selective and sensitive methods for the analysis of glucose include colorimetric [1-5], chemiluminescent [6, 7], and electrochemical approaches [8-15]. These approaches are all rely on glucose oxidation reaction catalyzed by enzyme glucose oxidase (GOx). Among these methods, electrochemical detection by a biosensor [8-15] is one of the most commonly used because of inherent high sensitivity and simplicity of instrumentation. Most of the electrochemical glucose biosensors are based on GOx immobilized on a high conductive material to prepare glucose sensors. Although GOx is relatively more stable than other enzymes, use of the biosensor is limited by relatively high cost, inherent stability, complicated immobilization procedures, and certain critical operational and storage conditions e.g. temperature, pH and ionic strength [8, 10, 11, 15]. Besides glucose, sulfite (SO_3^{2-}) one of the most wide applications as food preservative, is considerable interest to develop sensor for the detection in food quality control.

In addition, electrochemical oxidation of sulfite using non-enzymatic sensors are currently interesting because of sulfite is widely used as an additive in pickle food and beverages to prevent oxidation and bacterial growth and to control enzymatic reactions during production and storage. Despite these advantages, the sulfite content in food and beverages should be strictly limited amounts due to its the severe harmful effects to skin, mutagenic, or gastrointestinal signs [16-18]. The United States Food and Drug Administration (FDA) has required labeling of food products containing more than

10 $\mu\text{g mL}^{-1}$ of sulfite [19-21]. Therefore, it is important to develop a rapid, high accurate and precision methods for determination of sulfite in food and beverages. Several methods were developed to quantify of sulfite such as spectrophotometry [22-23], chemiluminescence [24-25], capillary electrophoresis [26] and electrochemical methods [27-29]. Among these methods, electrochemical detection is the most attractive because of its high sensitivity, simplicity, fast response and inexpensive equipment when comparison with several methods. Sulfite biosensor for determination of sulfite are developed based on sulfite oxidases (SOx) enzyme immobilized with nanomaterials. SOx enzyme catalyzes $2e^-$ oxidation of sulfite (SO_3^{2-}) to sulfate (SO_4^{2-}) and H_2O_2 . This enzymatic sulfite sensor provides many good characteristics including high activity, sensitivity and selectivity in detection of sulfite [30-32]. However, the biosensors are normally processed the limitation of using enzyme as same as using GOx in glucose biosensor.

To solve of the disadvantages of enzymatic biosensors such as instability, the high cost of enzymes, complicated immobilization procedures, and critical operating conditions. Therefore, considerable attention had been paid to developing non-enzymatic electrodes to overcome these problems. As a result, there is an ever-growing demand to create electrochemical sensors with high sensitivity, high reliability, short response times, good recyclability, and low cost, especially non-enzymatic amperometric sensors [14-15].

Recently, nanomaterials, such as carbon nanotubes (CNTs) and nanoparticles (NPs) of metals, have been widely applied in sensors and biosensors. Carbon nanotubes (CNTs) to the forefront of micro and nanotechnology ever since the discovery [33]. Their high thermal conductivity in fluid suspension made them can be used as molecular wires in molecular electronics and as smallest possible electrodes [34-35]. CNTs can display metallic, semiconducting and super conducting because of their electron transport properties that are able to promote electron or proton transfer reaction and provide mechanical properties due to their low mass, high surface area and chemical stability [36-39]. Moreover, they are friendly to the environment.

Metallic NPs, including nickel (Ni), gold (Au), platinum (Pt), palladium (Pd), copper (Cu), and silver (Ag), can be used to increase electrochemical activities. Chemical sensors and biosensors modified with metallic NPs have demonstrated good

performances due to their high surface area, superb high mass transport and high catalytic activity as well as good bio-compatibility, with control over the microenvironment, relative to macro electrodes [14, 39-40]. Moreover, there have been recently various trials to employ new nanomaterials in fabricating chemically modified electrodes. Their good biocompatibility, strong super paramagnetic behavior, low toxicity, large surface area and easy preparation process make them be very promising materials. In addition, magnetic nanoparticles (MNs), especially iron oxide nanoparticles have been one of the most widely investigated and applied to immobilize different biomolecules and enzymes [41-44].

In this work, a simple and effective method for constructing glucose and sulfite non-enzymatic sensors using hybrid materials of magnetite (Fe_3O_4) and nickel nanoparticles decorated carbon nanotubes (Fe_3O_4 -CNTs-NiNPs) was proposed. The combination of CNTs with magnetite and nickel nanoparticles (NiNPs) is expected to be an effective electrocatalyst for glucose and sulfite detection. However, most metals nanoparticles or metal oxide nanoparticles, including Fe_3O_4 and NiNPs, are unable to adhere to the CNTs surface. This work proposed simple and effective strategy to solve this problem by loading Fe_3O_4 nanoparticles in situ on the surface of carboxylated multi-walled carbon nanotubes (CNTs-COOH) via a chemical co-precipitation procedure. After that, NiNPs were decorated on Fe_3O_4 -CNTs using ultra-sonication. The simple and effective method enables the uniformly deposition of Fe_3O_4 and NiNPs onto the surface of CNTs. Construction of glucose as well as sulfite sensors using the Fe_3O_4 -CNTs-NiNPs nanocomposites coated on the surface of glassy carbon electrode was investigated. The Fe_3O_4 -CNTs-NiNPs/GC electrode showed an excellent activity for the electrocatalysis of glucose and sulfite oxidation. These modified electrodes exhibit high sensitivity and selectivity in the detection of glucose and sulfite.

1.2 Objectives

1.2.1 To synthesize and characterize of Fe₃O₄-CNTs-NiNPs by decorating of NiNPs on Fe₃O₄-CNTs via ultrasonication.

1.2.2 To investigate the possibility of using a developed chemical sensor based on Fe₃O₄-CNTs-NiNPs nanocomposites for evaluation of glucose and sulfite oxidation by using cyclic voltammetry.

1.2.3 To optimize parameters effecting the sensitive and selective chemical sensor based on Fe₃O₄-CNTs-NiNPs nanocomposites of glucose and sulfite in food applications.

1.3 Expected outcomes

1.3.1 Sensitive and selective non-enzymatic sensors were developed based on magnetite and nickel nanoparticles decorated carbon nanotubes for quantitative analysis of glucose and sulfite.

1.3.2 The fabricated non-enzymatic sensors (Fe₃O₄-CNTs-NiNPs/GC) have high selectivity and stability which can be applied to determine glucose and sulfite in real samples.

1.4 Scope of research

Development of chemical sensor for glucose and sulfite determination using Fe₃O₄-CNTs-NiNPs nanocomposites

1.4.1 Development of chemical sensors

Developed sensor was carried out by coating Fe₃O₄-CNTs-NiNPs nanocomposites on glassy carbon (GC) electrode. These nanocomposites were prepared by in situ loading of Fe₃O₄ nanoparticles on the surface of carboxylated multi-walled carbon nanotubes and then decorating of NiNPs on Fe₃O₄-CNTs via ultra-sonication. This process provided Fe₃O₄-CNTs-NiNPs nanocomposites. Then, the developed electrodes were applied to determine glucose and sulfite by amperometric and linear sweep votammetric techniques.

1.4.2 Characterization of the nanocomposites

1.4.2.1 Transmission Electron Microscopy (TEM)

1.4.2.2 X-Ray Diffraction (XRD)

1.4.3 Electrochemical oxidation of glucose on the developed sensor

1.4.3.1 Study of glucose oxidation using cyclic voltammetry.

1.4.3.2 Study of parameters that affect the sensitivity and selectivity of the glucose chemical sensor using cyclic voltammetry and amperometry.

- 1) Effect of Fe₃O₄-CNTs-NiNPs loading on the current response
- 2) Effect of pH (sodium hydroxide solution), 0.1 M
- 3) Scan rate dependence study
- 4) Reproducibility study
- 5) Applied potential for amperometric detection
- 6) Linearity range and limit of detection (LOD)
- 7) Interferences study (sucrose, maltose, fructose, citric acid, ascorbic acid, uric acid, dopamine, sodium chloride, and sodium carbonate).

1.4.4 Electrochemical oxidation of sulfite chemical sensor

1.4.4.1 Cyclic voltammetric study of sulfite oxidation.

- 1) Scan rate dependence study
- 2) Effect of Fe₃O₄-CNTs-NiNPs loading on the single response
- 3) Effect of pH (phosphate buffer solution), 0.1 M
- 4) Scan rate dependence study

1.4.4.2 Parameters that effect the sensitivity and selectivity of the linear sweep voltammetric detection.

- 1) Linear concentration range and limit of detection.
- 2) Interferences study (glucose, sucrose, maltose, fructose, ethanol, ascorbic acid, sodium chloride, sodium sulfate and sodium carbonate).
- 3) Method validation
- 4) Stability of the developed sulfite sensor and the possibility applied to determine sulfite in wine, pickled mustard green and pickled garlic.

CHAPTER 2

LITERATURE REVIEWS

2.1 Chemical sensor

A chemical sensor composed of two basic components which are an active layer (receptor) and a transducer [45, 46]. Mostly, the receptor interacts with analyte molecule. As a result, its physical properties are changed in such a way that the appending transducer can gain an electrical signal. Many materials such as organic, inorganic or hybrid organic-inorganic polymers can be used as receptor layers. Analyte can diffuse into the matrix and be trapped, thus modifying the chemical or physical properties of the material. The receptor can also be doped with specific transducer able to react selectively with the target chemical substance (analyte), thus provided the selectivity of the sensor. The ideal chemical sensor is low cost, simple design or portable device that responds with signal output at any required analyte concentration. Chemical sensors contain two basic functional units including a receptor part and a transducer part (Figure 2.1).

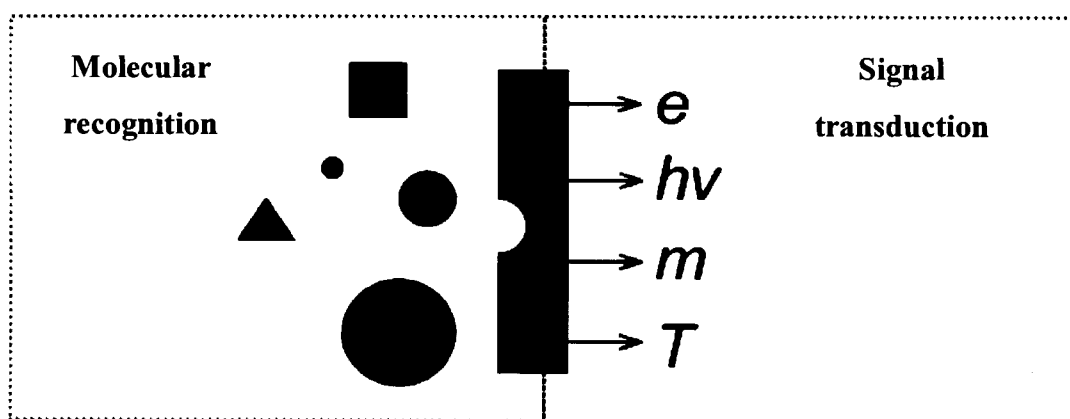


Figure 2.1 Diagram of chemical sensor [47].

The receptor part: Artificial sensing element interacts with analytes based on chemical, physical properties and transformed into a form of energy which may be measured by the transducer. The receptor part of chemical sensors may be based upon various principles:

- 1) physical, where no chemical reaction takes place. For examples are those based on measurement of absorbance, refractive index, conductivity, temperature or mass change.
- 2) chemical, in which a chemical reaction with participation of the analyte gives rise to the analytical signal.
- 3) biochemical, in which a biochemical process is the source of the analytical signal.

The transducer part: a device is used to convert the chemical signal transforming. The intensity of generated signal is directly or inversely proportional to the analyte concentration.

A chemical sensor is a device that transforms chemical information, ranging from the concentration of a specific sample component to total composition analysis, into an analytically useful signal [45, 48]. The chemical information, mentioned above, may originate from a chemical reaction of the analyte or from a physical property of the system investigated.

2.2 Carbon nanotubes

Carbon nanotubes (CNTs) to the forefront of micro and nanotechnology was discovered in 1991 by Iijima et al. [33]. CNTs is a tube-shaped material, made of carbon, have been constructed with diameter measurement on the nanometer scale. A nanometer is one-billionth of a meter, or about 10,000 times smaller than a human hair. The lamellar planes of sp^2 carbon in graphite sheets are organized in hexagons with a tremendously high degree delocalization of pi-electron. Thus, CNTs can display high thermal conductivity in fluid suspension uses in enhancing industrial heat transfer efficiency [34, 35]. CNTs have also been investigated for their mechanical properties due to their low mass, high surface to volume ratio and chemical stability [36-39]. The current energy crisis and concerns with environment have boosted our interest in renewable and eco-friendly sources of energy. CNTs are categorized as either single-walled carbon nanotubes (SWCNTs) and multi-walled carbon nanotubes (MWCNTs).

The structure of single-walled carbon nanotubes has only one layer, included a single graphene layer rolled up into a seamless [49, 50]. The structure of SWCNTs can be constructed by wrapping a single layer of graphite called graphene into a seamless cylinder as shown in Figure 2.2A. The chiral vector can be described by the following equation:

$$C_h = na_1 + ma_2 \quad (2.1)$$

where the integers (n, m) are the number of steps along the unit vectors (a_1, a_2) of hexagonal lattice, connects two lattice points O and A on the graphene sheet. An infinite strip is cut from the sheet through these two points, perpendicular to the chiral vector. The nanotube is uniquely specified by the pair of integer numbers n, m or by its radius $R = C_h/2\pi$ and chiral angle θ which is the angle between C_h and the nearest zigzag of C–C bonds. All different tubes have angles θ between zero and 30° . Special tube types are the achiral tubes (tubes with mirror symmetry): armchair tubes (n, n) ($\theta = 30^\circ$) (B(a)) and zigzag tubes $(n, 0)$ ($\theta = 0^\circ$) (B(b)). Otherwise, they are called chiral (B(c)). Schematic of different chiralities CNTs is shown in Figure 2.2B [50].

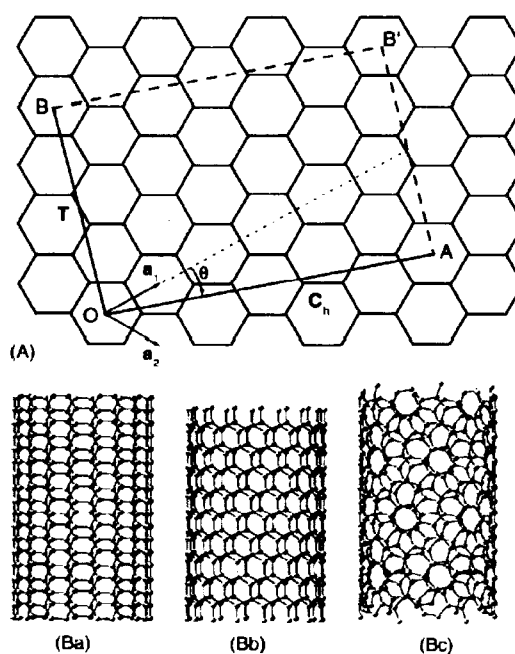


Figure 2.2 Schematic representation of the construction of a nanotube by rolling-up an infinite strip of graphene with different chiralities (Ba: armchair; Bb: zigzag and Bc: chiral) [50].

While MWCNTs consisting of multi rolled layer are a collection of nested tubes of continuously increasing diameters. They can range from one outer and one inner tube (a double-walled carbon nanotube) to as many as 100 tubes (walls) or more as shown in Figure 2.3.

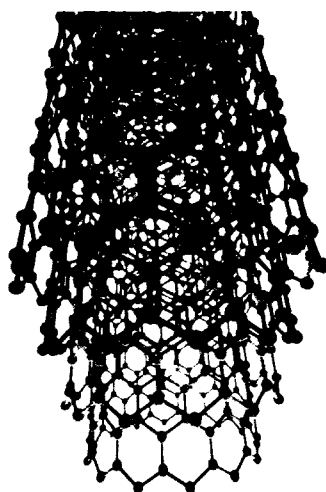


Figure 2.3 Structure representation of multi-walled carbon nanotubes (MWCNTs).

2.3 Magnetite nanoparticles (Fe_3O_4)

Magnetite nanoparticles (Fe_3O_4) are one of the most widely studied nanomaterials. The diameter range presents of micro and nano meter (diameter in 10^{-6} - 10^{-9} m) of Fe_3O_4 , an iron oxide with chemical structure Fe_3O_4 , particles; additionally, the properties of nano-particulate magnetite have been widely applied in various field including environmental engineering, mechano-electrical fields, sorting of biological species, biomedical imaging and site-specific drug delivery [51-53].

2.3.1 Structural Properties

Magnetite's crystal structure follows by spinel pattern with alternating octahedral and tetrahedral-octahedra layers [54, 55]. As shown in Figure 2.4, the ferrous (Fe^{2+}) species occupied by half of the octahedral lattice sites due to greater ferrous crystal field stabilization energy (CFSE); alternatively, ferric (Fe^{3+}) species occupied by the other octahedral lattice sites and all tetrahedral lattice sites.

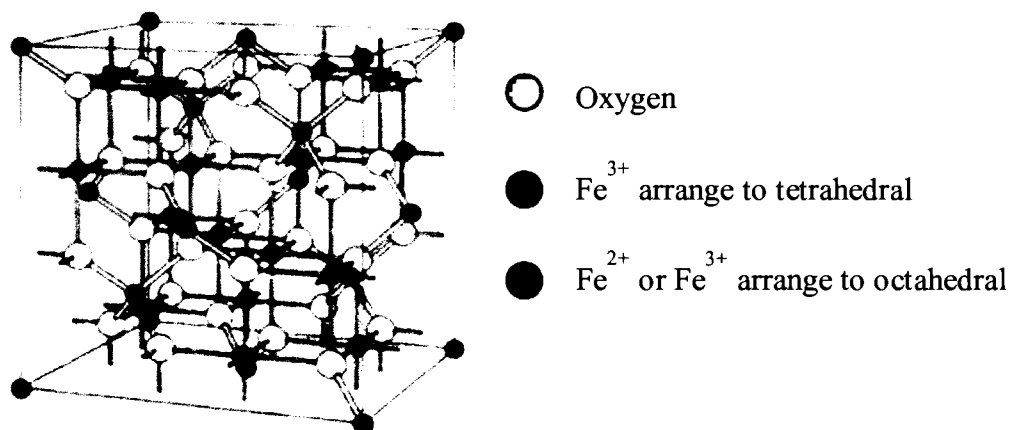


Figure 2.4 Structure and unit cell of magnetite (Fe₃O₄) [55].

The synthesis techniques of Fe₃O₄ based on two categories including polymer/surfactant assisted precipitation reactions and co-precipitation reactions. A simple and effective method for synthesizing magnetite nanoparticles by co-precipitation reactions was described [56, 57]. The method consists of stoichiometric mixtures of ferrous and ferric hydroxides in aqueous solution, yielding spherical magnetite particles homogeneous in size [57]. The reaction mechanism can be described by the following reaction equation.



Optimum conditions for this reaction are pH between 8 and 14, Fe³⁺/Fe²⁺ ratio of 2:1 and a non-oxidizing environment. Being highly susceptible to oxidation, magnetite (Fe₃O₄) is transformed to maghemite (γ-Fe₂O₃) in the presence of oxygen by the following equation



The size and shape of the nanoparticles can be controlled by adjusting pH, ionic strength, temperature, nature of the precursor salts (perchlorates, chlorides, sulfates, and nitrates), or the Fe(II)/Fe(III) concentration ratio [58, 59].

2.4 Magnetite decorated carbon nanotubes (Fe₃O₄-CNTs)

Recently, magnetic nanoparticles (MNs), especially iron oxide nanoparticles (Fe₃O₄) have been widely investigated and applied to immobilize different biomolecules and enzymes because of their good biocompatibility, strong super paramagnetic behavior, low toxicity, large surface area and easy preparation process. On the other hand, carbon nanotubes (CNTs) are considered as an important group of nanostructures with attractive electronic, chemical and mechanical properties [41, 60]. The intrinsic stability, large surface area and good biocompatibility applications of CNTs to immobilize a variety of species have been reported [61]. Furthermore, it has already been reported that the combination of Fe₃O₄ with CNTs provides hybrid nanocomposites with synergetic effect that leads to the improvement in the electrocatalytic properties and can be useful platform for immobilizing biomolecules or enzymes to enhance sensor performances of modified electrodes [41]. For these reasons, many studies increasingly focus interest in coating of CNT with Fe₃O₄ and/or in filling their cavity with Fe₃O₄. However, one of the major drawbacks that CNTs are very hydrophobic, low solubility in aqueous solutions a surface tension greater than approximately 100 or 200 mN m⁻¹ [60, 62, 63]. Thus, most metals nanoparticles or MNs, are unable to adhere to the CNTs surface. Our simple and effective strategy to solve this problem is loading Fe₃O₄ nanoparticles in situ on the surface of carboxylated multi-walled carbon nanotubes (CNTs-COOH) via a chemical co-precipitation procedure. The resulting Fe₃O₄-CNTs nanocomposite can be a useful in enhancing the capabilities for electrochemical sensing, biotechnological and biomedical field.

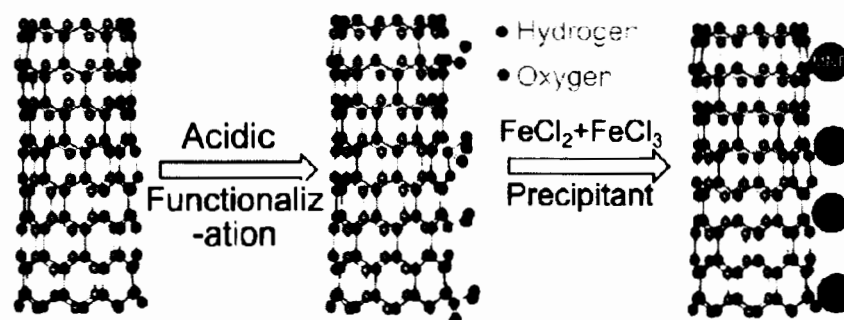
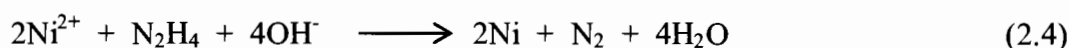


Figure 2.5 Magnetizing CNTs by coprecipitation. When CNTs are treated with strong oxidizing acids, COOH, C=O, and C–OH groups are formed at defect sites. In the presence of Fe^{+2} , Fe^{+3} and a precipitating base serve as nucleation sites for (Fe_3O_4) [61].

2.5 Nickel nanoparticles (NiNPs)

Recently, nickel nanoparticles (NiNPs) is increased in attention for chemical sensor development. The attention has been paid to the monodisperse because of their excellent physical and chemical properties and have been widely applied in various fields, such as hybrid with magnetic materials, using in sensor materials, enhancing of optical properties and catalytic activities. The unique properties of NiNPs show excellent catalytic activity and high stability [64-66]. However, their stability and catalytic activity in depend strongly on the size, morphology, and homogeneous dispersion of the nanoparticles It is a big challenge to find the method to minimize the aggregation of NiNPs. Therefore, in this work propose the preparation of NiNPs through reducing nickel chloride by hydrazine hydrate to obtain the monodisperse NiNPs. The reaction can be described by the following reaction equation [67].



NiNPs can be easily synthesised by dissolving 0.952 g of nickel chloride and 5.0 g of hydrazine hydrate in 395.0 mL ethylene glycol. Then, 4.0 mL of 1.0 M sodium hydroxide solution was added to the solution. The solution was further stirred in a capped flask for 1 h at 60 °C. The obtained black Ni nanoparticles (NiNPs) was washed thoroughly with ethanol and dried at 60 °C for 24 h NiNPs were obtained as a black powder.

2.6 Reaction of glucose

The mechanism for electro-oxidation of glucose are believed that Ni(II) and Ni(III) redox couple on the electrode surface in an alkaline medium are involved. First, NiNPs (Ni^0) at the surface of electrode was transformed to $\text{Ni}(\text{OH})_2$. Then $\text{Ni}(\text{OH})_2$ is oxidized to the catalytically active NiOOH . After that, the glucose undergoes hydrogen abstraction at the surface to form a radical intermediate and reform the $\text{Ni}(\text{OH})_2$ species. Finally, the hydroxyl anions in the solution rapidly oxidize the organic radical intermediate to form gluconolactone [68, 69]. The couple of peaks are corresponding to the Ni(II)/Ni(III) can be described by the following reactions [70, 71]:



Mechanism of the glucose sensor as described above can be schematically shown in Figure 2.6.

The electro-catalytic in glucose oxidation by NiNPs in Fe_3O_4 -CNTs-NiNPs/GC electrode is accordance to the previous reports of non-enzymatic glucose sensing fabricated from three-dimension porous nickel nanostructure [72], CNTs-nickel nanocomposites [70] and ultrathin $\text{Ni}(\text{OH})_2$ nanoplates [72] synthesized by hydrogen-evolution-assisted electro-deposition [71], atomic layer deposition [70] and pyrolysis melamine foam followed by the microwave process [72]. These electrodes showed highly sensitive, selective and satisfactorily stable response toward glucose at low over potential under alkaline condition. However, the methods for synthesizing nanostructured Ni or Ni-hybrid materials are somehow relatively complicated. In practice, the high cost of the electrode due to the sophisticated method and expensive instruments may limit their real applications. Herein, this work proposed the good electrochemical performance of Fe_3O_4 -CNTs-NiNPs nanocomposites, such as large surface area and electrical conductivity, with the electrocatalytic activity of the hybrid nanocomposites towards glucose oxidation. Our method for prepared Fe_3O_4 -CNTs-NiNPs nanocomposites is very simple using uncomplicated precipitation method and

common laboratory equipment. The fabricating process was cost-effective, time-saving and easy by preparation under ultrasonication.

$\text{Fe}_3\text{O}_4\text{-CNTs-NiNPs/GC}$

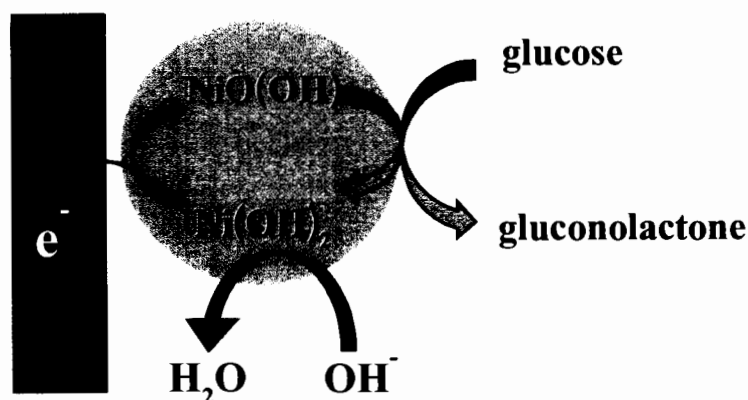


Figure 2.6 Schematic diagram showing the mechanism of glucose oxidation reactions occur during operation of the developed glucose chemical sensor.

2.7 Voltammetry

The voltammetric (volt-amperometric) techniques discussed here record the resulting current (I) via a working electrode as a function of time (t) [73]. Voltammetry is the general term to be used when current potential relationships are being investigated.

2.7.1 Cyclic voltammetry

Cyclic voltammetry (CV) is a subset of voltammetry, that is one of the most widely used for studying redox reactions of both organic and inorganic compounds and electroanalytical techniques for analysis of electron transfer related reactions. Their ability to provide information on the steps involved in electrochemical processes is very well known. The CV consists of scanning linearly the applied potential (E) to a working electrode (WE) using a triangular potential wave form is shown in Figure 2.7a. During the experiment the electrode is stationary, the "electrochemical detection" is performed. Typical result or cyclic voltammogram is presented in Figure 2.7b [74]. As shown in Figure 2.7b, the voltage is measured between the working electrodes and reference electrode, while the current is measured

between the working electrode and counter electrode. The CV system consists of three electrodes defined as the working electrode (WE), surface where the electrochemical reaction takes place, the reference electrode (RE), which tracks the potential solution and the counter electrode (CE), which supplies the current required for the electrochemical reaction at WE.

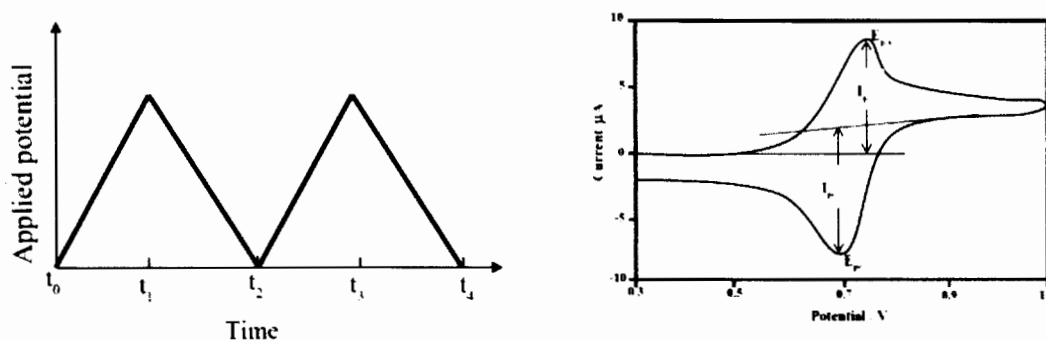


Figure 2.7 Typical of a) cyclic voltammogram wave from: variation of the potential applied to the working electrode with time and b) cyclic voltammogram: resulting current-potential curves [74].

2.7.2 Linear sweep voltammetry (LSV)

Linear sweep voltammetry is simply cyclic voltammetry without a vertex potential and reverse scan. The basic setup for linear sweep voltammetry at the applied potential scan at the $1\text{--}5\text{ mV s}^{-1}$ is shown in Figure 2.8a. User (s) can choose an initial potential, final potential and sweep rate. Finally, the resulting current plot versus applied potential and follows the general shape illustrated in Figure. 2.8b, which is called a linear sweep voltammogram.

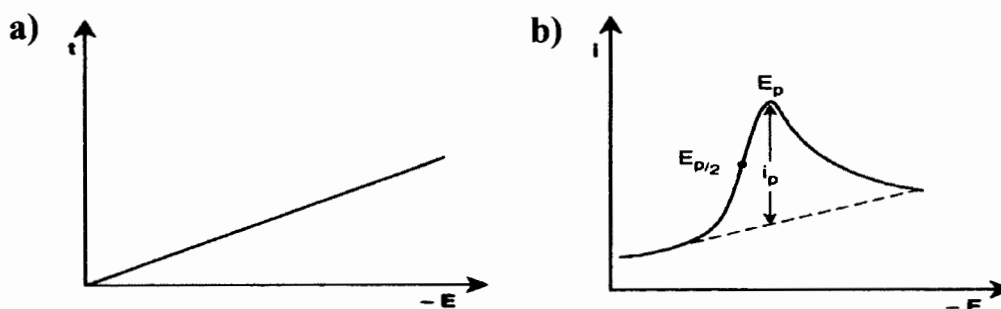


Figure 2.8 Linear sweep voltammetry of a) the variation of the potential applied to the working electrode with time and b) linear sweep voltammogram: resulting current-potential curves [75].

2.8 Amperometry

The term amperometry involves the technique in which a fixed potential is applied to a working electrode and the current resulting from oxidation or reduction reactions occurred at the working electrode is measured. It is a method of electrochemical analysis in which the signal of interest, current, is linearly dependent based on the concentration of the analyte and can be controlled by the electric potential applied to the working electrode [75]. To maintain charge neutrality within the sample, a counter-reaction occurs at a second electrode. The third electrode acts as a reference. During electrolysis, working electrode may acts as an anode or a cathode, according to the nature of analyte. The typical amperogram shows in Figure 2.9

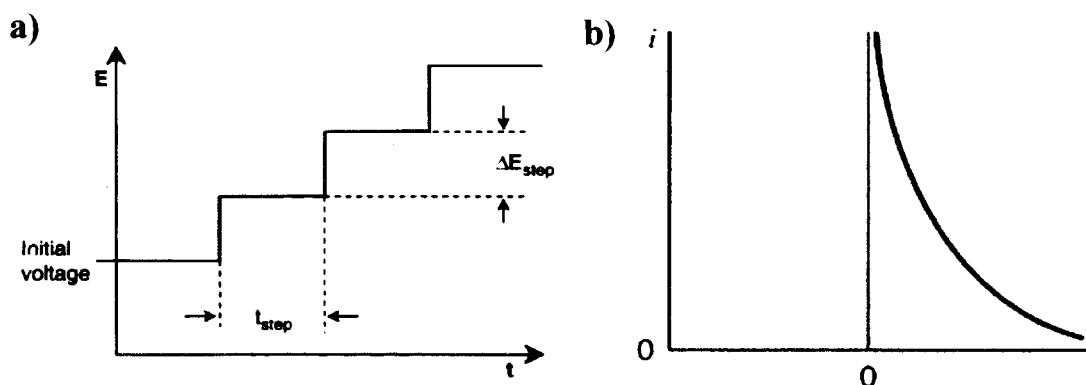


Figure 2.9 Amperometry of a) the potential-time profile for the stepped or staircase voltage applied to the working electrode. T_{step} , time interval of the voltage step ($=t_0$), ΔE_{step} , voltage step of the applied staircase waveform (adopt from [76]) and b) typical amperometric i - t curve.

Amperometric detector, which are the most commonly used in electroanalysis, are of the three electrodes type. The potential applied to working electrode is set at a constant relative to the reference electrode. The iR drop between the working and auxiliary electrode is compensated by the potentiostat and the current flowing through the working electrode is the measured signal. The current, which is in the range of pA to μA , is amplified and recorded as a function of the time in a suitable flow-cell, through which the eluent stream passes. This gives the concentration-time profile or chromatogram of the analyte in the effluent [76]. However, when the surface area of

the working electrode in amperometry is a smaller 0.5 cm^2 , so the Faradaic reaction of the analyte is incomplete. This may be caused only a fraction of the total analyte to react. In fact, less than 10% of the analyte is reacted in a typical amperometric flow-cell at flow-rates around 1 mL min^{-1} . While using the larger surface area of working electrodes can lead to quantitative reaction of the analyte at the electrode, and when this occurs, the technique used is described as high-efficiency amperometry [76].

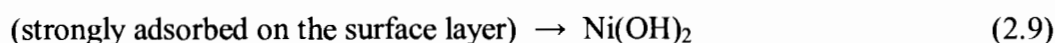
2.9 Related research

2.9.1 Detection of glucose

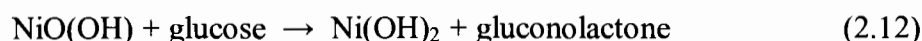
In 2010, M. Shamsipur. et al. [77] presented the improvement of electro-oxidation for glucose detection based on GC electrode coated with nickel(II) oxide and multi-walled carbon nanotubes (MWCNTs). Cyclic voltammetry and chronoamperometry were employed for the examination. The non-enzymatic glucose sensor was fabricated by dispersing 1 mg of MWCNTs in 10 mL N,N-dimethylformamide (DMF) with the ultrasonic agitation to give a 0.1 mg mL^{-1} black solution. Then 20 μL of the black solution was dropped cast at the GC electrode surface and evaporated at $50 \text{ }^\circ\text{C}$ to prepare the GC/MWCNTs modified electrode. After that one drop of 2 mM nickel (II) nitrate aqueous solution to the GC/MWCNTs electrode surface. The electrode was allowed to dry at $50 \text{ }^\circ\text{C}$ in an air oven for 25 min and then applied the potential cycling between 0.1 and 0.6 V vs. Ag/AgCl to electrode in 0.10 M NaOH solution. The resulting electrode provided a linear range between 0.2 mM - 12 mM and limit of detection of 0.16 mM (3σ) for glucose. The developed electrode displayed satisfied stability and better self life stored at ambient conditions.

In 2011, Y. Mu et al. [78] developed a fast and sensitive non-enzymatic glucose sensor to solve the disadvantages of the previous enzyme-modified electrode. The modified carbon paste electrodes (CPEs) was fabricated by nano nickel oxide (NiO). CPEs were prepared firstly by hand mixing of graphite powder and paraffin with ratio of 5:1. The resulting carbon paste was packed firmly into the cavity of capillary (diameter 1 mm). The electric contact was established via a conductive brass wire. After that nano NiO and carbon paste were mixed in the ratio of 1:9. The mixture then was carefully packed into CPEs to a depth of about 1 mm. In this step, nano NiO modified CPEs was obtained. The nano NiO modified CPEs were processed by

potential scan for 5 cycles from 0 to 1.2 V to activate non-enzymatic glucose sensors before the determination. The hydroxyl phenomenon also could be found on the surface of various metals. A transformation could be speed up further in alkaline condition when the nano NiO modified electrodes are immersed into 0.5 M alkaline electrolyte. The reaction process was as follows:



In the presence of glucose, oxidation of glucose to gluconolactone was catalyzed by the $\text{Ni}^{3+}/\text{Ni}^{2+}$ redox couple according to the following reactions.

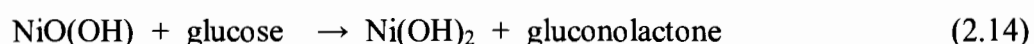


The resulting from modified electrode provided the linear range between 1 - 110 μM and limit of detection of 0.16 μM ($\text{S/N} = 3$). The nano NiO modified electrodes displayed the enhancing of glucose oxidation and satisfy sensitivity for the detection.

In 2011, H. Nie et al. [79] presented the fabrication of non-enzymatic glucose sensor based on NiNPs and straight multi-walled carbon nanotube (SMWNTs) nanohybrids modified GC electrode. This nanohybrids were synthesized by in situ precipitation procedure. NiNPs/SMWNTs nanohybrids were obtained from the reduction of $\text{Ni(OH)}_2/\text{SMWNTs}$ complex. Briefly, 20 mg $\text{Ni(NO}_3)_2$ was added into 20 mL of the treated SMWNTs solution and ultrasonicated for 1 h at room temperature. After that, 60 mL of 2.2 mM NaOH solution was added dropwise to the above mixture solution under stirring at 80 °C. Then the $\text{Ni(OH)}_2/\text{SMWNTs}$ complex was formed and the reaction was carried out under magnetic stirring for 2 h at room temperature. Finally, the $\text{Ni(OH)}_2/\text{SMWNTs}$ complex was separated and rinsed with distilled water several times and heated in furnace at 650 °C for 2 h in the H_2/N_2 mixture atmosphere to reduce Ni^{2+} and get NiNPs/SMWNTs nanohybrids. The NiNPs/SMWNTs/GC electrode was prepared by dropping a 10 μL of NiNPs/SMWNTs (0.2 mg mL^{-1}) on to the GC electrode surface. The electrode was dried slowly at the atmosphere. A non-enzymatic electrochemical sensor device

showed the linear range from 1 μM - 1 mM and limit of detection of 0.5 μM . Moreover, the modified electrode possessed good selectivity and sensitivities and stability for determination of glucose. However, this methods for synthesized nanostructured Ni or Ni-hybrid materials are somehow relatively complicated.

In 2012, A. Sun et al. [80] presented a novel non-enzymatic glucose sensor based on nickel combined with multi-walled carbon nanotubes (Ni-MWCNTs) to fabricate nanohybrid films coated on GC electrode. Nanohybrid film modified electrode was synthesized by heating ethylene glycol and choline chloride (2:1 ratio) while stirring constantly for 20 min until a homogeneous suspension, then the colorless liquid was obtained. After that 10 mg of the acid treated MWCNTs and 3.0 mmol NiCl_2 were added into 10 mL ionic liquid ethaline and the dispersion was ultrasonicated for 30 min to obtain a homogeneous black-blue solution. Then, the MWCNTs and NiCl_2 dispersion solution were used for the electrodeposition of the Ni-MWCNTs nanohybrid films. The potential for applied to cyclic voltammetry (CVs) experiments ranged from 0.0 V to 1.6 V (vs. SCE) with a scan rate of 20 mV s^{-1} for 20 cycles. Then electrode was washed with distilled water. The fabricated sensor exhibited high electrocatalytic activity and good response to glucose and a wide linearity range. The mechanism of electrocatalytic oxidation of glucose due to the existence of Ni^{2+} explain by reactions equation:.



Under optimal conditions, the sensor showed high sensitivity, rapid response time (<2 s) and a limit of detection of 0.89 μM (S/N = 3).

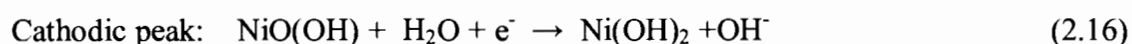
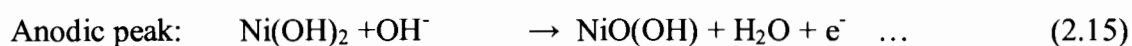
In 2013, X. Zhu et al. [81] reported an amperometric non-enzymatic glucose sensor based on a composite incorporating with nickel(II) oxides and reduced graphene (GR) modified GC electrode. The modified dispersion was prepared by dispersing GR in N, N dimethylformamide (DMF) at a concentration of 1 mg mL^{-1} with the aid of ultrasonic agitation for 1 h, resulting in a homogeneous black suspension. Then drop casting 2 μL of 1 mg mL^{-1} GR dispersion onto the surface of cleaned GC electrode and then evaporating the solvent under an infrared heat lamp. After that, the GR/GC electrode was immersed into a 0.01 mol L^{-1} of NiSO_4 solution,

and a potentiostat was employed for the direct electrodeposition of Ni particles. In the first series of experiments, a pulse potential of 200 mV (500 ms) ~-1,200 mV (100 ms) ~200 mV (500 ms) (vs. Ag/AgCl) was applied and 15 pulses were used for each deposition. The electrode was then conditioned by potential cycling in a successive (0.2 – 0.5 V vs. Ag/AgCl) of 0.2 mol L⁻¹ NaOH solution until a steady state voltammogram was obtained. The modified NiO-GR/GC electrode was used for the study of glucose oxidation. Nickel(II) oxides-graphene modified GC electrode (NiO-GR/GCE) provide the larger current response toward the nonenzymatic oxidation of glucose in alkaline media when compare with NiO/GCE about 1.5 times. The modified electrode exhibited a linear range from 20 μM to 4.5 mM and limit of detection was 5 μM (S/N = 3) for glucose with very short response time (<3 s). Other beneficial features included selectivity, reproducibility and stability. This non-enzymatic sensor designed in this work was used for determination of glucose in commercial red wines.

In 2013, K-C. Lin et al. [82] developed a novel sensitive non-enzymatic glucose sensor based on multiwall-carbon nanotubes (MWCNTs) decorated with nickel and copper nanoparticles (Ni/Cu/MWCNTs). The non-enzymatic glucose sensor was fabricated by drop casted 10 μL MWCNTs solution on the cleaned GC electrode surface and dried in an oven at 40 °C. After that, Ni was electrodeposited on the surface MWCNT/GCE by cyclic voltammetry in the applied potential between 0.5 - 1.1 V, scan rate 0.1 V s⁻¹ and 30 cycles, using a precursor of 0.05 M nickel chloride in a tetraborate solution (pH 9.0). Finally, the Cu was electrodeposited on the electrode surface by cyclic voltammetry in the applied potential between 0.5 - 0.6 V, scan rate 0.1 V s⁻¹ and 30 cycles. This method was used to prepare Ni/Cu/MWCNTs modified electrode. The optimum ratio of Ni:Cu nanoparticles was 1:1. Amperometric sensor produced its optimum response within 1 s when operated at 0.57 V in 0.1 M NaOH (pH 13.0). Two linear ranges of 0.025 μM - 0.8 mM and 2 - 8 mM were obtained with a limit of detection of 0.025 μM (S/N = 3). Moreover, this modified electrode exhibited a high selectivity, good selectivity, low cost and good performance in glucose quantification in human serum samples.

In 2015, T. Choi et al. [70] proposed a strategy to fabricated CNTs-NiNPs through atomic layer deposition (ALD) of Ni followed by chemical vapor deposition

of functionalized CNTs. The synthesized nanocomposites for application to free enzyme for glucose analysis. Carbon nanotube-nickel nanocomposites was prepared by ALD of Ni using A bis(dimethylamino-2-methyl-2-but-oxo) nickel ($\text{Ni}(\text{dmamb})_2$) as a Ni precursor. One ALD cycle consisted of four steps: $\text{Ni}(\text{dmamb})_2$ precursor exposure, Ar purging, ammonia (NH_3) gas reactant exposure, and another cycle of Ar purging. The ALD process temperature was maintained at 300 °C. These CNT-Ni nanocomposites were characterized by scanning electron microscopy (SEM), transmission electron microscopy (TEM), and X-ray photo electron spectroscopy (XPS) analysis. Electrochemical studies indicated that the CNT-Ni nanocomposites exhibited high electrocatalytic activity for glucose oxidation in alkaline media. Cyclic voltammogram showed an anodic peak at +0.45 V and a cathodic peak at +0.36 V. The redox couple peaks are due to the reaction of $\text{Ni}^{3+}/\text{Ni}^{2+}$ couple on the electrode surface. The reaction process was as follows:



The resulting electrode provided a wide linear range between 5 μM - 2 mM and limit of detection of 2 μM . However, the methods for synthesized nanostructured Ni-hybrid materials are somehow relatively complicated. In practice, the high cost of the electrode due to the sophisticated method and expensive instruments may limit their real applications.

2.9.2 Detection of sulfite

In 2003, M. H. Pournaghi-Azar et al. [83] developed a voltammetric and amperometric sensor based on nickel pentacyanonitrosylferrate (NiPCNF) film modified aluminum electrode for determination of sulfite in some real samples. The Al electrode was deposited in metallic nickel by dropping single drop of 0.7 M NiCl_2 saturated with KF solution on the cleaned surface and stand for 10 min. The electrode coated by metallic nickel was derivatized by immersing in a mixture reagent of 0.5 M NaNO_3 and 10 mM $\text{Na}_2(\text{Fe}(\text{CN})_5\text{NO})$ (pH 2.5 adjusted by HNO_3) for 2 h. After that, the modified electrode was stored in air for at least 1 day. The catalytic current was measured on a NiPCNF/Al modified electrode at potential of 0.65 V in 10 mL of phosphate buffer solution (pH 6.2). This electrode showed linearly dependent on the

sulfite concentration and limit of detection was 3 μM . In particular, the proposed method was used for determination of sulfite in sugar, boiler water, sulfur dioxide treated raisins, and dried apricots.

In 2008, H. Zhou et al. [84] developed a novel amperometric sulfite sensor based on multiwalled carbon nanotube ferrocene-branched chitosan (CHIT-Fc/CNTs) modified GC electrode. The modified electrode was prepared by dissolving 0.5 mg CHIT-Fc in 0.5 mL of 0.1 M acetic acid and dispersing 0.5 mg of CNTs-COOH in 0.1 M acetic acid and the dispersion was ultrasonicated for 15 min. Then 3 μg CHIT-Fc and 3 μg CNTs of this solution was drop-casted on the surface of cleaned GC electrode and dried at room temperature for 2 h. The CHIT-Fc/CNTs modified GC electrode. After use, electrode was immersed into 0.1 M phosphate buffer solution (pH 7.0) for 5 min. The sulfite sensor showed a good electrocatalytic activity towards the oxidation of sulfite at peak potential less than 0.33 V. The resulting electrode provided a wide linear range between 5 μM - 1.5 mM and the detection limit was 2.8 μM (S/N = 3). In addition, the sensor has good stability and reproducibility were obtained.

In 2010, L.S.T. Alamo et al. [85] developed an amperometric sensor coupled with pervaporation-flow injection method based on copper hexacyanoferrate-carbon nanotube (CuHCF-CNT) modified carbon paste electrode for determination of sulfite in food products. In this work, CNT was purified using acid treatment in conc. HNO_3 and ultrasonication of 12 h. In addition, the CuHCF was prepared by mixing of 0.2 M $\text{Cu}(\text{NO}_3)_2$ and 0.1 M $\text{K}_4\text{Fe}(\text{CN})_6$. The solution was heated in a water bath until dry. After that, the resulting solid of CNT and CuHCF was mixed using various ratio compositions of graphite powder and mineral oil. Then the composites was mixed again in mortar and packed into the cavity of a tube with diameter 3.0 mm. Teflon tube with a stainless steel screw was served as the electrical contact. Before determination, the electrode surfaces was pressed using an oil-removing film for surface smooth. The modified electrode used as a working electrode in the amperometric flow-through cell in flow injection system. The method involved the injection of a standard or sample solution into a sulfuric acid donor stream to generate sulfur dioxide gas and evaporated into the headspace of the pervaporation unit. The amperometric detection of sulfite was a constant applied potential at +0.55 V (vs. Ag/AgCl). This sensor

provided linear calibration over the range of 0.5 – 50 ppm. The detection limit was 0.4 ppm. Sample throughput was 11 samples h⁻¹.

In 2013, X. Wang et al. [86] presented the development of an electrochemical sensor for the simultaneous determination of sulfite and nitrite based on gold nanoparticles/grapheme-chitosan (GR-CS/AuNPs) modified GC electrode. The dispersion was prepared by dispersing 1 mg of graphene in 1 mL of a 0.5 wt% chitosan solution (2% acetic acid) and the solution was stirred for 1 h until a homogeneous dispersion was obtained. Next, 10 µL of the composite solution was drop-casted into the clean GC electrode and dried at room temperature for 24 h. After that, The GR-CS modified electrode was immersed in a solution containing of 0.01 M K₂SO₄ and 0.04% HAuCl₄. The AuNPs were electrochemically formed on the surface of the GR-CS GC electrode via cyclic voltammetry. The potential was applied from -0.6 V to 1.5 V (vs. SCE) then the GR-CS/AuNPs/GCE was obtained. The results from electrochemical behaviors demonstrated that the long term stability, sensitivity and good detection range were obtained.

In 2014, M. Amatatongchai et al. [17] presented the development of simple flow injection system, which employed an amperometric detection based on CNTs-PDDA-AuNPs modified glassy carbon electrode for determination of sulfite in beverages. The CNTs was chemically shorten and carboxylated by acid treatment (H₂SO₄:HNO₃ 3:1) under ultrasonication for 5 h. After that, the suspension was centrifuged and washed several time with deionization water until the pH water was 7.0 and then dried at 110 °C. The CNTs was then functionalized with PDDA by stirring 10 mg of CNTs in 20 mL of a 0.25% PDDA aqueous solution containing of 0.5 M NaCl for 30 min. The resulting dispersion was centrifuged and washed with water to remove residual PDDA. The collected product was dispersed in 1 mL water and the solution was sonicated for 5 min before use. The CNTs-PDDA-AuNPs composites was prepared by dispersing the 0.5 mL of CNTs-PDDA (4 mg mL⁻¹) in 0.25% AuNPs solution and then solution was sonicated for 15 min. The negatively charged AuNPs was adsorbed on the positively charged CNTs-PDDA by electrostatic attraction. Finally, 40 µL of the CNTs-PDDA-AuNPs solution was casted on the surface of the cleaned GC electrode, and then dried at room temperature. The resulting electrode provided linear range from 2 – 200 ppm for sulfite ($r^2 = 0.998$) and the

detection limit was 0.03 ppm (3σ of blank). Sample throughput was 23 samples h^{-1} . Moreover, this method was successfully applied for detection of sulfite in real samples.

In 2015, E.M. Silva et al. [87] developed a voltammetric measurement of sulfite in commercial beverages based on CNTs modified carbon paste electrode. The CNTs suspension was prepared by dispersing in HNO_3 : H_2SO_4 3:1 at room temperature and then the suspension was centrifuged and washed several time with ultrapure water until the pH water was ~ 7.0 . Finally, the collected product was dried at $80\text{ }^\circ\text{C}$ for 24 h. hand-mixing of 5% CNTs and 55% graphite powder was performed in a mortar and pestle for 20 min. After that 40% mass mineral oil was added and mixed thoroughly. The mixture was grinded until this mixture homogeneously mixed to the carbon paste. This final the mixture was packed in a Teflon cylinder with internal diameter 3 mm containing a copper rod as an electrical contact. Teflon cylinder protects lateral parts of carbon paste from contact with supporting electrolyte solution. At the optimum condition, the modifying electrode provide a linear response to sulfite concentrations from 1.6 - 32 ppm with a limit of detection of 1.0 ppm. In addition, this modified electrode did not interfere from the other common beverage additives. The electrochemical behaviors demonstrated that the fast response for determination of sulfite in beverages was achieved.

CHAPTER 3 EXPERIMENTAL

3.1 Instrumentation

Equipments used in this work were list in table 3.11

Table 3.1 Instrumentation used for electrochemical measurements.

Instrument	Model	Company
Potentiostat	EA 161	eDAQ, Australia
e-corder	210	eDAQ, Australia
Data System	e-Chem (v2.0.13)	eDAQ, Australia
Ultrasonicator	CT360D	Scientific promotion
Working electrode	glassy carbon electrode (3 mm diameter)	CH Instrument, USA
Reference electrode	Ag/AgCl (3 M KCl)	CH Instrument, USA
Counter electrode	Pt wire	CH Instrument, USA
Stirrer	COLOR SQUID	Prodigy Science Instrument

3.2 Reagents and Chemicals

All chemicals used in this work were summarized in table 3.2

Table 3.2 List of reagents, grade and their suppliers.

Chemical and reagent	Grade	Suppliers
Carbon nanotubes (CNTs-COOH)	95% pure	Nanolab inc. (MA, USA)
Iron(II) chloride tetrahydrate (FeCl ₂ ·4H ₂ O)	AR	Carlo Erba
Iron(III) chloride hexahydrate (FeCl ₃ ·6H ₂ O)	AR	Carlo Erba
Nickel chloride (NiCl ₂)	Laboratory	ACROS ORGANICS
Hydrazine hydrate (NH ₂ NH ₂ ·H ₂ O)	AR	Carlo Erba
Ethylene glycol (C ₂ H ₆ O ₂)	> 99.75%	ACROS ORGANICS
Sodium sulfite (Na ₂ SO ₃)	ACS	Sigma-Aldrich
Glucose (C ₆ H ₁₂ O ₆)	ACS	Sigma-Aldrich
Sodium dihydrogen phosphate (NaH ₂ PO ₄)	Analysis	Carlo Erba
<i>N,N</i> -Dimethylformamide (C ₃ H ₇ NO)	AR	Sigma-Aldrich
di-Sodium hydrogen phosphate anhydrous (Na ₂ HPO ₄ ·H ₂ O)	Analysis	Carlo Erba
Fructose (C ₆ H ₁₂ O ₆)	AR	Sigma-Aldrich
Sucrose (C ₁₂ H ₂₂ O ₁₁)	AR	Sigma-Aldrich
Ascorbic acid (C ₆ H ₈ O ₆)	ACS	Sigma-Aldrich
Sodium chloride (NaCl)	ACS	Carlo Erba
Potassium iodide (KI)	ACS	Carlo Erba
Ethanol (C ₂ H ₅ OH)	ACS	Carlo Erba
Uric acid (C ₅ H ₄ N ₄ O ₃)	Laboratory	ACROS ORGANICS
Dopamine (C ₈ H ₁₁ NO ₂)	ACS	Sigma-Aldrich

3.3. Chemical preparation

Preparation of NiNPs.

Nickel nanoparticles (NiNPs) was synthesized through the reduction of nickel chloride by hydrazine hydrate as described by Wu's method [64]. The reaction was described by the following reaction equation,



In brief, 0.952 g of nickel chloride and 5.0 g of hydrazine hydrate were dissolved in 395.0 mL ethylene glycol. Then, 4.0 mL of 1.0 M sodium hydroxide solution was added into the solution. The solution was further stirred in a capped flask for 1 h at 60°C. The obtained black Ni nanoparticles (NiNPs) was washed thoroughly with ethanol and dried at 60°C for 24 h. NiNPs were obtained as a black powder.

Preparation of Fe₃O₄-CNTs nanocomposites.

Fe₃O₄-CNTs nanocomposite was prepared according to a methods described previously by Teymourian *et al.* [41] with a slightly modification. The Fe₃O₄-CNTs nanocomposite was synthesized under N₂ atmosphere. 20 mg of carboxylated carbon nanotubes (CNTs-COOH) were dispersed in 20 mL of distilled water using an ultrasonic bath for 20 min. Then 30 mg of FeCl₃·6H₂O was added under vigorous stirring. The mixture was stirred further for 30 min. 40 mg of FeCl₂·4H₂O was added and the mixture was stirred continuously for 30 min. 2 mL of solution prepared from diluted concentrated NH₃ with 10 mL of deionized water was slowly added into the mixture. The solution was then heated at 60°C for another 2 h. Fe₃O₄-CNTs nanoparticles were separated using an external magnetic field, then washed with ethanol and deionized water. After drying in a desiccator, Fe₃O₄-CNTs nanoparticles were obtained as powder.

Preparation of the Fe₃O₄-CNTs-NiNPs nanocomposites.

Fe₃O₄-CNTs-NiNPs nanocomposites was firstly prepared by dispersing 2 mg of Fe₃O₄-CNTs into 1.0 mL of aqueous solution containing 1% DMF and ultrasonicated for 30 min. After that, 2 mg NiNPs was added into the resulting dispersion and ultrasonicated for 30 min. Finally, homogeneous Fe₃O₄-CNTs-NiNPs dispersion was obtained and the solution was sonicated for 5 min before use.

0.1 M Glucose solution

0.1 M Glucose solution was prepared by dissolving 0.450 g of glucose in deionized water and diluting to 25 mL in a volumetric flask.

0.1 M sulfite solution

Solution of 0.1 M sulfite solution was prepared by dissolving 0.3151 g of sodium sulfite (Na_2SO_3) in deionized water and diluting to 25 mL in a volumetric flask.

1% Dimethylformamide (DMF)

Solution of 1% DMF was prepared by pipetting 0.2 mL of 99.99% DMF and diluting with deionized water to 20 mL in a volumetric flask.

0.1 M NaOH solution

2 g of sodium hydroxide was dissolved with deionized water to 500 mL in a beaker.

0.1 M (Na_2HPO_4) solution

14.20 g of di-sodium hydrogen phosphate (Na_2HPO_4) was dissolved and diluted with deionized water to 1000 mL in a volumetric flask

0.1 M (NaH_2PO_4) solution

13.80 g of sodium dihydrogen phosphate monohydrate ($\text{NaH}_2\text{PO}_4 \cdot \text{H}_2\text{O}$) was dissolved and diluted with deionized water to 1000 mL in a volumetric flask.

0.1 M Phosphate buffer pH 7.0

0.1 M Phosphate buffer pH 7.0 was prepared by mixing 58.7 mL of 0.1 M Na_2HPO_4 and 41.3 mL of 0.1 M $\text{NaH}_2\text{PO}_4 \cdot \text{H}_2\text{O}$, then the mixture was adjusted to pH 7.0.

3.4 Electrode preparation**Preparation of the Fe_3O_4 -CNTs-NiNPs modified GC electrode**

Prior to the electrochemical experiments, glassy carbon (GC) electrodes (diameter of 3 mm, from CH Instrument inc.) were polished using 1.0, 0.3 and 0.05 μm alumina slurry, successively. The electrode was rinsed with distilled water and the sonicated in deionized water of 5 min to remove residual abrasive particles. Fe_3O_4 -CNTs-NiNPs/GC electrode was prepared by casting 40 μL of the Fe_3O_4 -CNTs-NiNPs dispersion (2 mg mL^{-1}), mentioned above, on the surface of the polished glassy

carbon (GC) electrode, and then left to dry at room temperature. Figure 3.1 shows diagram for preparation of $\text{Fe}_3\text{O}_4\text{-CNTs-NiNPs/GC}$ electrode.

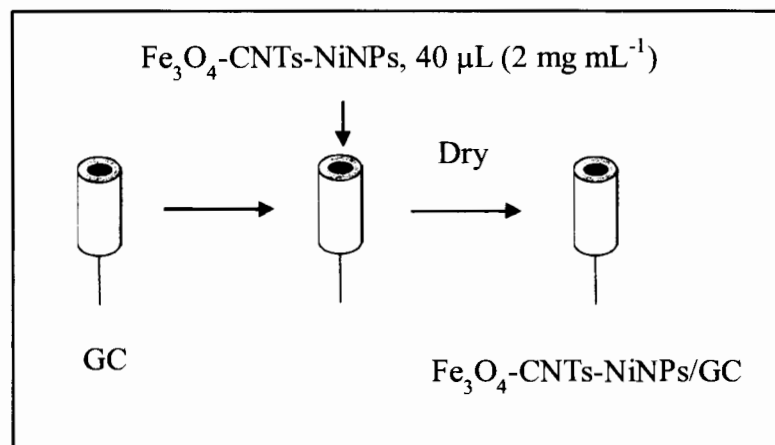


Figure 3.1 Schematic diagram of preparation steps for the chemical sensor modification ($\text{Fe}_3\text{O}_4\text{-CNTs-NiNPs/GC}$).

3.5 Measurement procedures

3.5.1 Voltammetry and amperometric detection

An eDAQ potentiostat (model EA 161) equipped with e-Corder (model 210) with three electrodes system was used for all the voltammetric and amperometric studies. Electrochemical oxidation of glucose and sulfite were studied at the developed chemical sensor. The modified electrode ($\text{Fe}_3\text{O}_4\text{-CNTs-NiNPs/GC}$) was used as a working electrode, Ag/AgCl as a reference electrode and Pt wire as an auxiliary electrode. Solution of 0.1 M NaOH and 0.1 M phosphate buffer pH 7.0 were used as supporting electrolytes for glucose and sulfite detection, respectively. Figure 3.2 showed the setup of the system used for all of the electrochemical studies.

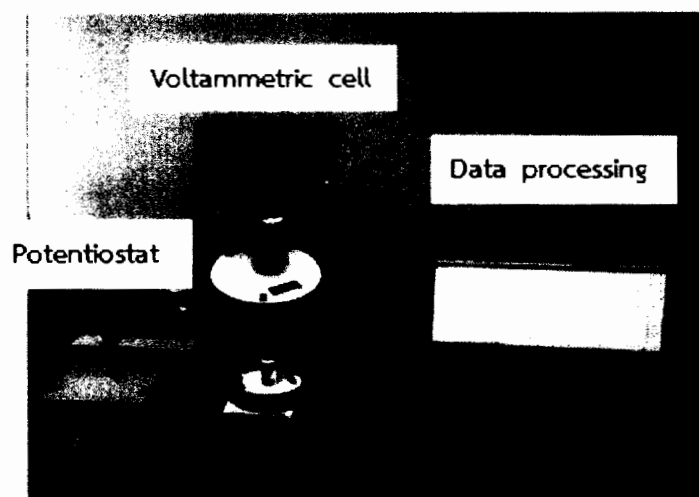


Figure 3.2 Photograph of the set up for electrochemical measurements using a potentiostat (eDAQ) data processing and a voltammetric cell.

3.6 Sample preparation

3.6.1 Sample preparation for glucose detection

Samples of energy drink and honey were employed in method validation for glucose determination. Those products were bought from local supermarket in Ubon Ratchathani province. A picture of sample used in this work is shown in Figure 3.3. The energy drink and honey were diluted 500 and 1000 times with 0.1 M sodium hydroxide pH 13.0 before the measurement using the developed method.



Figure 3.3 Sample of energy drinks (100 plus, Sponsor be fresh and Sponsor active) and honeys (Vejpong, Good.b and Floral longan honey).

3.6.2 Sample preparation of sulfite detection

All commercial products of wine, pickled mustard green and pickled garlic were employed in method validation for sulfite determination. Picture of samples used in this work, shown in Figure 3.4. Those samples were bought from supermarket in Ubon Ratchathani province. Prior to the analysis, wine samples were filtered with 0.45 μm syringe filter. Then sample 19 mL was added into 20 mL volumetric flask and diluted with 1.0 M phosphate buffer pH 7.0. For food samples (pickled mustard green and pickled garlic samples) liquid extraction was applied to extract sulfite from sample matrices. The sample was chopped, and a portion of 50 g was transferred to a blender and then 50 mL of 0.1 M phosphate buffer pH 7.0 was added. After that, the sample and extraction solvent were blended vigorously until the homogenized sample was obtained. After that the collected residual solution and centrifuge at 4,000 rpm. The supernatant clear solution of sample was collected and 10 mL was added into 20 mL volumetric flask and diluted with 0.1 M phosphate buffer pH 7.0.



Figure 3.4 Sample of wines (Boones pina colada, Boones cheek berry and Fresco berry red), pickled mustard green (Songheng, Songpueng and House wife) and pickled garlic (Ma jin, Big C and Vanusnun), respectively.

3.7 Procedure

3.7.1 Characterization of the nanocomposites

3.7.1.1 Transmission Electron Microscopy (TEM)

The morphology of the nanocomposites modified electrode (CNTs, NiNPs, Fe₃O₄-CNTs and Fe₃O₄-CNTs-NiNPs) surface was study with the transmission electron microscopy. The TEM model: JEM-1230; JEOL from Japan as shown in Figure 3.5. The TEM samples were prepared by dispersing the nanocomposites in de-ionized water with ultrasonicated for 1 h and then drying a drop of the suspension on a copper grid. Results are presented in Section 4.3.1.

3.7.1.2 X-ray Diffraction (XRD)

X-ray diffraction (XRD) is an important technique to identify the crystal structure of nanocomposites. In this work, X-ray diffractometer model X' Pert MPD, Philip in Finland as shown in Figure 3.6 was used to characterize the as-prepared nanocomposites. The XRD patterns of NiNPs, Fe₃O₄-CNTs and Fe₃O₄-CNTs-NiNPs was obtained by studied with a Siemens D5000 diffractometer with Cu K_α monochromatized radiation source, operated at 40 kV and 100 mA The XRD pattern was recorded from 20° to 80° at a scanning rate of 4° min⁻¹. Results are discussed in Section 4.3.2.

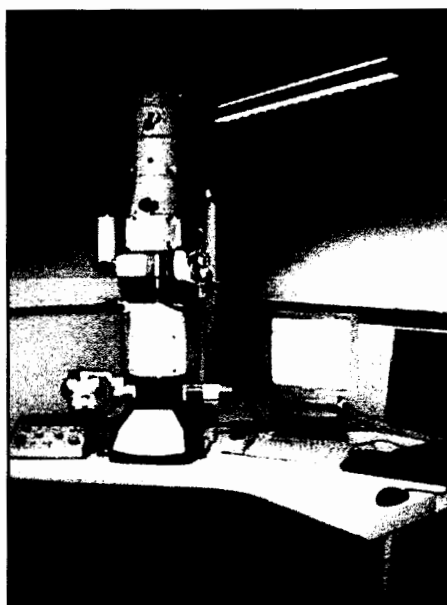


Figure 3.5 Transmission electron microscope (JEM-1230; JEOL).



Figure 3.6 X-ray diffractometers (X' Pert MPD, Philip).

3.7.2 Development of glucose chemical sensor based on Fe_3O_4 -CNTs-NiNPs/GC

3.7.2.1 Cyclic voltammetric study of glucose oxidation

The unique electrochemical behavior of glucose oxidation was studied at different modified electrode materials. The cyclic voltammograms at the bare GC (a) and modified electrodes of NiNPs/GC (b), Fe_3O_4 /GC (c), Fe_3O_4 -CNTs/GC (d), NiNPs-CNTs/GC (e) and Fe_3O_4 -CNTs-NiNPs/GC (f) were investigated in 0.1 M sodium hydroxide solution and 4 mM glucose using cyclic voltammetry. Electrode codes for bare and modified glassy carbon electrodes are shown in Table 3.3. The results were discussed in Section 4.2.1.

Table 3.3 Electrode codes for bare and modified glassy carbon electrodes.

Electrode code	Modified electrode
a	GC
b	NiNPs/GC
c	Fe ₃ O ₄ /GC
d	Fe ₃ O ₄ -CNTs/GC
e	NiNPs-CNTs/GC
f	Fe ₃ O ₄ -CNTs-NiNPs/GC

3.7.2.2 Studies of parameters that effect the sensitivity of glucose sensor

1) Effect of Fe₃O₄-CNTs-NiNPs modified amount on the detection of glucose

Optimization of the Fe₃O₄-CNTs-NiNPs modified amount was investigated using cyclic voltammetry to find the most sensitive condition for glucose detection. The Fe₃O₄-CNTs-NiNPs amount ranged from 2 to 8 mg mL⁻¹ in 1% DMF was used for modified electrode of Fe₃O₄-CNTs-NiNPs/GC. Results of Fe₃O₄-CNTs-NiNPs amount coated in GCE were illustrated in Section 4.2.2.

2) Effect of buffer pH (0.1 M sodium hydroxide)

The effect of pH on the performance of the Fe₃O₄-CNTs-NiNPs/GC for detection oxidation of glucose were varied at pH 9.0, 10, 11, 12, 13 and 14 using 0.1 M sodium hydroxide and adjust these pH with 0.1 M hydrochloric acid for using as supporting electrolyte. Cyclic voltammograms of glucose were recorded using electrolyte solution of varied pH. Results are presented in Section 4.2.3.

3.7.2.3 Scan rate dependence study

The cyclic voltammograms of anodic and cathodic peaks current of glucose on the glucose chemical sensor were examined in 0.1 M sodium hydroxide pH 13.0. The effect of various scan rate (0.03, 0.04, 0.05, 0.06, 0.08 and 0.09 V s⁻¹) on the voltammograms were investigated. The results are discussed in Section 4.2.4.

3.7.2.4 Concentration dependence study

The electrochemical behavior of glucose oxidation was studied at the developed glucose chemical sensor ($\text{Fe}_3\text{O}_4\text{-CNTs-NiNPs/GC}$) using cyclic voltammetry (CV). The modified electrode was used as a working electrode, Ag/AgCl as a reference electrode and Pt wire as a counter electrode. The variation of glucose concentration from 0 to 6 mM in 0.1 M sodium hydroxide (pH 13.0) was used as a supporting electrolyte. The results are presented in Section 4.2.5.

3.7.2.5 Amperometric detection of glucose

1) Optimum potential for amperometric detection

The effect of applied potential on amperometric response of 1 mM glucose oxidation were investigated. The applied potential was studied at 0.40, 0.45, 0.50, 0.55, 0.60, 0.65 and 0.70 V in 0.1 M sodium hydroxide solutions (pH 13.0). The results were discussed in Section 4.2.6.1

2) Linear concentration range

Calibration standards of glucose were studied by spike the appropriate amount of standard glucose solution in 15 mL of 0.1 M sodium hydroxide solutions (pH 13.0) to give working solutions in the range of 10 μM to 3.0 mM. Amperometric responses were recorded using an applied potential of +0.55 V and solution was stirred at 1,000 rpm. The results were shown in Section 4.2.6.2.

3) Limit of detection

In this study, the limit of detection was calculated from anodic current from glucose standard solution at a concentration of 0.02 mM (6 replicates). The signal value of 3 times of the standard deviation from 0.02 mM glucose was convert to limit of detection for glucose. Results were presented in Section 4.2.6.3.

4) Interference study

In this study, the effect of foreign ions that are likely to exist in the glucose samples were examined. The interested ions and compounds such as fructose, maltose, sucrose, carbonic acid, citric acid and sodium chloride were selected as the interferences. The concentration of the interferent species that provide a signal change greater than $\pm 5\%$ was considered as the tolerance limit. The results are discussed in Section 4.2.6.4.

5) Reproducibility and stability of developed glucose chemical sensor

The electrode-to-electrode reproducibility of Fe_3O_4 -CNTs-NiNPs/GC was investigated from the sensitivity of the calibration curve (0.5 to 2.0 mM) of five sensors. The repeatability of the electrode was estimated from six amperometric measurements of 0.5 mM glucose. The results are discussed in Section 4.2.6.5.

3.7.2.6 Application of the developed glucose sensor in real samples

The samples were diluted 500 and 1000 times with 0.1 M sodium hydroxide (pH 13.0) before measured using the developed method. Glucose concentration was examined by standard addition method. Results were presented in Section 4.2.6.6.

3.7.3 Development of sulfite sensor based on Fe_3O_4 -CNTs-NiNPs/GC

3.7.3.1 Cyclic voltammetric study of sulfite oxidation

The unique electrochemical behavior of sulfite oxidation was studied at different modified electrode materials. The cyclic voltammograms at the bare GC (a) and modified electrodes of NiNPs/GC (b), Fe_3O_4 /GC (c), CNTs/GC (d), Fe_3O_4 -CNTs/GC (e), NiNPs-CNTs/GC (f) and Fe_3O_4 -CNTs-NiNPs/GC (g) in 0.1 M phosphate buffer solution (pH 7.0) were investigated using cyclic voltammetry both with and without 4 mM sulfite. Electrode codes for bare and modified glassy carbon electrodes are shown in Table 3.4. The results discussed in Section 4.3.1.

Table 3.4 Electrode codes for bare and modified glassy carbon electrodes.

Electrode codes	Modified electrode
a	GC
b	NiNPs/GC
c	Fe_3O_4 /GC
d	CNTs/GC
e	Fe_3O_4 -CNTs/GC
f	NiNPs-CNTs/GC
g	Fe_3O_4 -CNTs-NiNPs/GC

3.7.3.2 Studies of parameters that effect the sensitivity of sulfite sensor

1) Effect of Fe₃O₄-CNTs-NiNPs modified amount on the detection of sulfite

Optimization of the Fe₃O₄-CNTs-NiNPs modified amount was investigated using cyclic voltammetry to find the most sensitive condition for sulfite detection. The Fe₃O₄-CNTs-NiNPs amount ranged from 2 to 8 mg mL⁻¹ in 1% DMF was used to modify of the electrode. Results of Fe₃O₄-CNTs-NiNPs amount coated in GCE were illustrated in Section 4.3.2.1.

2) Effect of buffer pH (0.1 M phosphate buffer solution)

The effect of buffer pH on the performance of the Fe₃O₄-CNTs-NiNPs/GC for sulfite detection were studied over the range of 5.0-8.5 using 0.1 M phosphate buffer solution as supporting electrolyte. Cyclic voltammograms of sulfite were recorded using electrolyte solution of varied pH. Results were presented in Section 4.3.2.2.

3.7.3.3 Scan rate dependence study

The cyclic voltammograms of sulfite on the sulfite sensor were examined in 0.1 M phosphate buffer solution (pH 7.0). This cyclic voltammograms using various scan rate over range from 0.01 - 0.09 V s⁻¹ were investigated. The results were discussed in Section 4.3.3.

3.7.3.4 Concentration dependent study

The electrochemical behavior of sulfite oxidation was studied at the developed sulfite sensor (Fe₃O₄-CNTs-NiNPs/GC) using CV. The modified electrode was used as a working electrode, Ag/AgCl as a reference electrode and Pt wire as a counter electrode in 0.1 M phosphate buffer solution pH 7.0 as a supporting electrolyte. The results were presented in Section 4.3.4.

3.7.3.5 Linear sweep votammetric detection of sulfite

1) Linearity

Calibration standards of sulfite were studied by spiking the appropriate amount of standard sulfite solution in to 15 mL of 0.1 M phosphate buffer solution (pH 7.0) to give a working concentration in the range of 0.1 to 10 mM. Linear sweep voltamograms were recorded using an applied potential from 0 to 1.0 V at scan rate 20 mV s⁻¹. The results were shown in Section 4.3.5.1

2) Limit of detection

In this study, the limit of detection was calculated from anodic peak current of sulfite standard solution at a concentration of 0.1 mM. The signal value of 3 times of the standard deviation from signal of 0.1 mM sulfite standard solution was calculated as limit of detection for glucose. Results were presented in Section 4.3.5.2.

3) Interference study

In this study, the effect of foreign ions that are likely to exist in the sulfite samples were examined. The interested ions and compounds such as glucose, sucrose, maltose, fructose, ethanol, ascorbic acid, sodium chloride, sodium sulfate and sodium carbonate were selected as the interferences. The concentration of the interferent species that provide a signal change greater than $\pm 5\%$ was considered as the tolerance limit. The results were discussed in Section 4.3.5.3.

4) Stability of sulfite chemical sensor

The stability of the $\text{Fe}_3\text{O}_4\text{-CNTs-NiNPs/GC}$ electrode for detection of sulfite oxidation was studied. The modified electrode was stored in room temperature when not use. The anodic current of sulfite were measured at a $\text{Fe}_3\text{O}_4\text{-CNTs-NiNPs/GC}$ electrode when stored for 0, 1, 2, 3, 4, 5, 6, 7, 15 and 21 days. Results were presented in Section 4.3.5.4.

3.7.3.6 Application of developed sulfite chemical sensor in real samples

Standard method for sulfite quantitation (iodometric titration method).

The iodometric titration of sulfite was performed according to the Association of Official Agricultural Chemists (AOAC) method. A back titration was used to avoid sulfite loss in the form of SO_2 in acidic environment. 5 mL of standard potassium iodate (KIO_3) 0.00021 M was added in the 250 mL conical flask followed by 2.5 mL of 3 M sulfuric acid (H_2SO_4). Then 2.5 mL of 0.15 M potassium iodide (KI) was pipetted into the conical flask and 5.0 mL of sample was added. After that, this mixture solution was immediately titrated with 0.0025 M sodium thiosulfate ($\text{Na}_2\text{S}_2\text{O}_3$) to a light yellow color. Then 0.5 mL of starch indicator was added and continued the titration until the iodine-starch complex become colorless.

The samples were dilute with 0.1 M phosphate buffer solution pH 7.0 before measurement using the developed method. The sulfite concentration was calculated by standard addition method. Results were presented in Section 4.3.5.5.

CHAPTER 4

RESULTS AND DISCUSSION

4.1 Characterization of the synthesized nanocomposites

4.1.1 Transmission electron microscopy (TEM)

In this thesis, the morphology of the different synthesized composites was studied by transmission electron microscopy (TEM) and X-ray diffraction (XRD). The TEM samples were prepared by dispersing the nanocomposites in de-ionized water with ultrasonicator and then drying a drop of the dispersion on a copper grid. Fig. 4.1 (a-d) showed TEM images of a) the fine nanotubular morphology of CNTs-COOH at the light grey region, b) a homogenous dispersion of NiNPs. In this work NiNPs were prepared by reduction of Ni^{2+} by hydrazine in the presence of ethylene glycol, as a stabilizing agent [63]. The average diameter of synthesized NiNPs was 21.6 ± 3.2 nm (count = 50). The TEM images of Fe_3O_4 -CNTs (Fig. 4.1c)) indicated that a lot of Fe_3O_4 nanoparticles have been surrounded on the surface of the carbon nanotubes. The TEM image of Fe_3O_4 -CNTs-NiNPs (Fig. 4.1 d) shows a typical deposition of Fe_3O_4 and NiNPs on the surface of CNTs nanotubular structure. The average diameter of the nanoparticles synthesized on CNTs surface was estimated to be 20.3 ± 1.6 nm (count = 50), and the nanoparticles tends to homogeneously dispersed all over the CNTs tubes.

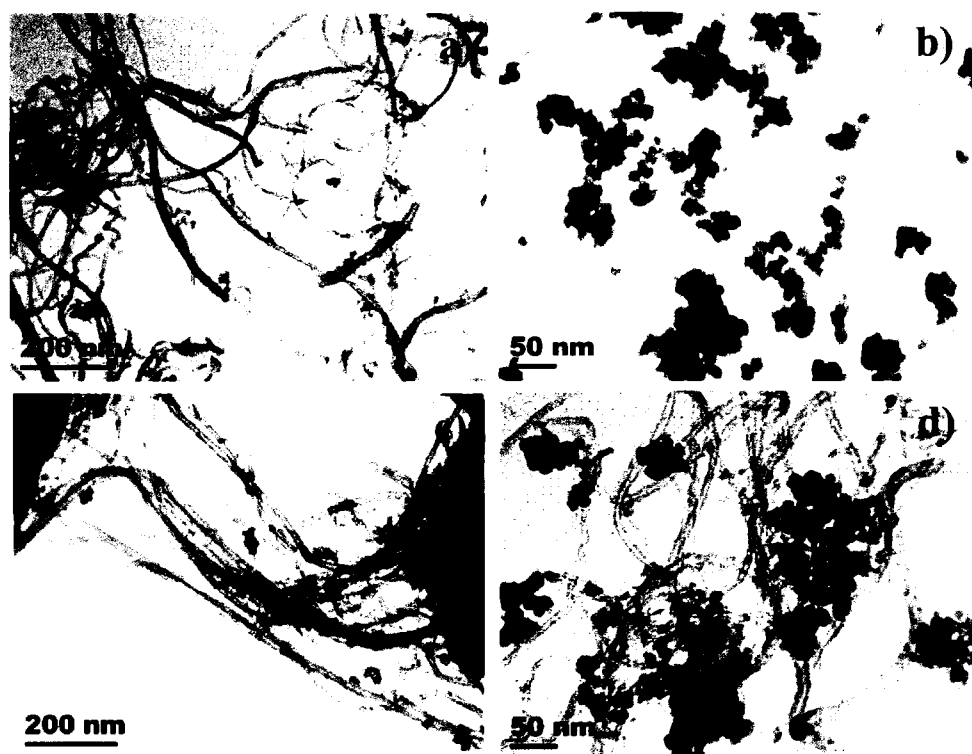


Figure 4.1 TEM images of a) CNTs, b) NiNPs, c) Fe_3O_4 -CNTs and d) Fe_3O_4 -CNTs-NiNPs.

4.1.2 X-ray diffraction

Figure 4.2 shows the X-ray diffraction patterns of NiNPs, Fe_3O_4 -CNTs and Fe_3O_4 -CNTs-NiNPs obtained under our synthesis conditions. The three well-resolved peaks at 2θ of approximately 44.7° , 52.1° and 76.6° was assigned to the (111), (200) and (220) planes of pure fcc nickel, which accorded to the previous report [64, 67]. This suggests that the as-prepared nanoparticles are nickel nanoparticles. XRD patterns for the Fe_3O_4 -CNTs is observed the peaks at 2θ of approximately 30.4° , 35.7° , 43.6° , 57.8° and 63.4° that were marked by their indices (220), (311), (400), (511) and (440), correspond to the spinel structure of magnetite phase [5, 31], (JCPDS No. 82-15330). The XRD pattern of Fe_3O_4 -CNTs-NiNPs displayed indices corresponding peaks for both NiNPs and Fe_3O_4 which is indicated formation of Fe_3O_4 and NiNPs decorated on the CNTs.

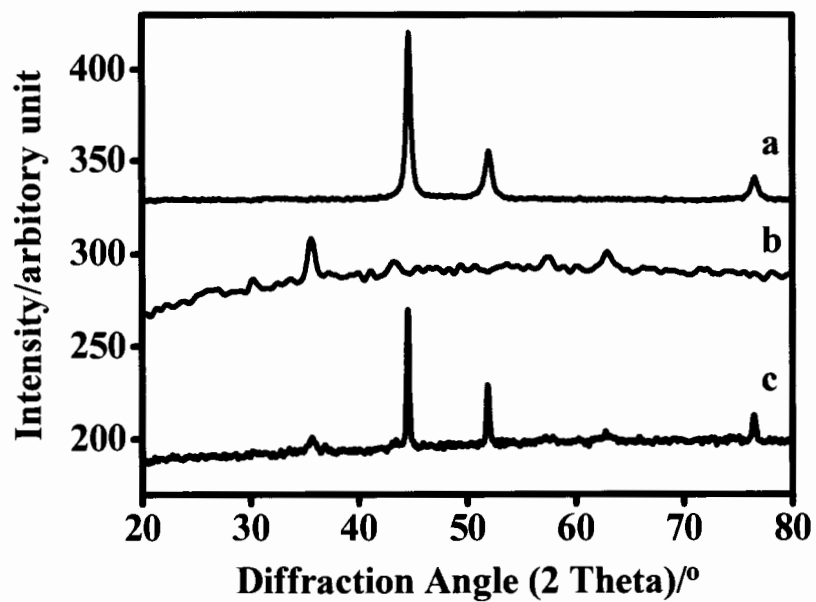
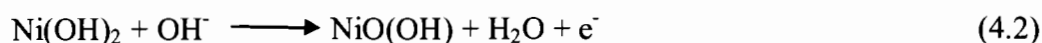
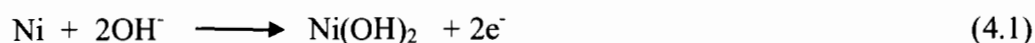


Figure 4.2 XRD patterns of, a) NiNPs, b) Fe₃O₄-CNTs and c) Fe₃O₄-CNTs-NiNPs nanocomposites.

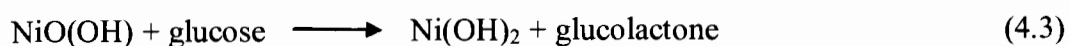
4.2 Development of glucose sensor based on Fe₃O₄-CNTs-NiNPs/GC

4.2.1 Cyclic voltammetric study of glucose oxidation

The electrochemical behavior of glucose at various modified electrodes (bare GC, NiNPs/GC, Fe₃O₄/GC, Fe₃O₄-CNTs/GC, CNTs-NiNPs/GC and Fe₃O₄-CNTs-NiNPs/GC) were examined by CV. Results in Figure 4.3 showed the cyclic voltammograms for different electrodes in 0.1 M NaOH (dash line) with containing 4 mM glucose (solid line). According to Figure 4.3, bare GC, NiNPs/GC, Fe₃O₄/GC, Fe₃O₄-CNTs/GC were not shown well defined redox peaks at a potential range of 0-0.8 V while NiNPs-CNTs/GC and Fe₃O₄-CNTs-NiNPs/GC displayed a pair of well-defined redox peak, which can be assigned to the electrochemical redox reaction of Ni(II)/Ni(III) couple on the electrode surface in the alkaline medium, which accorded to the previous report [70, 71] However, the electrode modified with only NiNPs produced very small current. The Fe₃O₄-CNTs-NiNPs/GC electrode shows much larger peak currents than that of NiNPs-CNTs/GC. This result reveals that electrochemical performance of the hybrid nanocomposites is greatly enhanced compared to its individual counterparts. Fe₃O₄-CNTs-NiNPs/GC provided a pair of well-defined redox peaks, an anodic peak at +0.54 V and a cathodic peak at +0.32 V, respectively. The couple of peaks are corresponding to the Ni(II)/Ni(III) can be described by the following reactions [70, 71]:



Glucose oxidation is an electrochemically irreversible process. The enhancement of anodic current obtained from this chemical sensor (Fe₃O₄-CNTs-NiNPs/GC) is attributed to the electro-oxidation of glucose with the participation of Ni (III) may be as the following process:



In this study, the Fe₃O₄-CNTs-NiNPs/GC which provided the highest sensitive and selective for glucose detection was selected as the optimum modified electrode.

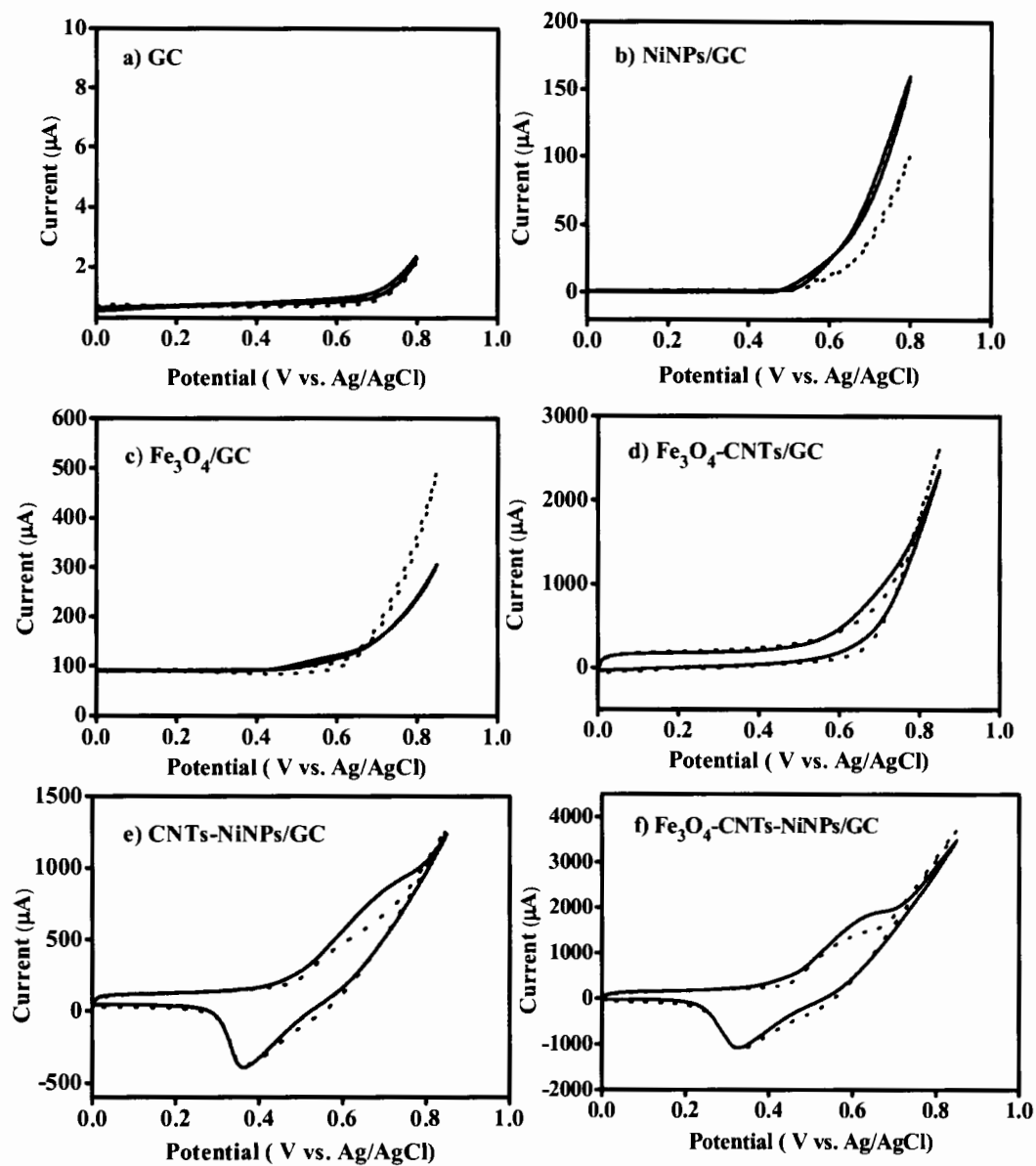


Figure 4.3 Cyclic voltammogram of a) bare glassy carbon electrode (GC), b) NiNPs/GC, c) Fe_3O_4 /GC, d) Fe_3O_4 -CNTs/GC, e) CNTs-NiNPs/GC and f) Fe_3O_4 -CNTs-NiNPs/GC electrodes in 0.1 M sodium hydroxide solution, pH 13.0 (dashed line) and in 4 mM glucose (solid line), scan rate 0.05 V s^{-1} .

4.2.2 Effect of Fe_3O_4 -CNTs-NiNPs modified amount on the detection of glucose

The effect of Fe_3O_4 -CNTs-NiNPs loading from 2 to 8 mg mL^{-1} used for electrode modification on the oxidation peak current of glucose was investigated. As show in Figure 4.4 the current response increased with increasing amount of Fe_3O_4 -CNTs-NiNPs from 2 to 4 mg mL^{-1} . This result assumed that increasing of Fe_3O_4 -CNTs-NiNPs amount can be improve the electro-conductivity and enhance active surface area of the nanocomposite. The current response a slightly decreased at the modified concentration above 4 mg mL^{-1} . Therefore, 4 mg mL^{-1} Fe_3O_4 -CNTs-NiNPs was chosen as the optimum concentration for modified electrode in the further experiments.

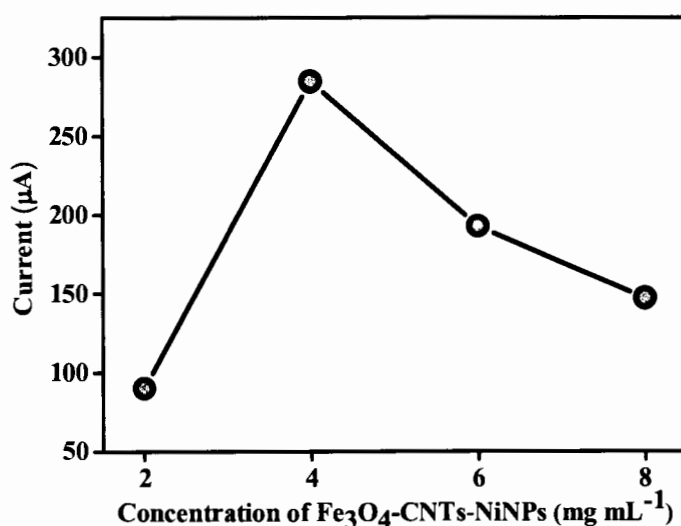


Figure 4.4 The effect of the concentration of Fe_3O_4 -CNTs-NiNPs (mg mL^{-1}) on the oxidation peak current of 4 mM glucose in 0.1 M sodium hydroxide solution (pH 13.0).

4.2.3 pH dependence study (0.1 M sodium hydroxide solution)

The influence of the pH is very important for sensitivity of the glucose sensor and catalytic activity of NiNPs [68, 69]. The effect of pHs on the developed sensor ($\text{Fe}_3\text{O}_4\text{-CNTs-NiNPs/GC}$) was investigated over the range of pH 9.0 to 14.0 using 0.1 M sodium hydroxide solution as supporting electrolyte. Figure 4.7 shown the oxidation current of 1 mM glucose at various pHs values in alkaline condition. The result showed that anodic peak current of glucose were not well define oxidation peaks at pH lower than 12.0 at the studied potential from 0 – 0.8 V. When increasing the concentrate presence of OH^- anions the anodic peak current was increased from pH 12.0 to 13.0 and once pH 14.0, it began to decrease. So the optimum pH for the electro-catalytic detection of glucose was determined to pH 13.0 it gave the highest current response. The result indicated that NiO(OH) electro catalytic activity is highly dependent on the concentrated presence of hydroxyl anions OH^- more than low or neutral pH solution. The oxidation potential was shift to more positive potential and the anodic peak currents was decreased when as pH is decreased. This result accorded to the previous report [68, 69]. There for we used 0.1 M sodium hydroxide solution at pH 13.0 for enhanced sensitivity of glucose sensor.

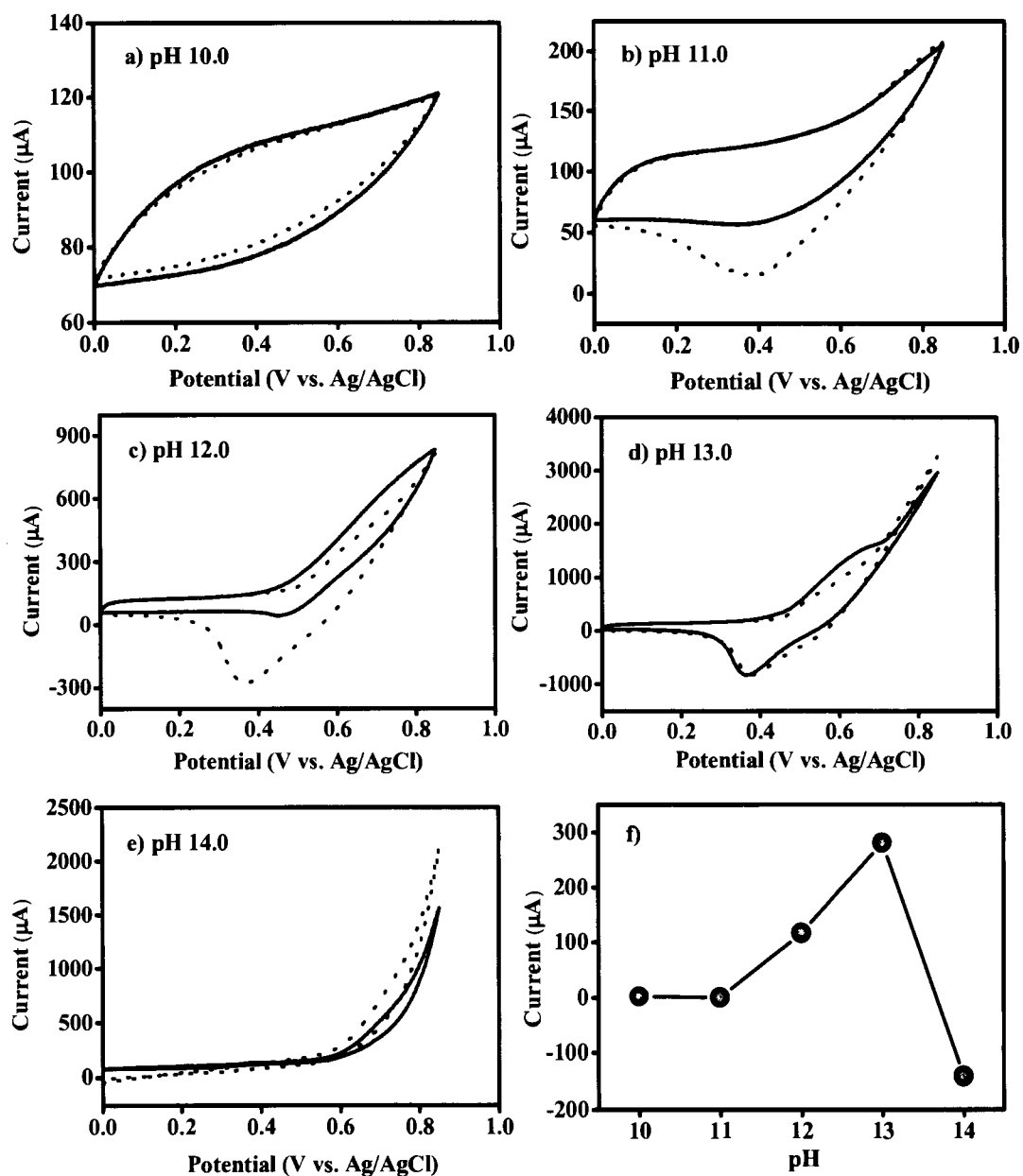


Figure 4.5 Cyclic voltammograms of $\text{Fe}_3\text{O}_4\text{-CNTs-NiNPs/GC}$ electrode at various sodium hydroxide solution a) pH 10.0, b) pH 11.0, c) pH 12.0, d) pH 13.0, e) pH 14.0 and f) peak current obtained from the chemical sensor in the presence of 1 mM glucose (solid line), scan rate 0.05 V s^{-1} .

4.2.4 Scan rate dependence study

The influence of scan rate at $\text{Fe}_3\text{O}_4\text{-CNTs-NiNPs/GC}$ electrode was investigated in 0.1 M NaOH solution (pH 13.0) containing 0.5 mM glucose at different scan rates of 0.03-0.09 V s^{-1} . The results are displayed in Figure 4.6. It can be observed in Figure 4.6a that the anodic peak current ($I_{p,a}$) and cathodic peak current ($I_{p,c}$) of glucose increased with increasing scan rates while the anodic and cathodic peak potential shift to a more positive potentials (from 0.54 to 0.70 V and 3.20 to 2.10 V), respectively. Also, 4.5b) peak currents (μA) for both the oxidation and the reduction were linearly proportional to the square root of scan rate ($\text{V}^{1/2} \text{ s}^{-1/2}$) were found to be linear in the range from 0.03-0.09 V s^{-1} . The linear regression equations were $I_{p,a} = 2327.55 v^{1/2} + 1.60$ ($r^2 = 0.994$) and $I_{p,c} = -6625.05 v^{1/2} + 487.13$ ($r^2 = 0.993$), respectively. This result indicated a diffusion-controlled process at the $\text{Fe}_3\text{O}_4\text{-CNTs-NiNPs/GC}$ electrode, which accorded to the previous report [80].

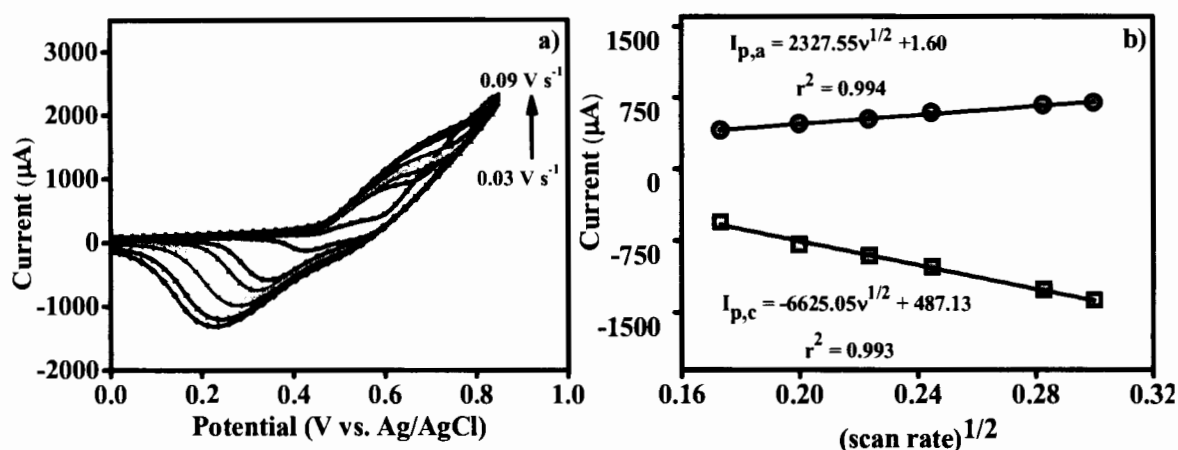


Figure 4.6 a) Cyclic voltammogram of $\text{Fe}_3\text{O}_4\text{-CNTs-NiNPs/GC}$ electrode for 0.5 mM glucose in 0.1 M sodium hydroxide solution (pH 13.0) with the variation of scan rate ranging from 0.03 to 0.09 V s^{-1} . b) linear relationship is the plot of the anodic ($I_{p,a}$) and cathodic peak current ($I_{p,c}$) versus the square root of the scan rate.

4.2.5 Concentration dependence study

The electrochemical behavior of glucose oxidation was studied at the developed chemical glucose sensor ($\text{Fe}_3\text{O}_4\text{-CNTs-NiNPs/GC}$) using cyclic voltammetry (CV). Glucose concentration was examined from 0 to 6 mM. Figure 4.7a displayed cyclic voltammograms of $\text{Fe}_3\text{O}_4\text{-CNTs-NiNPs/GC}$ electrode in the absence and presence of different glucose concentration in 0.1 M NaOH solution under the optimum conditions. It can be observed that by increasing the glucose concentration, the oxidation peak current increased and the potential shifted to a more positive value, demonstrating the good catalytic effect of the Ni(II)/Ni(III) redox couple in glucose oxidation. This potential was similar to previous work reported by [70, 72]. Linear calibration ($r^2 = 0.999$) was obtained with the slope of $128.31 \mu\text{A}\cdot\text{mM}^{-1}$. These results have demonstrated that the $\text{Fe}_3\text{O}_4\text{-CNTs-NiNPs/GC}$ electrode is appropriate for the quantitation of glucose.

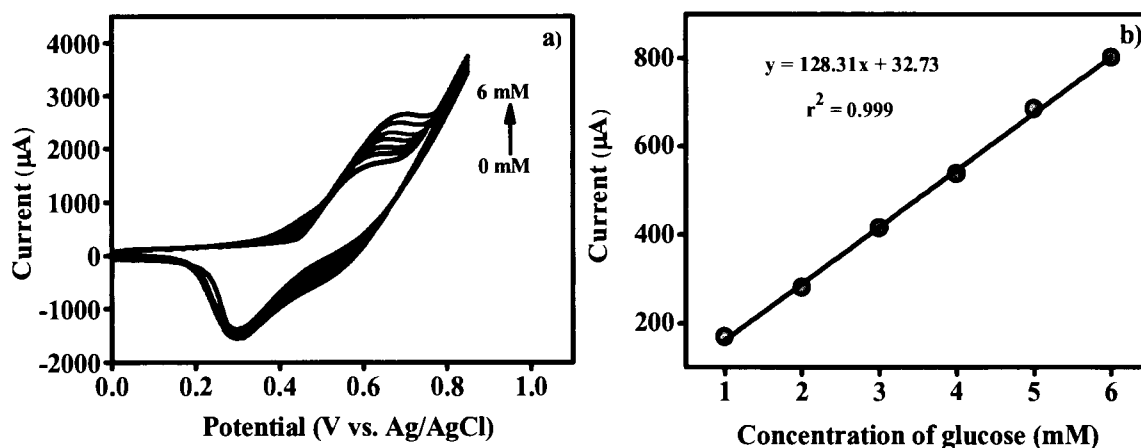


Figure 4.7 a) Cyclic voltammogram of glucose in 0.1 M NaOH with the variation of glucose concentration from 0 to 6 mM and b) Calibration plot of anodic peak currents versus glucose concentration.

4.2.6 Amperometric detection of glucose

4.2.6.1 Optimum potential for amperometric detection

The applied potential is an important parameter in amperometry because it strongly affects the size of the current signal of an analyte. The proposed amperometric method for detection of glucose is based on the electrochemical monitoring of the oxidation signal from glucose at the $\text{Fe}_3\text{O}_4\text{-CNTs-NiNPs/GC}$ electrode. In this study, we investigated the optimal potential for amperometric detection at the electrode over the potential range from 0.40 to 0.70 V. As shown in Figure 4.8, the anodic current response increases rapidly from 0.45 to 0.55 V, and then decreased from 0.55 to 0.70 V. The potential at 0.55 V (versus Ag/AgCl) provided the maximum anodic current response of and thus, it was used this optimal voltage for amperometric detection.

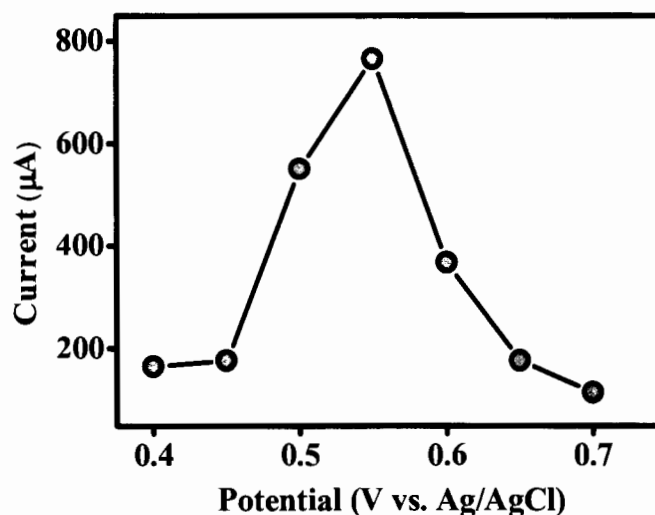


Figure 4.8 Anodic current of $\text{Fe}_3\text{O}_4\text{-CNTs-NiNPs/GC}$ electrode at different potentials from 0.40 V to 0.70 V upon addition of 1 mM glucose to 0.1 M sodium hydroxide solution (pH 13.0).

4.2.6.2 Linear concentration range

The amperometric response at the developed glucose sensor ($\text{Fe}_3\text{O}_4\text{-CNTs-NiNPs/GC}$) was investigated by successive addition of glucose standard in a continuously stirred of 0.1 M sodium hydroxide solution (15 mL, pH 13.0). Figure 4.9 displayed the amperometric signals corresponding to its calibration plot at optimal potential of 0.55 V. As shown in Figure 4.9 a) the anodic current increased with increasing the concentration of glucose ranging from 10 μM to 3.0 mM. The developed chemical sensor showed very fast current responses ($\sim 5\text{s}$) indicated that the electrode is very sensitive to glucose. As shown in Figure 4.9 b) the linear response range of the developed chemical sensor for glucose concentration was from 10 μM to 1.8 mM. The result demonstrated the regression equation $y = 335.246x + 11.812$ ($r^2 = 0.998$).

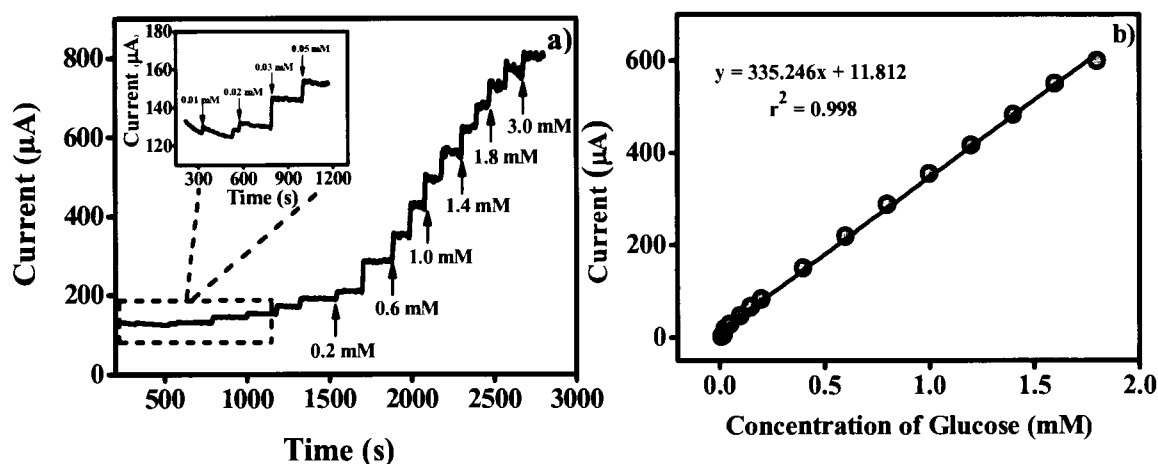


Figure 4.9 a) Typical amperometric *i-t* curve of $\text{Fe}_3\text{O}_4\text{-CNTs-NiNPs/GC}$ electrode to successive additions of glucose solution into a stirred system of 0.1 M sodium hydroxide solution (pH 13.0) at 0.55 V. b) The linear calibration plot of the corresponding oxidation peak current versus glucose concentration.

Table 4.1 provides a comparison of the analytical characteristics of the $\text{Fe}_3\text{O}_4\text{-CNTs-NiNPs/GC}$ with related modified electrodes from the literature. The analytical characteristics of developed glucose sensor are comparable to, or better than, those reported for other nanomaterial based-glucose sensor designs. Additionally, the applied potential for developed sensor is lower [80, 90, 96], or comparable to, those in previous reports [82, 89, 91, 93, 94]. Moreover, the use of the $\text{Fe}_3\text{O}_4\text{-CNTs-NiNPs/GC}$ electrode offers a higher sensitivity [80, 82, 88, 89, 92-96], or comparable [90] to those previously reported values for other modified electrodes. The developed sensor provides a satisfying wide range of linearity and low detection limit.

Table 4.1 Response characteristics of the $\text{Fe}_3\text{O}_4\text{-CNTs-NiNPs/GC}$ electrode and other non-enzymatic glucose sensors.

Electrode	E_{app} (V)	Sensitivity ($\mu\text{A mM}^{-1}$)	Linear range (mM)	Detection limit (μM)	Ref.
$\text{MnO}_2/\text{CNTs}^{\text{a}}$	0.30	33.19	0.01-28	-	[88]
$\text{RGO-Ni(OH)}_2^{\text{b}}$	0.54	11.43	0.002-3.1	0.6	[89]
$\text{CS-RGO-NiNPs}^{\text{c}}$	0.60	318.4	0.2-9	4.1	[90]
$\text{Ni/NiO-GP}^{\text{c}}$	0.55	1997	0.029-6.4	1.8	[91]
NiO-GP^{b}	0.35	7.57	0.02-4.5	5	[92]
$\text{Ni(OH)}_2/\text{TiO}_2^{\text{d}}$	0.50	192	0.03-14	8	[93]
Ni nanowires ^b	0.55	131.1	0.0005 – 7	0.1	[94]
Ni(OH)_2 nanoflowers ^b	0.49	265.3	0.1-1.1	0.5	[95]
$\text{Cu nanoclusters/CNTs}^{\text{b}}$	0.65	17.8	0.0007 – 3.5	0.21	[96]
$\text{Ni-CNTs}^{\text{b}}$	0.60	67.2	0.003 – 17.5	0.89	[80]
$\text{Ni/Cu/CNTs}^{\text{b}}$	0.58	186.2	0.00003 – 0.8	0.03	[82]
$\text{Fe}_3\text{O}_4\text{-CNTs-Ni}^{\text{b}}$	0.55	335.3	0.01-1.8	6.7	This work

RGO-Ni(OH)_2 = reduced graphene oxide assembled with Ni(OH)_2 nanoplates, CS = chitosan, RGO = reduced graphene oxide, NiNPs= nickel nanoparticles, GP = Graphene, E_{pp} = applied potential, ^aCarbon nanotubes electrode (CNTsE), ^bGlassy Carbon Electrode (GCE), ^cScreen Printed Electrode (SPE), ^dNiTi alloy sheet

4.2.6.3 Limit of detection

The limit of detection was determined by measuring signal of successive addition of 0.02 mM glucose with six replicates. Results are shown in Figure 4.10. The detection limit estimated based on the signal-to-noise ratio ($S/N=3$) was $6.7 \mu\text{M}$.

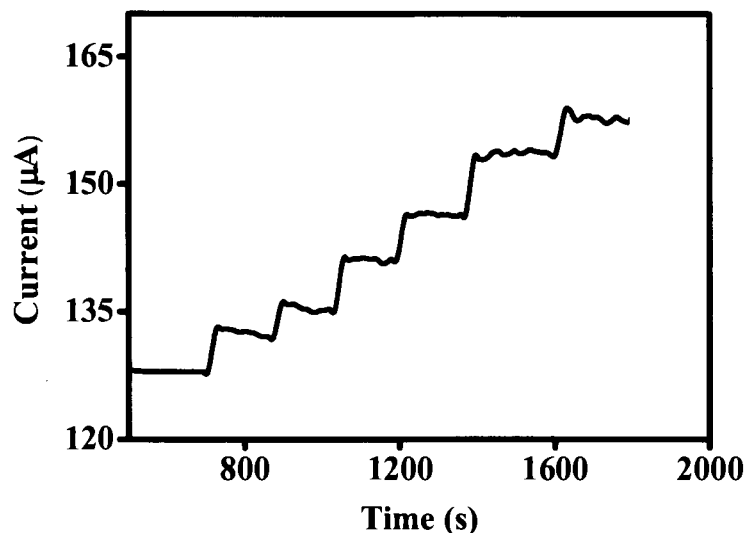


Figure 4.10 An amperometric response obtained from the developed glucose sensor for six replicates with the addition of 0.02 mM glucose in to 0.1 M sodium hydroxide solution (pH 13.0), applied potential at 0.55 V.

4.2.6.4 Interference study

In this study, the effects of possible interferences were conducted to identify specie that may affects the analysis. Interference studies were performed by divided into two categories of samples containing low matrix such as soft-drinks and honey and samples containing high matrices e.g. body fluids. The interference used in this study for high matrix samples such as ascorbic acid (AA), dopamine (DA) and uric acid (UA). That are normally co-existed with glucose in real samples like body fluids. The normal range for blood glucose concentration is about 4.4-6.6 mM, while those of AA, DA and UA are about 0.1 mM [97, 98]. Therefore, the anti-interference performance of the $\text{Fe}_3\text{O}_4\text{-CNTs-NiNPs/GC}$ electrode against these foreign species

was examined. It can be seen that a well-defined glucose response was obtained, while insignificant responses were observed for the interfering species (Fig. 4.11). Tolerances toward these compounds are satisfied, and negligible interference were observed during testing.

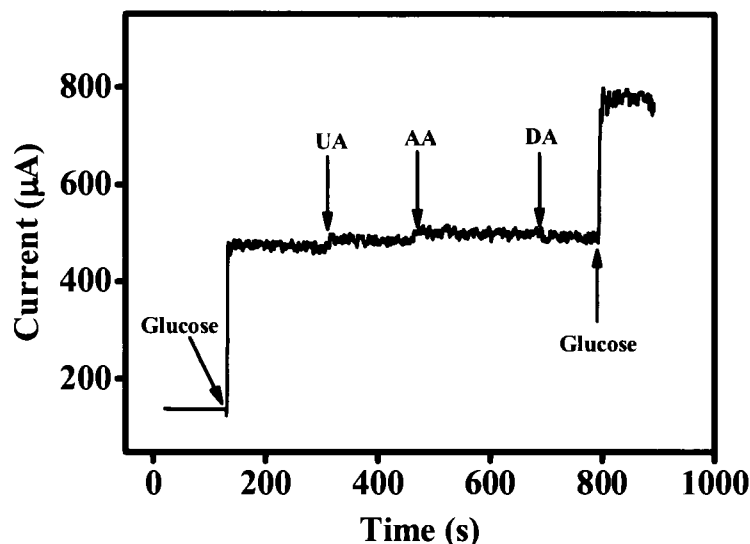


Figure 4.11 Amperometric response of glucose chemical sensor in 0.1 M NaOH (pH 13.0) upon the successive addition of 1 mM glucose, 0.5 mM uric acid (UA), 0.1 mM ascorbic acid (AA), 0.01 mM dopamine (DA) and 1 mM glucose, respectively.

In addition, to assess the selectivity of the developed glucose sensor ($\text{Fe}_3\text{O}_4\text{-CNTs-NiNPs/GC}$) in sample containing low matrix, we investigated possible interference with glucose detection from competing ions and compounds, such as fructose, maltose, sucrose, carbonic acid, citric acid and sodium chloride, which are always present in energy drinks. This work studied the effects of foreign species on the amperometric signals obtained from standard 1 mM glucose. The tolerance limit was taken as the amount of substance needed to cause a signal alteration of greater than $\pm 5\%$. Table 4.2 displays the results of the tolerance limit for fructose, maltose, sucrose, sodium carbonate, citric acid and sodium chloride was found to be 20, 5, 15, 70, 20 and 100 mM, respectively. These results demonstrated that different sugars (fructose, maltose and sucrose) and anions (CO_3^{2-} , $\text{C}_6\text{H}_5\text{O}_7^{3-}$ and Cl^-) produce very low interference signals at molar concentration of 5 mM or greater (100 mM) with respect

to glucose. However, because samples were diluted between 100 and 1,000 times prior to analysis, the presence of these foreign species is assumed not to be problematic. Thus the selectivity of Fe₃O₄-CNTs-NiNPs/GC electrode for glucose detection was satisfied in the presence of possible interfering reagents and sample ingredients.

Table 4.2 Effect of foreign ions on the amperometric signals obtained from standard 1 mM glucose.

Interference	Investigated concentration (mM)	Tolerance limit^a (mM)
Fructose/ C ₆ H ₁₂ O ₆	0.5-50	20
Maltose/ C ₁₂ H ₂₂ O ₁₁	0.5-20	5
Sucrose/ C ₁₂ H ₂₂ O ₁₁	0.5-50	15
Sodium carbonate/ Na ₂ CO ₃	0.5-300	70
Citric acid/ C ₆ H ₈ O ₇	0.5-300	20
Sodium chloride/ NaCl	0.5-30	100

^aGreater than ±5% signal alteration is classified as interfering condition.

4.2.6.5 Reproducibility and repeatability of the developed glucose sensor

Reproducibility and stability experiments were also undertaken to evaluate the performance of the developed sensor. The electrode-to-electrode reproducibility of Fe₃O₄-CNTs-NiNPs/GC was investigated from the sensitivity or slope of the calibration curve (0.5 to 2.0 mM) of five sensors. As shown in Figure 4.12, the sensitivity obtained from five electrodes was acquired with a relative standard deviation (RSD) of 3.08%. The repeatability of the electrode was estimated from six amperometric measurements of 0.5 mM glucose. The sensor showed RSD of 4.13% which indicates that the modified electrode possesses a good stability.

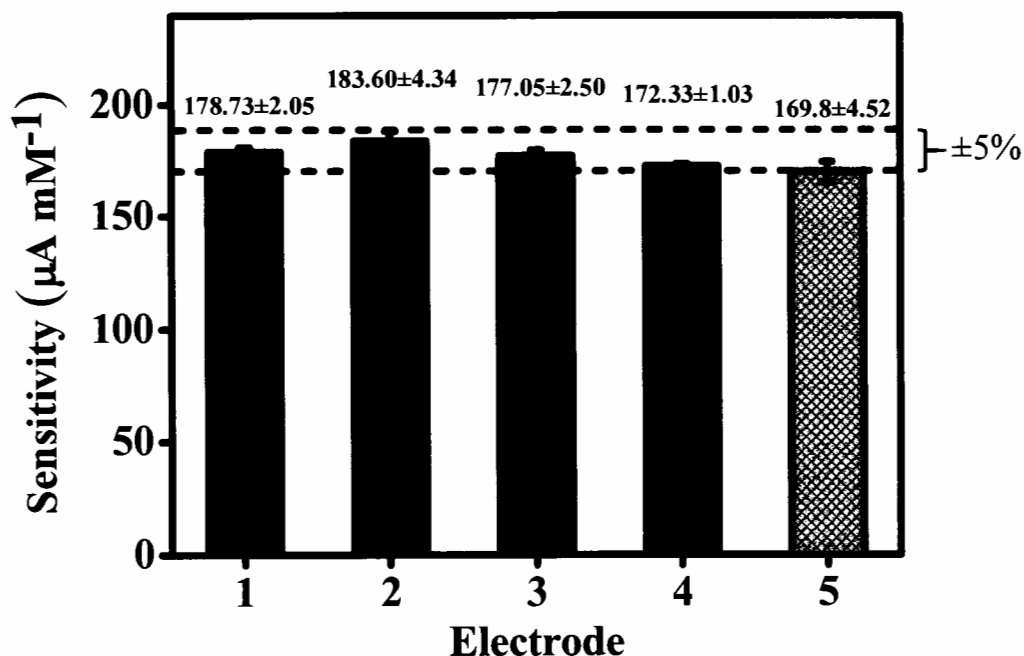


Figure 4.12 Sensitivity of the calibration curves obtained from five electrodes fabricated independently, calibration curves were performed using the concentration of glucose from 0.5 to 2.0 mM.

4.2.4.6 Application of developed glucose chemical sensor in real samples

In order to test the usefulness of the developed sensor, the electrode $\text{Fe}_3\text{O}_4\text{-CNTs-NiNPs/GC}$ was applied to the quantitative analysis of glucose in energy drinks and honey. Three different brands of energy drinks were Sponsor active, Sponsor be fresh and 100 plus (D-1, D-2 and D-3) and three brands of honeys were Floral longan honey, Vejpong and Good.b (H-1, H-2 and H-3). These samples were analyzed in triplicate by amperometry and the results shown in Table 4.2. Glucose concentration found in D-1, D-2 and D-3 by our method is close to the label values. Additionally, the results of glucose content obtained from H-1, H-2 and H-3 were compared well with the measurements obtained from a commercially available glucose meter. The differences between this method and the reference values range from 0.63% to 3.96% indicating that our test results are in good agreement with those of the drink manufacturers and the glucose meter. These results indicated that this developed method is sufficient accurate and suitable for the determination of glucose in these samples. Furthermore, to validated techniques of the developed method

compared with reference values by paired t-test at the 95% confidence level. According to the t-test values of glucose contents determined in energy drinks and honey from the two methods agree no significant difference in the means of each sample ($t_{cal} = 0.37$, $t_{table} = 4.30$) and ($t_{cal} = 0.19$, $t_{table} = 4.30$), respectively.

Table 4.3 Glucose contents found in energy drinks (D-1 to D-3) and honey (H-1 to H-3), which were obtained by the developed method and comparative values from labeled value and glucose meter.

Samples	Glucose content (%w/v)		Developed method (%w/v)	Relative difference (%)
	Label	Glucose meter		
D-1	8.50	-	8.63 ± 0.11	+1.53
D-2	8.00	-	7.91 ± 0.11	-2.38
D-3	4.80	-	4.83 ± 0.12	+0.63
H-1	-	20.10	19.27 ± 0.76	+3.96
H-2	-	15.00	15.46 ± 0.14	+1.95
H-3	-	8.20	8.35 ± 0.10	+1.83

4.3 Development of sulfite sensor based on GC/ Fe₃O₄-CNTs-NiNPs

4.3.1 Cyclic voltammetric study of sulfite oxidation

The electrochemical behavior of sulfite oxidation was studied at different modified electrode materials using cyclic voltammetry (CV). The bare GC or GC modified electrode was used as a working electrode, Ag/AgCl as a referent electrode and Pt wire as a counter electrode, respectively. Cyclic voltammograms of sulfite were measured in a 0.1 M phosphate buffer pH 7.0 (dash line) and in the solution containing 4 mM of sulfite (solid line) and the results shown in Figure 4.13. The oxidation peak sulfite obtained from bare GC, NiNPs/GC and Fe₃O₄/GC were not well defined oxidation peaks at the studied applied potential range of 0 - 1.0 V. While CNTs/GC, Fe₃O₄-CNTs/GC and NiNPs-CNTs/GC modified electrodes provide the lower current signal of sulfite oxidation than Fe₃O₄-CNTs-NiNPs/GC. These modified electrodes shown the oxidation potentials of sulfite at 0.38, 0.30 and 0.32 V, respectively. In this study, Fe₃O₄-CNTs-NiNPs/GC modified electrode displayed a highest current signal for sulfite oxidation. The electrode present an anodic peak of sulfite oxidation at 0.35 V (Figure 4.13 g). Results of anodic peak potentials ($E_{p,a}$) and current signals ($I_{p,a}$) of 4 mM sulfite obtained from difference modified electrode were summarized in table 4.4. This result indicated that the Fe₃O₄-CNTs-NiNPs nanocomposite improved the electrocatalytic activity and promoted electron transfer between analytes and the electrode surface for sulfite oxidation. Therefore, this electrode Fe₃O₄-CNTs-NiNPs/GC was selected as the optimum modified electrode because provided the highest sensitivity of sulfite.

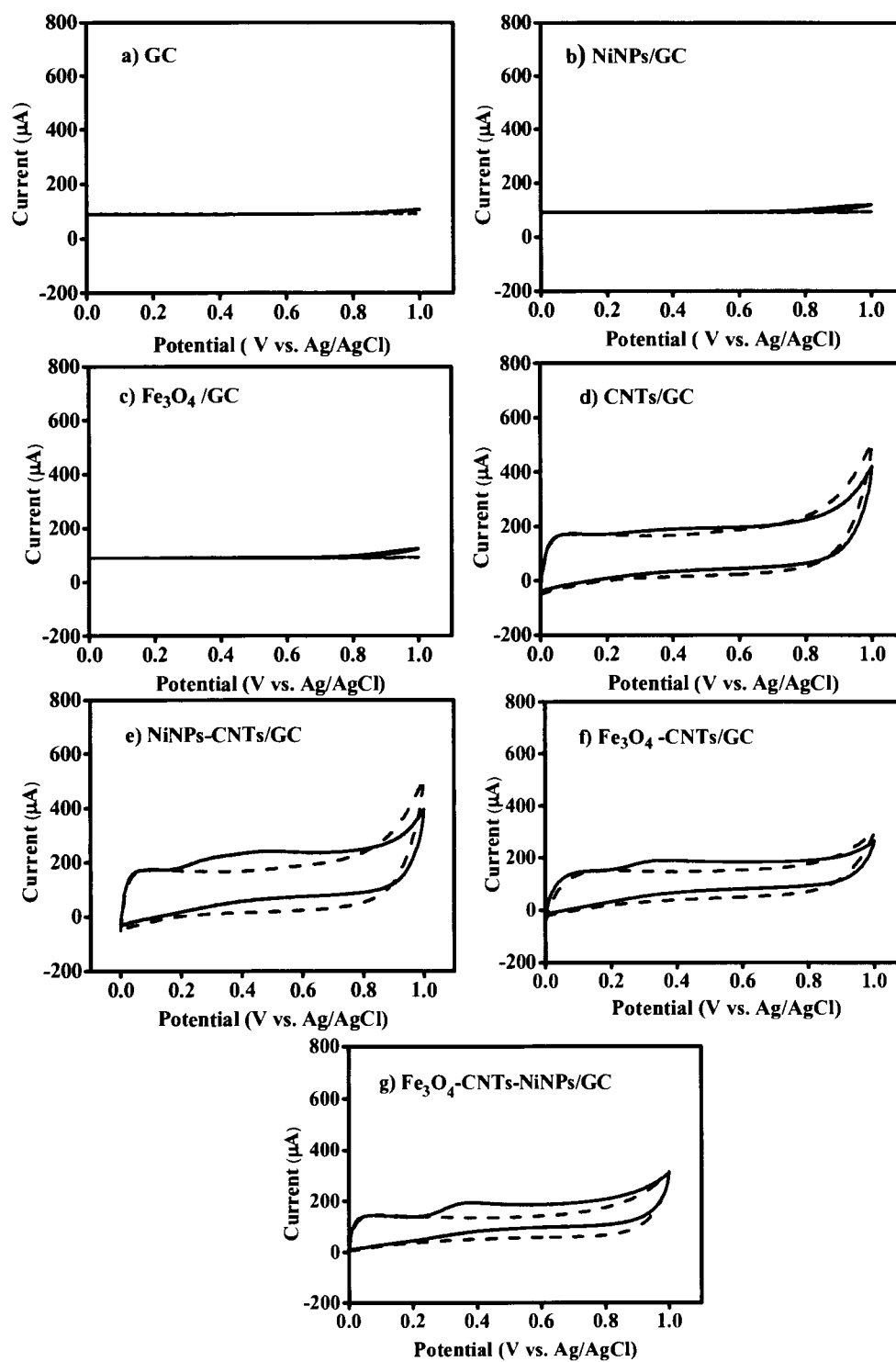


Figure 4.13 Cyclic voltammograms of a) bare glassy carbon electrode (GC), b) NiNPs/GC, c) Fe_3O_4 /GC, d) CNTs /GC e) NiNPs-CNTs /GC, f) Fe_3O_4 -CNTs/GC and g) Fe_3O_4 -CNTs-NiNPs/GC electrodes in 0.1 M phosphate buffer solution (pH 7.0) (dashed line) and in the presence of 4 mM glucose (solid line), scan rate 0.05 V s^{-1} .

Table 4.4 Anodic peak potentials ($E_{p,a}$) and current signals ($I_{p,a}$) of 4 mM sulfite using different modified electrodes.

Electrode code	Electrode	$E_{p,a}$ (V)	$i_{p,a}$ (μ A)
a	GC	>1.0	-
b	NiNPs/GC	>1.0	-
c	Fe ₃ O ₄ /GC	>1.0	-
d	CNTs /GC	0.4	22.77
e	CNTs-NiNPs/GC	0.3	47.71
f	Fe ₃ O ₄ -CNTs/GC	0.32	39.40
g	Fe ₃ O ₄ -CNTs-NiNPs/GC	0.35	55.92

4.3.2 Studies of parameters that effect the sensitivity of sulfite sensor

4.3.2.1 Effect of Fe₃O₄-CNTs-NiNPs modified amount on the detection of sulfite

The effect of Fe₃O₄-CNTs-NiNPs loading from 2 to 8 mg mL⁻¹ used for electrode modification on the oxidation peak current of sulfite was investigated. As shown in Figure 4.14 the current response increased with increasing amount of Fe₃O₄-CNTs-NiNPs from 2 to 6 mg mL⁻¹. This result assumed that increasing of Fe₃O₄-CNTs-NiNPs amount improved the electro-conductivity and enhanced active surface area of the nanocomposite. The current response was decreased at the concentration above 6 mg mL⁻¹. Therefore, the concentration of 6 mg mL⁻¹ Fe₃O₄-CNTs-NiNPs dispersion solution was chosen for modified electrode.

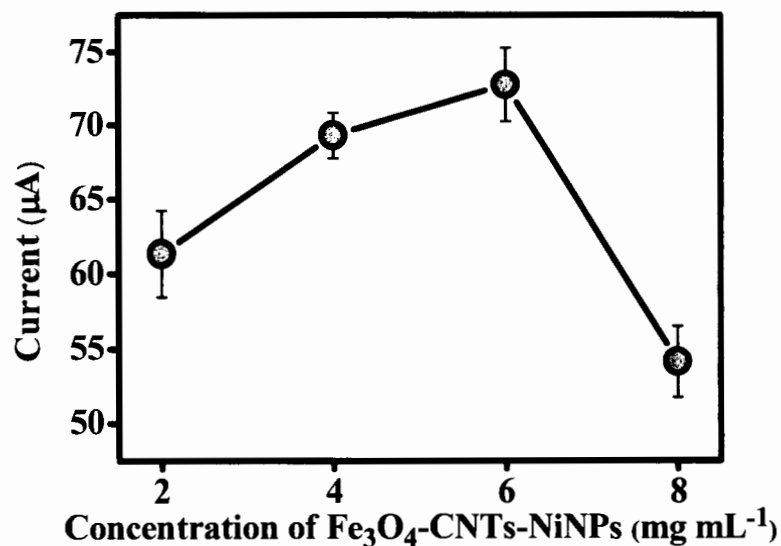


Figure 4.14 The effect of the concentration of Fe₃O₄-CNTs-NiNPs mg mL⁻¹ on the oxidation peak current of 4 mM sulfite in 0.1 M phosphate buffer solution, (pH 7.0).

4.3.2.2 Effect of buffer pH (0.1 M phosphate buffer solution)

pH is one of an important parameters that affect the developed sulfite sensor's performance. The effect of pHs on the analytical response of modified sulfite sensor was studied in the range 5.0 to 8.5 using 0.1 M phosphate buffer solution as supporting electrolyte. Figure 4.15 a) shown the oxidation current of 1 mM sulfite at various pHs buffer. It was observed that the peak potentials shifted slightly toward less positive values when the pH was increased (Figure 4.15 b). Results obtained from Figure 4.15 c) indicated that current responses was increased when the pH increased until the pH 7.0. The pH further than 7.0 provided the decreased of current responses. This result indicated that pH 7.0 gave the highest current response and therefore selected as the optimum pH.

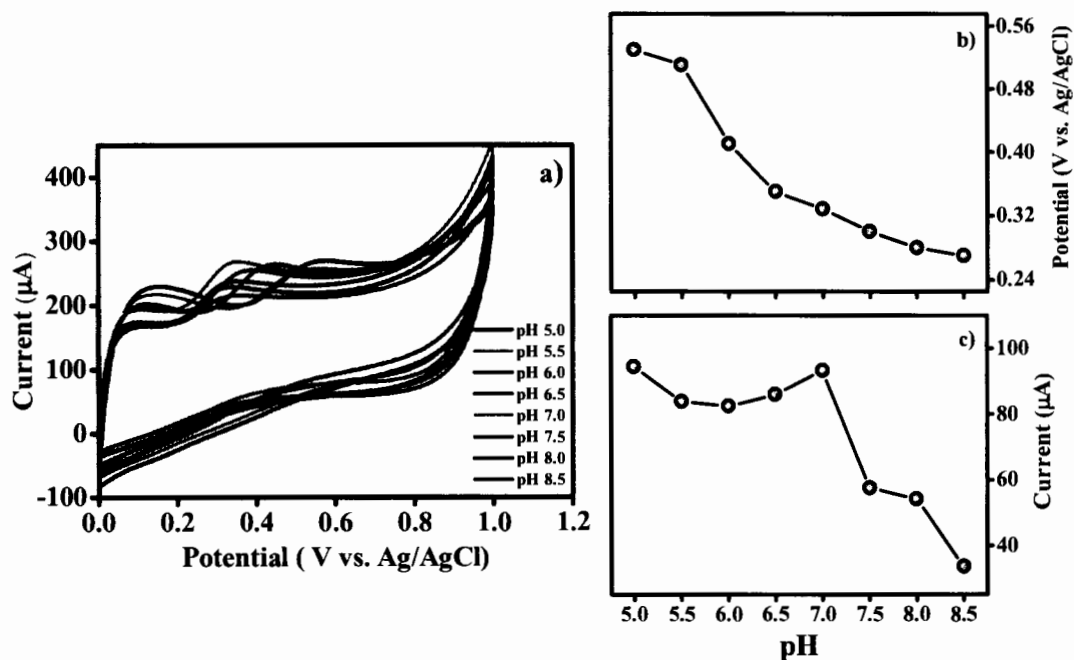


Figure 4.15 a) Cyclic voltammetric responses of 4 mM sulfite at various buffer pHs and the dependence of buffer pH on the b) peak potential and c) peak current obtained from the chemical sensor, scan rate 0.05 V s^{-1} .

4.3.3 Scan rate dependence study

The influence of potential scan rate at the $\text{Fe}_3\text{O}_4\text{-CNTs-NiNPs/GC}$ electrode was investigated in 0.1 M phosphate buffer solution containing 1 mM sulfite. Results shown in Figure 4.16 a) revealed that the oxidation peak potential shift to high positive potentials. Plot of anodic peak currents (μA) versus square root of scan rate as in Figure 4.16 b) showed linearly proportional of the current and the square root of scan rate ($\text{V}^{1/2} \text{ s}^{-1/2}$) in the range of 0.01-0.09 V s^{-1} . The linear regression equations were $I_{p,a} = 2362.20v^{1/2} + 21.27$ ($r^2 = 0.991$). This result indicated a diffusion-controlled process at the $\text{Fe}_3\text{O}_4\text{-CNTs-NiNPs/GC}$ electrode.

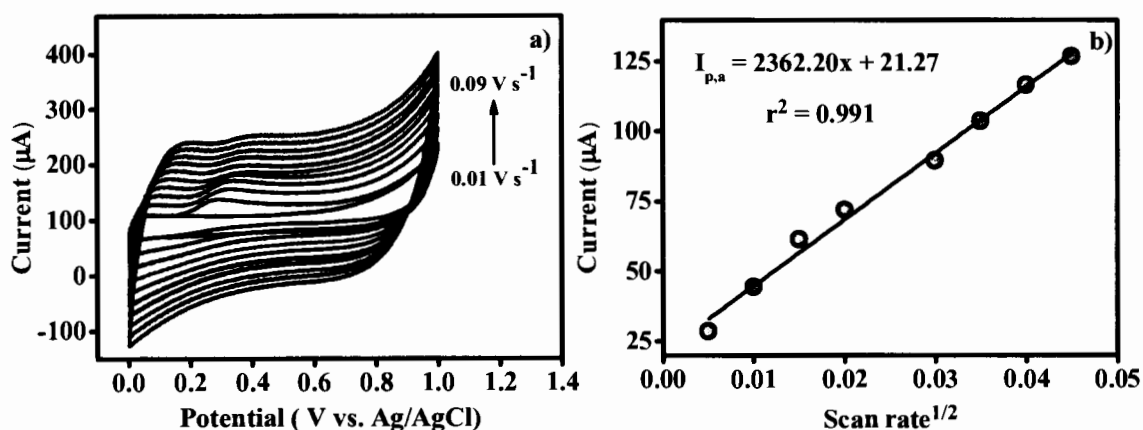


Figure 4.16 a) Cyclic voltammograms, obtained at various scan rates for 4 mM sulfite 4 mM sulfite in 0.1 M phosphate buffer solution, (pH 7.0) at modified sulfite sensor and b) linear relationship between oxidation peak currents and square root of the scan rate.

4.3.4 Concentration dependent study

The electrochemical behavior of sulfite oxidation was studied at the developed sulfite sensor ($\text{Fe}_3\text{O}_4\text{-CNTs-NiNPs/GC}$) using CV. Figure 4.17 displayed cyclic voltammograms obtained from the $\text{Fe}_3\text{O}_4\text{-CNTs-NiNPs/GC}$ electrode in the absence (0.1 M phosphate buffer solution) and presence of sulfite under the optimum conditions. It was observed that by increasing sulfite concentration, the anodic peak current increased and the potential shifted to a more positive value, demonstrating the good catalytic effect of the matrix of $\text{Fe}_3\text{O}_4\text{-CNTs-NiNPs}$ coated on electrode surface in sulfite oxidation. The relationship between oxidation peak current (μA) and sulfite concentration was examined from 0 to 8 mM. Linear calibration ($r^2 = 0.998$) was obtained with the slope of $15.539 \mu\text{A.mM}^{-1}$. These results demonstrated that the $\text{Fe}_3\text{O}_4\text{-CNTs-NiNPs/GC}$ electrode was appropriate for the quantitation of sulfite.

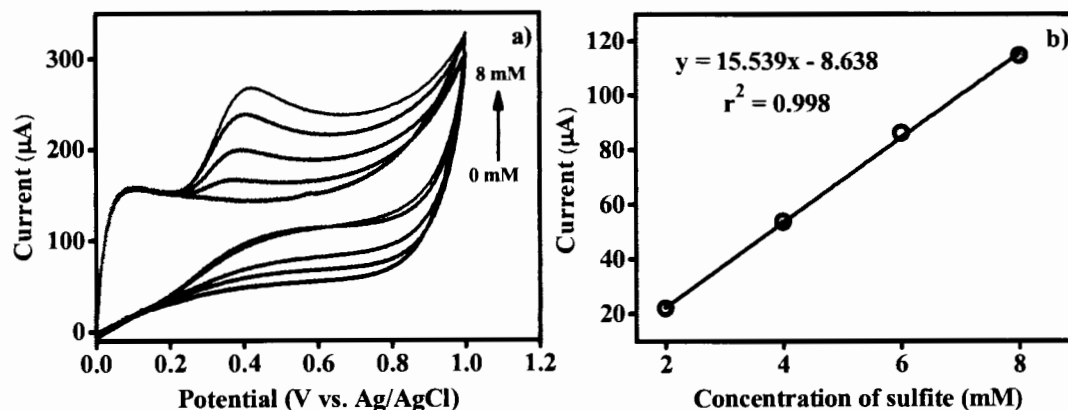


Figure 4.17 a) Cyclic voltammogram of sulfite in 0.1 M phosphate buffer solution, (pH 7.0) with the variation of sulfite concentration from 0 to 8 mM and b) calibration plot of anodic peak currents versus sulfite concentration.

4.3.5 Linear sweep voltammetric detection of sulfite

4.3.5.1 Linearity

The Linear sweep voltammograms of sulfite on the developed sensor ($\text{Fe}_3\text{O}_4\text{-CNTs-NiNPs/GC}$) was investigated by successively addition of sulfite standard in 0.1 M phosphate buffer solution (pH 7.0). Figure 4.18 displayed the oxidation current of sulfite corresponding to its concentration at optimal condition. As shown in Figure 4.18 a) the anodic current increased with increasing the concentration of sulfite ranging from 0.1 to 10 mM. The developed sensor was very sensitive to sulfite detection. As shown in Figure 4.18 b), the linear response of the developed sensor for sulfite concentration was ranged from 0.1 mM to 10 mM. The result demonstrated the regression equation $y = 12.75x + 6.35$, when y is current response (μA) and x is sulfite concentration (mM). The sensitivity of the developed sulfite sensor is $12.75 \mu\text{A mM}^{-1}$ with a linear correlation of 0.994.

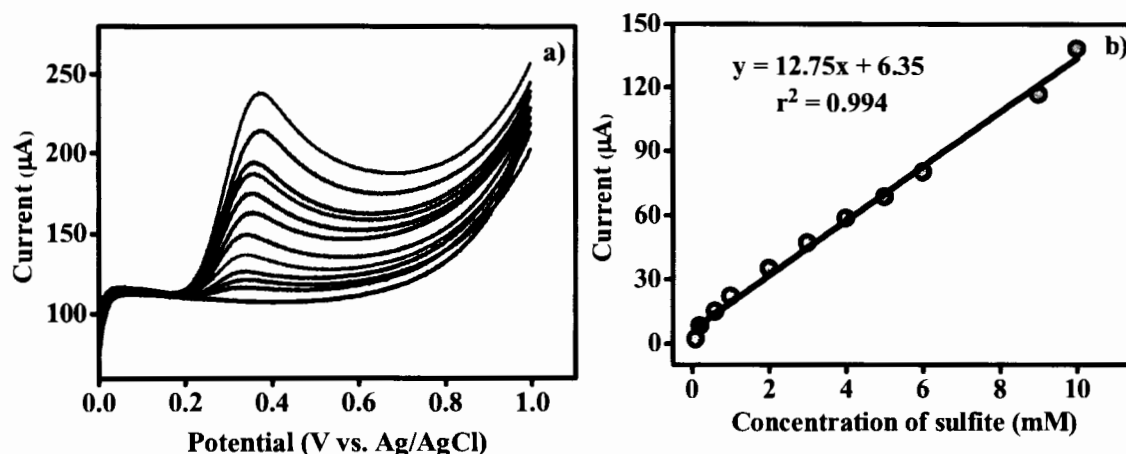


Figure 4.18 a) Linear sweep voltammograms of the $\text{Fe}_3\text{O}_4\text{-CNTs-NiNPs/GC}$ electrode to successive additions of sulfite standard into 0.1 M phosphate buffer solution, (pH 7.0), b) The linear calibration plot of the corresponding oxidation peak current versus sulfite concentration.

4.3.5.2 Limit of detection

The limit of detection at $\text{Fe}_3\text{O}_4\text{-CNTs-NiNPs/GC}$ electrode was investigated in 0.1 M phosphate buffer solution containing 0.1 mM sulfite. The detection limit was estimated based on the calculated as three times standard deviation of the lowest concentration in calibration curve (0.1 mM). In this study, limit of detection of sulfite in the signal-to-noise ratio ($S/N=3$) was 0.028 mM.

4.3.5.3 Interference study

The interference study is an important feature to assess the selectivity of the developed sensor ($\text{Fe}_3\text{O}_4\text{-CNTs-NiNPs/GC}$) for sulfite detection in real samples. We investigated possible interference of the competing ions and compounds such as sodium chloride, sodium sulfate and sodium carbonate, ethanol, glucose, fructose, maltose, sucrose, and ascorbic acid, which are always present in wine, pickled garlic and mustard green. This work, studied the effects of foreign species on the alteration of linear sweep voltammetric (LSV) responses obtained from 1 mM sulfite. The tolerance limit was taken as the amount of substance needed to cause a signal alteration of greater than $\pm 5\%$. The tolerance limit of possible

coexisting ions are summarized in table 4.5. The result shown the tolerance limit that other compounds (glucose, fructose sucrose maltose and ethanol) and competing ions (Cl^- , SO_4^{2-} and CO_3^{2-}) does not interfere signals at the concentration of 30 mM or greater (250 mM) with respect to sulfite detection. However, ascorbic acid produced considerable interference for sulfite analysis because of ascorbic acid is an organic compound that can be oxidized and the oxidation potentials is close to sulfite. However, the determination of sulfite in wine, pickled garlic and mustard green with the $\text{Fe}_3\text{O}_4\text{-CNTs-NiNPs/GC}$ electrode were diluted samples prior to analysis. Therefore, the proposed electrode provides the selectivity of for sulfite detection was satisfied in the presence of possible interfering reagents and sample ingredients.

Table 4.5 Effect of foreign ions on the linear sweep voltametric signals obtained from standard 1 mM sulfite.

Interference	Investigated concentration	Tolerance limit ^a
Ethanol/ $\text{C}_2\text{H}_6\text{O}$	0.5-15% v/v	15% v/v
Sodium chloride/ NaCl	} 0.5-300 mM	250 mM
Sodium sulfate/ NaSO_4		150 mM
Sodium carbonate/ Na_2CO_3		70 mM
Glucose/ $\text{C}_6\text{H}_{12}\text{O}_6$	} 0.5-100 mM	50 mM
Fructose/ $\text{C}_6\text{H}_{12}\text{O}_6$		50 mM
Sucrose/ $\text{C}_{12}\text{H}_{22}\text{O}_{11}$		50 mM
Maltose/ $\text{C}_{12}\text{H}_{22}\text{O}_{11}$		30 mM
Ascorbic acid/ $\text{C}_6\text{H}_8\text{O}_6$	0.1-5 mM	2 mM

^aGreater than $\pm 5\%$ signal alteration is classified as interfering condition.

4.3.5.4 Stability of sulfite chemical sensor

The storage stability of the developed sulfite sensor was investigated at room temperature when not used. The sulfite oxidation current at 0.1 mM sulfite was measured when stored for 0, 1, 2, 3, 4, 5, 6, 7, 14 and 21 days. The relative oxidation current was calculated and plot versus storage time. Relationship between percentages of relative oxidation current and storage time (day) was shown in Figure 4.19. The result indicated that relative oxidation current remain higher than 80% can be obtained after stored for 21 days. This indicated the high stability of the developed chemical sensor.

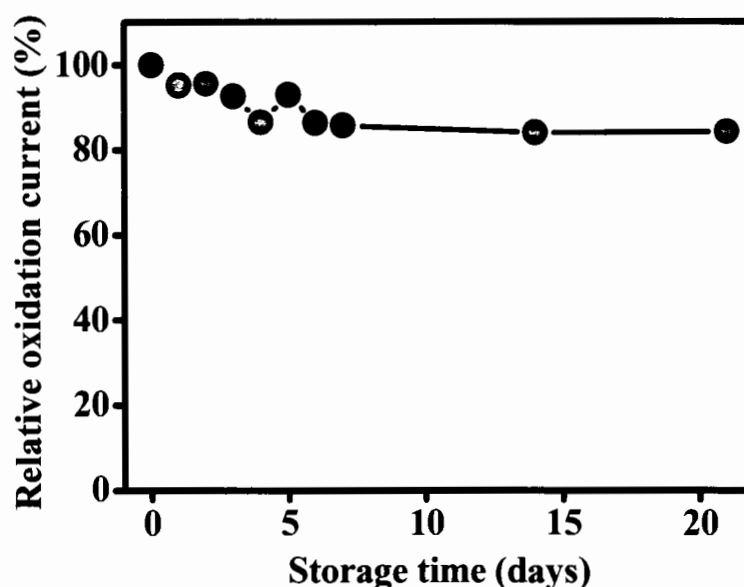


Figure 4.19 The storage stability of the developed sulfite sensor calculated from response of 1 mM sulfite in 0.1 M phosphate buffer solution, (pH 7.0).

4.3.5.5 Application of developed sulfite chemical sensor in real samples

The performance of the $\text{Fe}_3\text{O}_4\text{-CNTs-NiNPs/GC}$ modified electrode for practical application was evaluated the sensor was applied to determination sulfite in sample of wine, pickled mustard green and garlic. Three different brands of wine included Boones pina colada, Boones cheek berry and Fresco berry red wine (W-1, W-2 and W-3), pickled mustard green including House wife, Songpueng and Songheng, (M1, M-2 and M-3) and garlic including Ma jin, Big C and Vanusun

(G-1, G-2 and G-3) were analyzed in triplicate by linear sweep voltammetry. The sample were diluted with 0.1 M phosphate buffer pH 7.0. The results were compared with iodometric method as summarized in Table 4.6. The differences between our method and the reference values range from 0.28% to 4.66%. These results indicate that our developed method is sufficient accurate and suitable for the determination of sulfite in these samples. Moreover, validated techniques of the developed method compared with standard method (iodometric method) by t-test at the 95% confidence level. According to the t-test, sulfite contents determined from the two methods agree no significant difference in the means of each sample ($t_{cal} = 0.52$, $t_{table} = 2.31$).

Table 4.6 sulfite contents found in wine (W-1 to W-3), pickled mustard green (M-1 to M-3) and pickled garlic (P-1 to P-3), which were obtained by the developed method and comparative values from iodometric method was carried out in triplicate for a sample.

Samples	Developed method (mg L ⁻¹)	Iodometric method (mg L ⁻¹)	Relative error (%)
W-1	7.51±0.11	7.77±0.47	3.35
W-2	14.59±0.38	14.55±0.95	0.28
W-3	24.54±0.51	23.75±1.89	3.33
M-1	21.03±0.25	21.28±3.28	1.17
M-2	21.54±0.41	22.37±1.89	3.71
M-3	24.33±1.08	24.56±3.28	0.94
G-1	29.74±0.12	28.93±5.01	2.80
G-2	31.43±0.37	30.03±3.79	4.66
G-3	31.85±1.08	32.21±3.79	1.12

CHAPTER 5

CONCLUSIONS

This work presented the development of glucose and sulfite chemical sensor for in food applications. A simple new route for fabricated sensitive and selective glucose and sulfite chemical sensor based on the hybrid nanomaterials, Fe₃O₄ and NiNPs decorated on the surface of carbon nanotubes (Fe₃O₄-CNTs-NiNPs). The surface of carboxylic functionalized carbon nanotubes (CNTs-COOH) was loaded with Fe₃O₄ nanoparticle via a chemical co-precipitation procedure followed by decorated with NiNPs that prepared through reducing nickel chloride by hydrazine hydrate in the presence of ethylene glycol, as a stabilizing agent via ultrasonication. The stepwise preparation process of Fe₃O₄-CNTs-NiNPs nanocomposites were characterized using transmission electron microscopy (TEM) and X-Ray Diffraction (XRD). Furthermore, the as-prepared Fe₃O₄-CNTs-NiNPs nanocomposites was dispersed in aqueous solution containing 1% DMF and ultrasonicated until homogeneous and then drop cast on the surface of GC electrode (Fe₃O₄-CNTs-NiNPs/GC). The developed sensor (Fe₃O₄-CNTs-NiNPs/GC) was applied to studied electrochemical oxidation consists of two main parts; (i) electrochemical oxidation of glucose, and (ii) electrochemical oxidation of sulfite. Electrochemical cell using Fe₃O₄-CNTs-NiNPs/GC as a working electrode, Ag/AgCl and Pt wire as a reference and counter electrode was applied for the detection.

Characterization of the nanomaterials for the modified electrode, the morphology of the different composites by TEM and XRD. The TEM image shows the fine nanotubular morphology of CNTs-COOH and a homogenous dispersion of NiNPs with an average diameter of synthesized NiNPs of 21.6 ± 3.2 nm. The TEM images of Fe₃O₄-CNTs indicated that a lot of Fe₃O₄ nanoparticles have been surrounded on the surface of the carbon nanotubes. Fe₃O₄-CNTs-NiNPs shows a typical deposition of Fe₃O₄ and NiNPs on the surface of CNTs nanotubular structure. The average diameter of the nanoparticles on CNTs surface was estimated to be 20.3 ± 1.6 nm. The XRD

patterns of NiNPs displays the pure face centered cubic of nickel. The Fe₃O₄-CNTs nanocomposites were showed the spinel structure of magnetite phase and Fe₃O₄-CNTs-NiNPs were showed the peaks for both NiNPs and Fe₃O₄ which is indicated formation of Fe₃O₄ and NiNPs decorated on the CNTs.

The development of glucose sensor was studied the electrochemical oxidation of glucose based on Fe₃O₄-CNTs-NiNPs/GC modified electrode using cyclic voltammetry (CV) and amperometry. The electrochemical behavior of 4 mM glucose observed the anodic peak current at the potential +0.54 V and a cathodic peak at +0.32 V, respectively at the scan rate 0.05 V s⁻¹ in 0.1 M sodium hydroxide (pH 13.0) as supporting electrolyte. The mechanism of glucose are believed that Ni (II) and Ni (III) redox couple on the electrode surface in an alkaline medium. First, NiNPs (Ni⁰) in Fe₃O₄-CNTs-NiNPs nanocomposites at the surface of electrode was transformed to Ni(OH)₂. Then Ni(OH)₂ is oxidized to the catalytically active NiO(OH). After that, the glucose also be oxidized into gluconolactone. The result indicated that the optimum condition for modified electrode was observed by drop casted 40 μL of 4 mg mL⁻¹ of Fe₃O₄-CNTs-NiNPs on the glassy carbon (GC) electrode. The developed glucose sensor for amperometric detection show the electrochemical investigations indicated that the Fe₃O₄-CNTs-NiNPs/GC electrode exhibits excellent performance in the electrochemical oxidation of glucose at an applied potential of +0.55 V (vs. Ag/AgCl) in 0.1 M sodium hydroxide (pH 13.0). The proposed glucose sensor exhibits linear calibration over the range of 10 μM to 1.8 mM of glucose response with the regression equation $y = 335.25x + 11.81$ and a correlation coefficient of 0.998. The high sensitivity of 335.25 μA mM⁻¹ was obtained from the slope of the calibration curve. The limit of detection was 6.7 μM (S/N = 3). This sensor provide good repeatability of the electrode was estimated from six amperometric measurements of 0.5 mM glucose (RSD = 4.13%). In addition, the fabricated sensor was successfully applied to determine glucose in honey and energy drinks with good results.

In addition, the development of sulfite sensor was studied at the Fe₃O₄-CNTs-NiNPs/GC modified electrode for quantitative analysis of sulfite using linear sweep voltammetry (LSV) in 0.1 M phosphate buffer solution (pH 7.0) as supporting electrolyte. The oxidation of sulfite was found at +0.38 V using the scan rate at 0.05 V s⁻¹. The proposed sulfite sensor exhibits linear calibration over the range of

0.1 – 10 mM for sulfite response with the regression equation $y = 12.75x + 6.35$ and a correlation coefficient of 0.994. The sensitivity of $12.75 \mu\text{A mM}^{-1}$ was obtained from the slope of the calibration curve. The limit of detection was 0.028 mM (S/N = 3). The storage stability of $\text{Fe}_3\text{O}_4\text{-CNTs-NiNPs/GC}$ can be stored for up to 3 weeks at room temperature when not used with indicate the relative current response of 84% as compare to initial oxidation current of sulfite (1 mM). These results indicated the satisfactorily stability of the $\text{Fe}_3\text{O}_4\text{-CNTs-NiNPs/GC}$ modified electrode for detection of sulfite. In addition, the developed method are reliable measurement of sulfite in wine, pickled mustard green and pickled garlic. The proposed glucose and sulfite sensor provides a high sensitivity, acceptable selectivity with simples of preparation and low cost for preparation.

REFERENCES

REFERENCES

- [1] Wei, H. and Wang, E. "Fe₃O₄ magnetic nanoparticles as peroxidase mimetics and their applications in H₂O₂ and glucose detection", **Analytical Chemistry**. 80(6): 2250-2254; 15 March, 2008.
- [2] Caseli, L. and et al. "Controlled fabrication of gold nanoparticles biomediated by glucose oxidase immobilized on chitosan layer-by-layer films", **Materials Science and Engineering: C**. 29(5): 1687-1690; 22 January, 2009.
- [3] Palazzo, G. and et al. "Colorimetric detection of sugars based on gold nanoparticle formation", **Sensors and Actuators B**. 161(1): 366-371; 25 October, 2011.
- [4] Zhang, W. and et al. "Prussian blue nanoparticles as peroxidase mimetics for sensitive colorimetric detection of hydrogen peroxide and glucose", **Talanta**. 120: 362-367; 19 December, 2013.
- [5] Ponlakheth, K. and et al. "Development of sensitive and selective glucose colorimetric assay using glucose oxidase immobilized on magnetite-gold-folate nanoparticles", **Analytical Methods**. 8: 8288-8298; 3 November, 2016.
- [6] Qingwen, L. and et al. "Immobilization of glucose oxidase in sol-gel matrix and its application to fabricate chemiluminescent glucose sensor", **Materials Science and Engineering C**. 11: 67-70; 17 September, 1999.
- [7] Wang, C. and Huang, H. "Flow injection analysis of glucose based on its inhibition of electrochemiluminescence in a Ru(bpy)₃²⁺-tripropylamine system", **Analytica Chimica Acta**. 1-2: 61-68; 28 August, 2003.
- [8] Wang, J. and et al. "Oxygen independent poly(dimethylsiloxane)-based carbon-paste glucose", **Biosensors and Bioelectronics**. 17: 999-1003; 13 March, 2002.
- [9] Willner, I. and Katz, E. "Integration of Layered Redox Proteins and Conductive Supports for Bioelectronic Applications", **Angewandte Chemie International Edition**. 39(7): 1180-1218; 3 April, 2000.

REFERENCES (CONTINUED)

- [10] Mazeiko, V. and et al. "Gold nanoparticle and conducting polymer-polyaniline-based nanocomposites for glucose biosensor design", **Sensors and Actuators B**. 189: 187-193; 11 April, 2013.
- [11] Mani, V. and et al. "A novel glucose biosensor at glucose oxidase immobilized graphene and bismuth nanocomposite film modified electrode", **International Journal of Electrochemical Science**. 10: 691-700; 2 December, 2014.
- [12] Unnikrishnan, B., Palanisamy, S. and Chen, S.-M. "A simple electrochemical approach to fabricate a glucose biosensor based on graphene-glucose oxidase biocomposite", **Biosensors and Bioelectronics**. 39(1): 70-75; 15 January, 2013.
- [13] Rattanarat, P. and et al. "An Electrochemical Compact Disk-type Microfluidics Platform for Use as an Enzymatic Biosensor", **Electroanalysis**. 27(3): 703-712; 12 February, 2015.
- [14] Mena, M., Yez-Sedeo, L. P. and Pingarrn, J. M. "A comparison of different strategies for the construction of amperometric enzyme biosensors using gold nanoparticle-modified electrodes", **Analytical Biochemistry**. 336: 20-27; 5 November, 2004.
- [15] Fatoni, A. and et al. "A highly stable oxygen-independent glucose biosensor based on a chitosan-albumin cryogel incorporated with carbon nanotubes and ferrocene", **Sensors and Actuators B**. 185: 725-734; 27 May, 2013.
- [16] Satienerakul, S., Phongdong, P. and Liawruangrath, S. "Pervaporation flow injection analysis for the determination of sulphite in food samples utilising potassium permanganate-rhodamine B chemiluminescence detection", **Food Chemistry**. 121(3): 893-898; 16 January, 2010.
- [17] Amatongchai, M. and et al. "Simple flow injection for determination of sulfite by amperometric detection using glassy carbon electrode modified with carbon nanotubes-PDDA-gold nanoparticles", **Talanta**. 133: 134-141; 31 July, 2014.

REFERENCES (CONTINUED)

- [18] Isaac, A. and et al. "Electroanalytical methods for the determination of sulfite in food and beverages", **TrAC Trends in Analytical Chemistry**. 25(6): 589-598; June, 2006.
- [19] Bahmani, B. and et al. "Development of an electrochemical sulfite biosensor by immobilization of sulfite oxidase on conducting polyaniline film", **Synthetic Metals**. 160 (23-24): 2653-2657; 18 November, 2010.
- [20] Theisen, S. and et al. "A fast and sensitive HPLC method for sulfite analysis in food based on a plant sulfite oxidase biosensor", **Biosensors and Bioelectronics**. 26(1): 175-181; 12 June, 2010.
- [21] Yilmaz, M. T. and Somer, G. "Determination of trace sulfite by direct and indirect methods using differential pulse polarography", **Analytica Chimica Acta**. 603(1): 30-35; 22 September, 2007.
- [22] Hassan, S. S. M., Hamza, M. S. A. and Mohamed, A. H. K. "A novel spectrophotometric method for batch and flow injection determination of sulfite in beverages", **Analytica Chimica Acta**. 570(2): 232-239; 27 April, 2006.
- [23] Tzanavaras, P. D., Thiakouli, E. and Themelis, D. G. "Hybrid sequential injection flow injection manifold for the spectrophotometric determination of total sulfite in wines using o-phthalaldehyde and gas-diffusion", **Talanta**. 77(5): 1614-1619; 14 October, 2008.
- [24] Bonificio, R. L. and Coichev, N. "Chemiluminescent determination of sulfite traces based on the induced oxidation of Ni(II)/tetraglycine complex by oxygen in the presence of luminol: mechanistic considerations", **Analytica Chimica Acta**. 517(1-2): 125-130; 26 July, 2004.
- [25] Rawal, R., Chawla, S. and Pundir, C. S. "Polyphenol biosensor based on laccase immobilized onto silver nanoparticles/multiwalled carbon nanotube/polyaniline gold electrode", **Analytical Biochemistry**. 419(2): 196-204; 30 July, 2011.

REFERENCES (CONTINUED)

- [34] Kamali, R. and Binesh, A. R. "Numerical investigation of heat transfer enhancement using carbon nanotube-based non-Newtonian nanofluids", **International Communications in Heat and Mass Transfer**. 37(8): 1153-1157; 3 July, 2010.
- [35] Ding, Y. and et al. "Heat transfer of aqueous suspensions of carbon nanotubes (CNT) nanofluids", **International Journal of Heat and Mass Transfer**. 49(1-2): 240-250; 27 September, 2005.
- [36] Zhao, H. and Ju, H. "Multilayer membranes for glucose biosensing via layer-by-layer assembly of multiwall carbon nanotubes and glucose oxidase", **Analytical Biochemistry**. 350(1): 138-144; 20 December, 2005.
- [37] Merkoi, A. and et al. "New materials for electrochemical sensing VI: Carbon nanotubes", **TrAC Trends in Analytical Chemistry**. 24(9): 826-838; October, 2005.
- [38] Gavalas, V. and et al. "Carbon nanotube aqueous sol-gel composites: enzyme-friendly platforms for the development of stable biosensors", **Analytical Biochemistry**. 329(2): 247-252; 4 May, 2004.
- [39] Lin, Y., Cui, X. and Ye, X. "Electrocatalytic reactivity for oxygen reduction of palladium-modified carbon nanotubes synthesized in supercritical fluid", **Electrochemistry Communications**. 7(3): 267-274; 25 January, 2005.
- [40] Welch, C.M. and R.G. Compton, "The use of nanoparticles in electroanalysis: a review", **Analytical and Bioanalytical Chemistry**. 384(3): 601-619, 10 January, 2006.
- [41] Teymourian, H., Salimi, A. and Hallaj, R. "Low potential detection of NADH based on Fe₃O₄ nanoparticles/multiwalled carbon nanotubes composite: Fabrication of integrated dehydrogenase-based lactate biosensor", **Biosensors and Bioelectronics**. 33(1): 60-68; 26 December, 2011.
- [42] Kaushik, A. and et al. "Chitosan iron oxide nanobiocomposite based immunosensor for ochratoxin-A", **Electrochemistry Communications**. 10(9): 1364-1368; 8 July, 2008.

REFERENCES (CONTINUED)

- [43] Wang, Q. and et al. "Room-temperature ionic liquids/multi-walled carbon nanotubes/chitosan composite electrode for electrochemical analysis of NADH", **Electrochimica Acta**. 52(24): 6630-6637; 25 April, 2007.
- [44] Katz, E. and et al. "Dual Biosensing by Magneto-Controlled Bioelectrocatalysis", **Angewandte Chemie International Edition**. 41(8): 1343–1346; 15 April, 2002.
- [45] Hulanicki, A., Glab, S. and Ingman, F. "Chemical sensors: definitions and classification", **Pure and Applied Chemistry**. 63(9): 1247-1250; January, 1991.
- [46] Mowbray, D. J. and et al. "Designing multifunctional chemical sensors using Ni and Cu doped carbon nanotubes", **Physical Status Solidi B**. 247: 2678–2682; 5 October, 2010.
- [47] Ivaska, A. "Solid-state (Bio) Chemical Sensors", **Process chemistry centre**. <https://www.slideshare.net/TurkuSciencePark/solidstate-bio-chemical-sensors-bo-akademi-university-professor-ari-ivaska>. February, 2017.
- [48] Seitz, W.R. "Chemical sensors based on fiber optics", **Analytical Chemistry**. 56(1): 16–34; January, 1984.
- [49] Thostenson, E. T., Renb, Z. and Chou, T. W. "Advances in the science and technology of carbon nanotubes and their composites: a review", **Composites Science and Technology**. 61: 1899–1912; 21 June, 2001.
- [50] Popov, V. "Carbon nanotubes: properties and application", **Materials Science and Engineering: R**. 43(3): 61-102; 2004.
- [51] Blaney, L. "Magnetite (Fe₃O₄): Properties, Synthesis, and Applications", **Lehigh Preserve**. 15: 33-81; 2015.
- [52] Mascolo, M. C., Pei, Y. and Ring, T. A. "Room temperature co-precipitation synthesis of magnetite nanoparticles in a large pH window with different bases", **Materials**. 6: 5549-5567; 28 November, 2013.
- [53] Cabrera, L. and et al. "Magnetite nanoparticles: Electrochemical synthesis and characterization". **Electrochimica Acta**. 53(8): 3436-3441; 16 January, 2008.

REFERENCES (CONTINUED)

- [54] Martin F., Arno, S. and Matthias S. "Ab initio study of the half-metal to metal transition in strained magnetite", **New Journal of Physics**. 9: 1-15; January, 2007.
- [55] Charoenta, T. **Preparation and Characterization of Magnetic Nanoparticles for Hyperthermia Applications**. Master's Thesis: The University of Songkla, 2013.
- [56] Hariani, P. L. and et al. "Synthesis and properties of Fe₃O₄ nanoparticles by co-precipitation method to removal procion dye", **International Journal of Environmental Science and Development**. 4: 336-340; June, 2013.
- [57] Laurent, S. and et al. "Magnetic iron oxide nanoparticles: synthesis, stabilization, vectorization, physicochemical characterizations, and biological applications", **Chemical Reviews**. 108(6): 2064–2110; 11 June, 2008.
- [58] Tartaj, P. and et al. "Advances in magnetic nanoparticles for biotechnology applications", **Journal of Magnetism and Magnetic Materials**. 290-291: 28–34; 2 December, 2004.
- [59] Petri-Fink, A. and et al. "Development of functionalized superparamagnetic iron oxide nanoparticles for interaction with human cancer cells", **Biomaterials**. 26(15): 2685–2694; 11 September, 2004.
- [60] Masotti, A. and Caporali, A. "Preparation of magnetic carbon nanotubes (Mag-CNTs) for biomedical and biotechnological applications", **International journal of molecular sciences**. 14(12): 24619-24642; 18 December, 2013.
- [61] Abdalla, A. M., S. Ghosh and I. K. Puri. "Decorating carbon nanotubes with co-precipitated magnetite nanocrystals", **Diamond & Related Materials**. 66: 90–97; April, 2016.
- [62] Hrapovic, S. and et al. "Electrochemical biosensing platforms using platinum nanoparticles and carbon nanotubes", **Analytical Chemistry**. 76(4):1083-1088; 15 February, 2004.

REFERENCES (CONTINUED)

- [73] Bontempelli, G. and Toniolo, R. "Measurement methods electrochemical: Linear Sweep and Cyclic Voltammetry", **Encyclopedia of Electrochemical Power Sources**. 1: 643–654; December, 2009.
- [74] Nicholson, R. S. and Shain, I. "Theory of stationary electrode polarography. single scan and cyclic methods applied to reversible, irreversible, and kinetic systems", **Analytical Chemistry**. 36(4): 706–723; 1 April, 1964.
- [75] Thomas, F. G. and Henze, G. "Introduction to voltammetric analysis theory and practice", **Australia, Csiro**. 1-264; April, 2001.
- [76] Haddad, P. R. and Jackson, P. E. "Chapter 10 electrochemical detection (Amperometry, Voltammetry and Coulometry)", **Journal of Chromatography Library**. 46: 291-321; April, 1990.
- [77] Shamsipur, M., Najafi, M. and Hosseini, M. R. "Highly improved electrooxidation of glucose at a nickel(II) oxide/multi-walled carbon nanotube modified glassy carbon electrode", **Bioelectrochemistry**. 77(2): 120-1; 21 July, 2009.
- [78] Mu, Y. and et al. "Nano nickel oxide modified non-enzymatic glucose sensors with enhanced sensitivity through an electrochemical process strategy at high potential", **Biosensors & Bioelectronics**. 26(6): 2948-52; 4 December, 2010.
- [79] Nie, H. and et al. "Nonenzymatic electrochemical detection of glucose using well-distributed nickel nanoparticles on straight multi-walled carbon nanotubes". **Biosensors & Bioelectronics**. 30(1): 28-34; 25 August, 2011.
- [80] Sun, A., Zheng, J. and Sheng, Q. "A highly sensitive non-enzymatic glucose sensor based on nickel and multi-walled carbon nanotubes nanohybrid films fabricated by one-step co-electrodeposition in ionic liquids", **Electrochimica Acta**. 65: 64-69; 11 January, 2012.
- [81] Zhu, X. and et al. "Amperometric nonenzymatic determination of glucose based on a glassy carbon electrode modified with nickel(II) oxides and grapheme", **Microchimica Acta**. 180(5-6): 477-483; 8 February, 2013.

REFERENCES (CONTINUED)

- [82] Lin, K.-C., Lin, Y.-C. and Chen, S.-M. "A highly sensitive nonenzymatic glucose sensor based on multi-walled carbon nanotubes decorated with nickel and copper nanoparticles", **Electrochimica Acta**. 96: 164-172; 28 February, 2013.
- [83] Pournaghi-Azar, M. H., Hydarpour, M. and "Dastangoo, H., "Voltammetric and amperometric determination of sulfite using an aluminum electrode modified by nickel pentacyanonitrosylferrate film", **Analytica Chimica Acta**. 497(1-2): 133-141; 6 August, 2003.
- [84] Zhou, H., Yang, W. and Sun, C. "Amperometric sulfite sensor based on multiwalled carbon nanotubes/ferrocene-branched chitosan composites", **Talanta**. 77(1): 366-371; July, 2008.
- [85] Alamo, L. S., Tangkuaram, T. and Satienperakul, S. "Determination of sulfite by pervaporation-flow injection with amperometric detection using copper hexacyanoferrate-carbon nanotube modified carbon paste electrode". **Talanta**. 81(4-5): 1793-1799; 27 March, 2010.
- [86] Wang, X. "Simultaneous electrochemical determination of sulphite and nitrite by a gold nanoparticle/graphene-chitosan modified electrode". **Chinese Journal of Analytical Chemistry**. 41(8): 1232-1237; 21 March, 2013.
- [87] Silva, E. M., Takeuchi, R. M. and Santos, A. L., "Carbon nanotubes for voltammetric determination of sulphite in some beverages", **Food Chemistry**. 173: 763-769; 28 October, 2014.
- [88] Chen, J., Zhang, W. D. and Ye, J. S. "Nonenzymatic electrochemical glucose sensor based on MnO₂/MWNTs nanocomposite", **Electrochemistry Communications**. 10: 1268-1271; 29 June, 2008.
- [89] Zhang, Y. and et al. "Assembly of Ni(OH)₂ nanoplates on reduced graphene oxide: a two dimensional nanocomposite for enzyme-free glucose sensing", **Journal of Materials Chemistry**. 21: 16949-16954; May, 2011.

REFERENCES (CONTINUED)

- [90] Yang, J. and et al. "Nickel nanoparticle–chitosan-reduced graphene oxide-modified screen-printed electrodes for enzyme-free glucose sensing in portable microfluidic devices". **Biosensors and Bioelectronics**. 47: 530-538; 3 April, 2013.
- [91] Zhang, X. and et al. "Nonenzymatic glucose sensor based on in situ reduction of Ni/NiO-Graphene nanocomposite", **Sensors**. 16: 1791-1800; 26 October, 2016.
- [92] X. Zhu, "Amperometric nonenzymatic determination of glucose based on a glassy carbon electrode modified with nickel(II) oxides and graphene", **Microchimica acta**. 180: 477–483; 8 February, 2013.
- [93] Gao, A. and et al. "In situ synthesis of Ni(OH)₂/TiO₂ composite film on NiTi alloy for non-enzymatic glucose sensing", **Sensors and Actuators B**. 232: 150–157; 24 March, 2016.
- [94] Lua, L. M. and et al. "A nano-Ni based ultrasensitive nonenzymatic electrochemical sensor for glucose: Enhancing sensitivity through a nanowire array strategy", **Biosensors and Bioelectronics**. 25: 218–223; 7 July, 2009.
- [95] Yang, H. and et al. "Nickel hydroxide nanoflowers for a nonenzymatic electrochemical glucose sensor", **Journal of The Electrochemical Society**. 161(10): B216-B219; 15 July, 2014.
- [96] Kang, X. and et al. "A sensitive nonenzymatic glucose sensor in alkaline media with a copper nanocluster/multiwall carbon nanotube-modified glassy carbon electrode", **Analytical Biochemistry**. 363: 143–150; 8 January, 2007.
- [97] Wang, J. "Electrochemical Glucose Biosensors", **Chemical Reviews**. 108(2): 814–825; 23 December, 2007.
- [98] Canivell, S. and Gomis, R. "Diagnosis and classification of autoimmune diabetes mellitus", **Autoimmunity Reviews**. 13(4-5): 403-407; April, 2014.

APPENDICES

APPENDIX A
Characterization of nanocomposites

X-ray diffraction (XRD) (raw data for Figure 4.2)

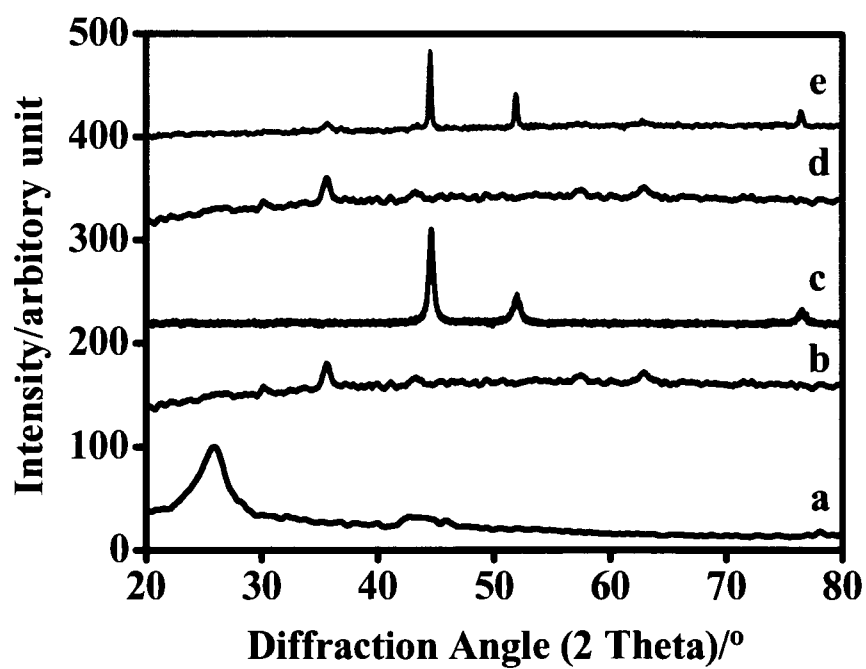


Figure A.1 XRD patterns of a) CNTs b) Fe_3O_4 c) NiNPs, d) Fe_3O_4 -CNTs and e) Fe_3O_4 -CNTs-NiNPs nanocomposites.

APPENDIX B

Development of glucose sensor based on Fe₃O₄-CNTs-NiNPs/GC

Effect of Fe₃O₄-CNTs-NiNPs modified amount on the detection of glucose (raw data for Figure 4.4)

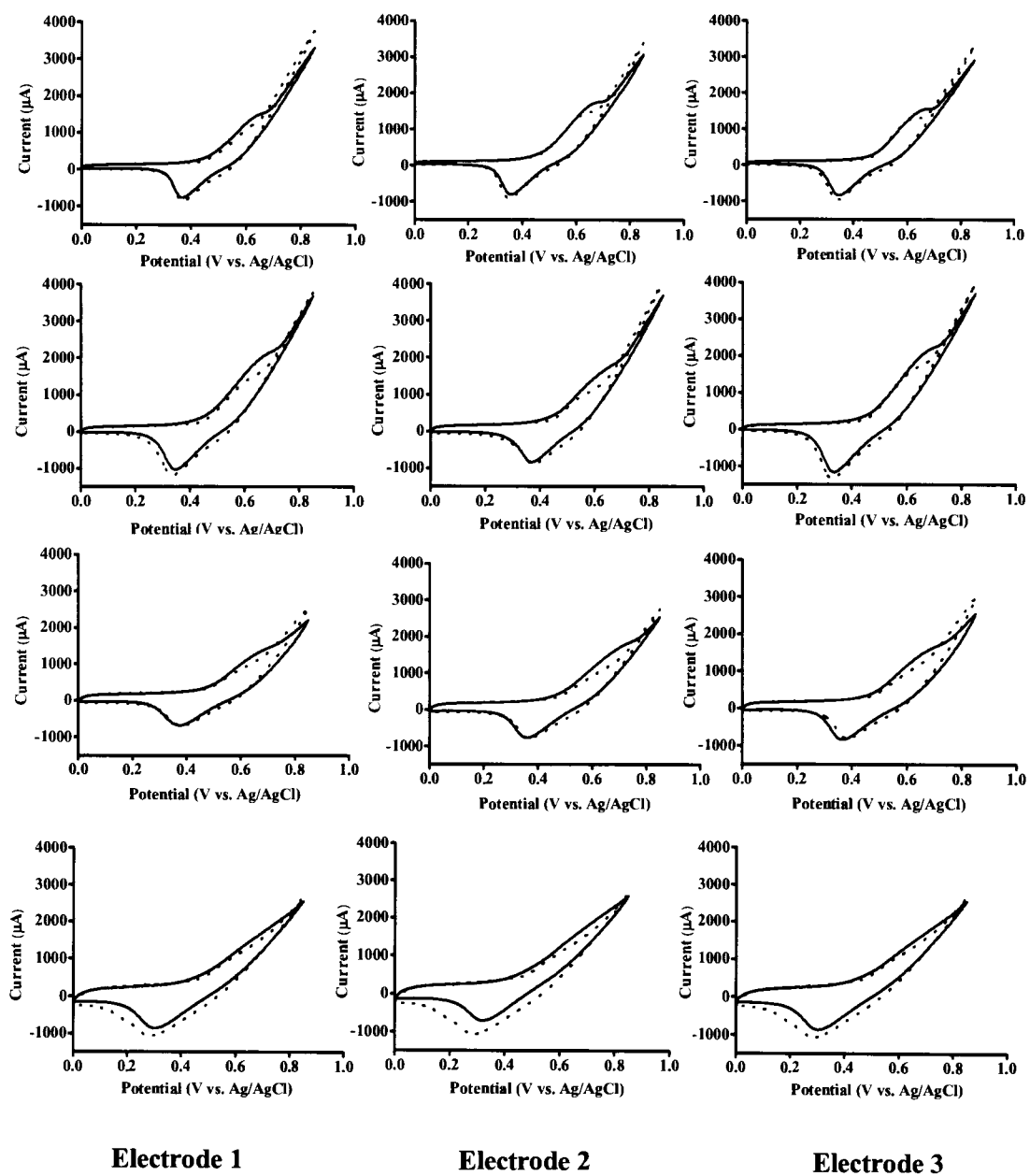
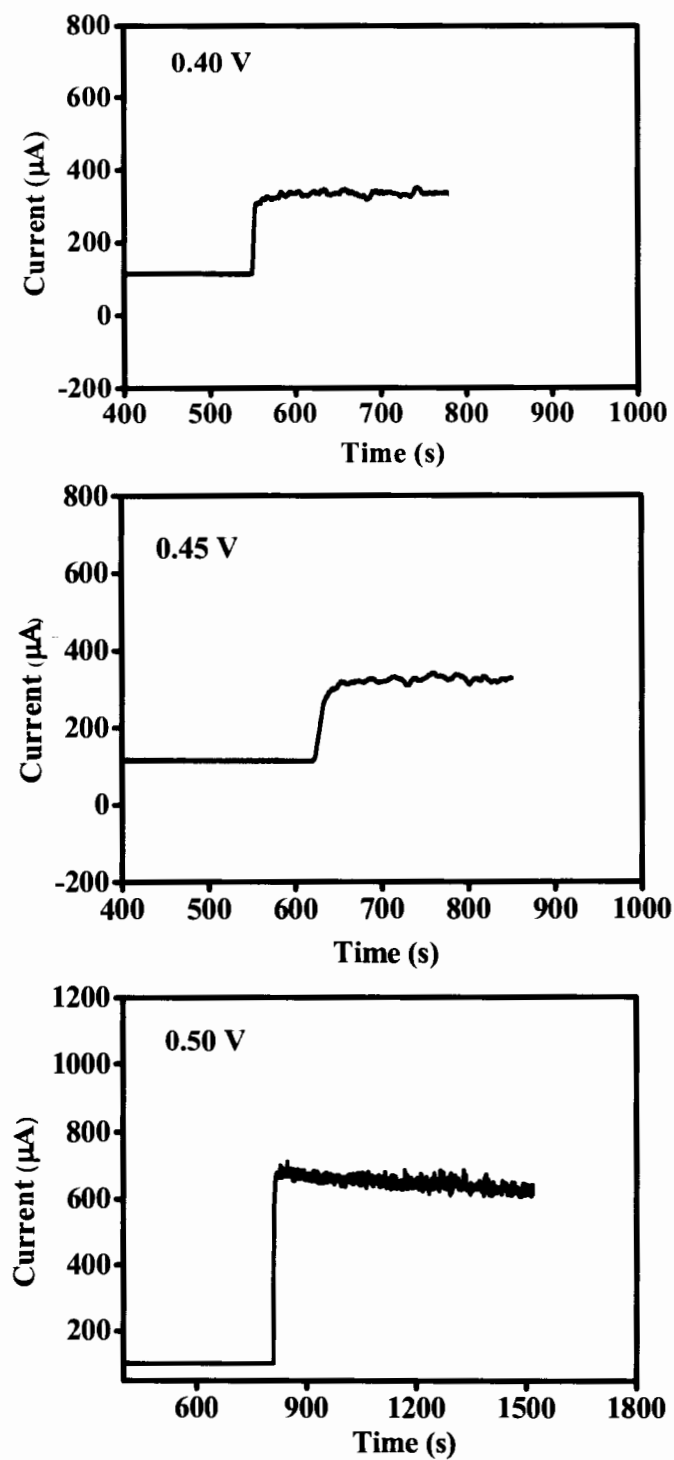


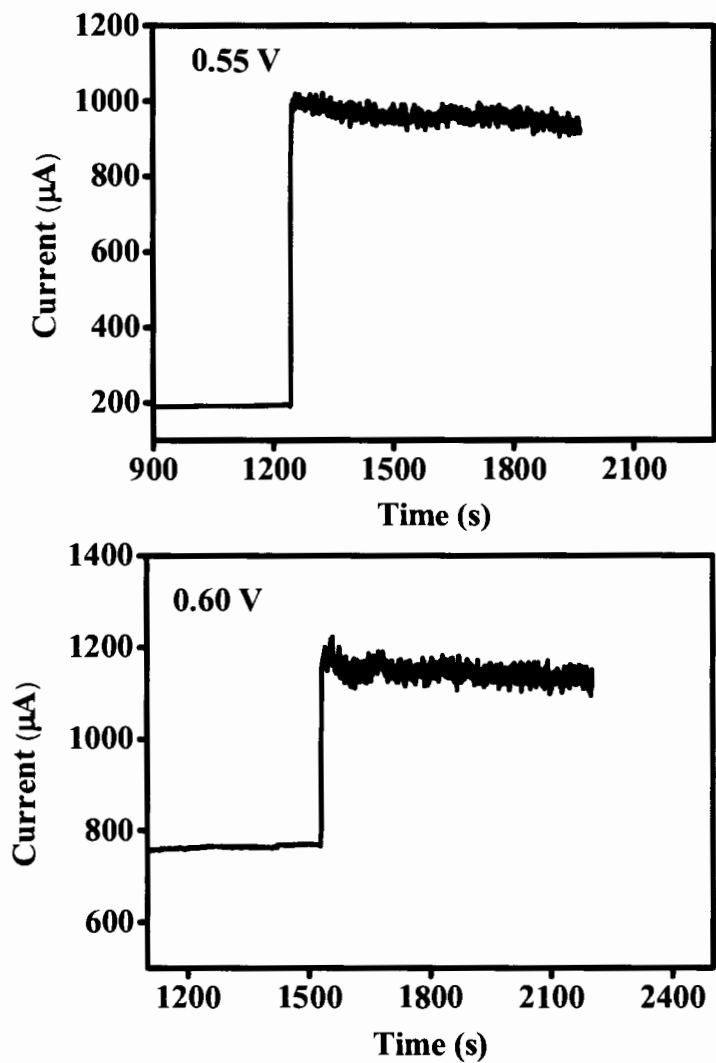
Figure B.1 Cyclic voltammograms of concentration of Fe₃O₄-CNTs-NiNPs (mg mL⁻¹).

Optimum potential for amperometric detection (raw data for Figure 4.8)

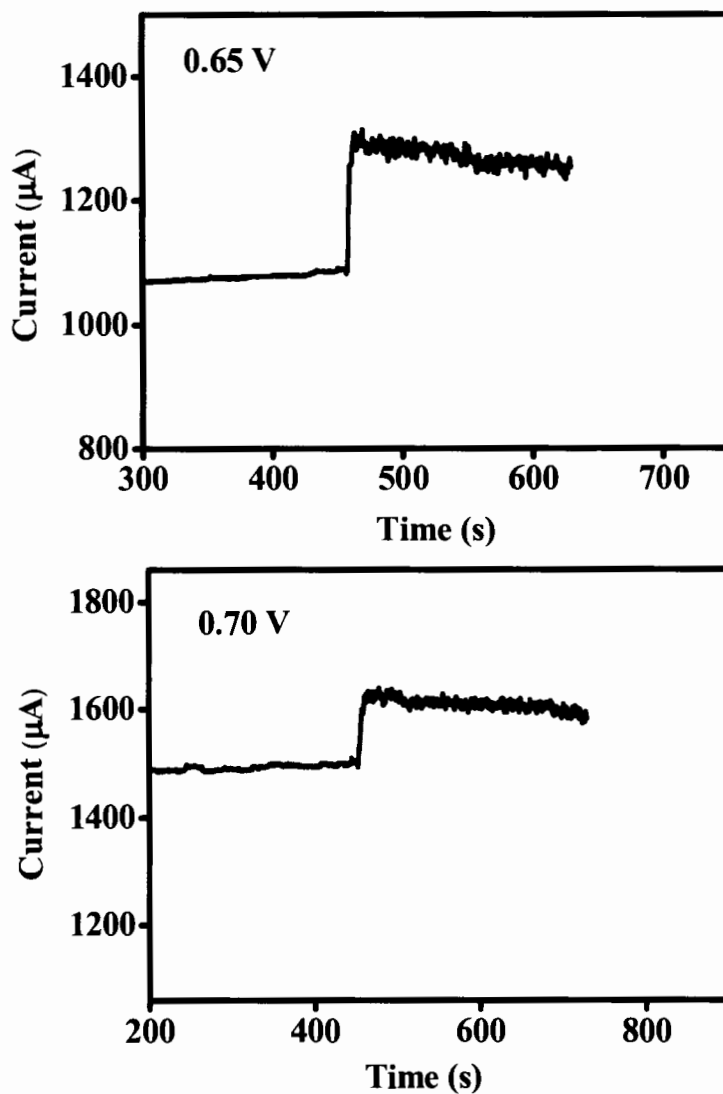
**Figure B.2 Amperograms of the applied potential on the glucose sensor response
0.1 mM glucose.**

Optimum potential for amperometric detection (raw data for Figure 4.8)

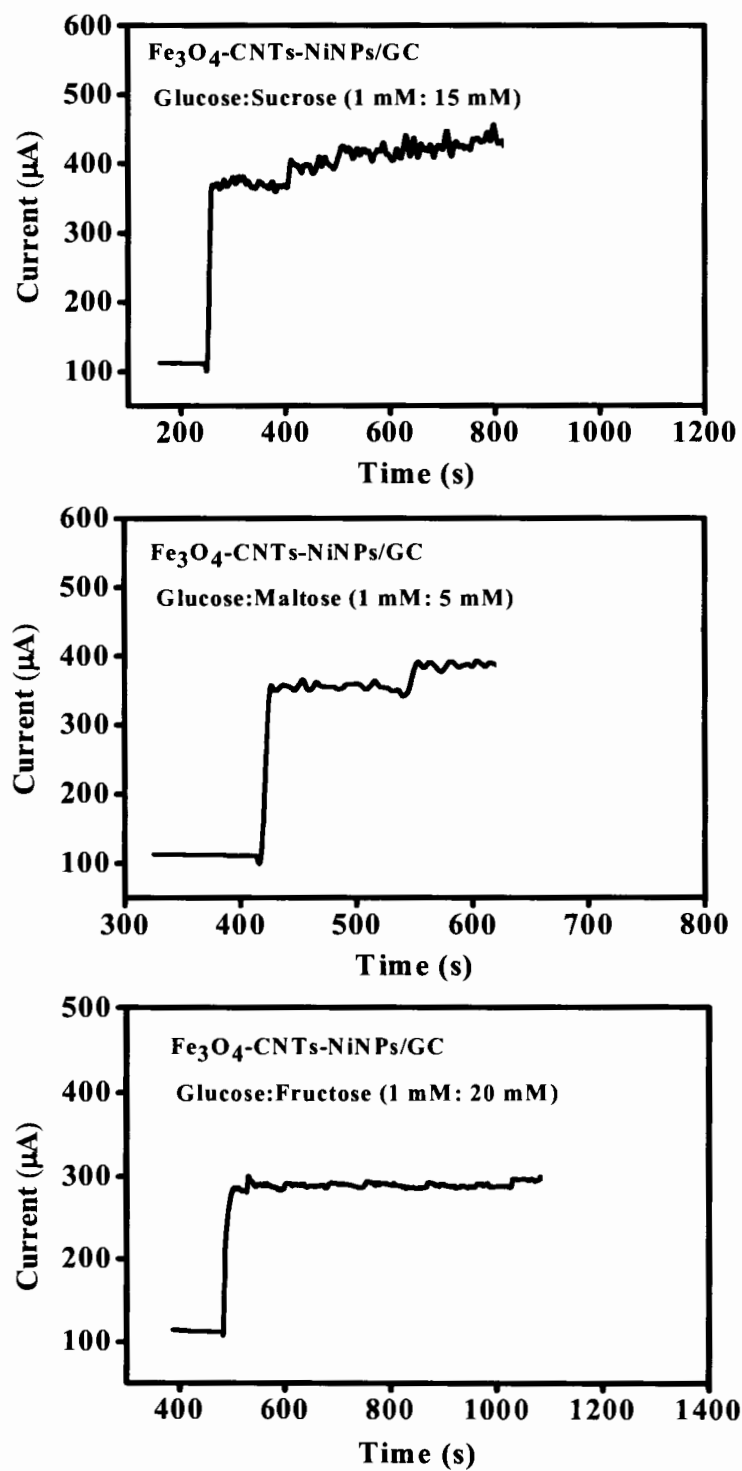
(Continued)



**Figure B.2 Amperograms of the applied potential on the glucose sensor response
0.1 mM glucose.**

Optimum potential for amperometric detection (raw data for Figure 4.8)**(Continued)**

**Figure B.2 Amperograms of the applied potential on the glucose sensor response
0.1 mM glucose.**

Interference study (raw data for Table 4.2)**Figure B.3 Amperograms of the interference on the glucose sensor.**

Interference study (raw data for Table 4.2) (Continued)

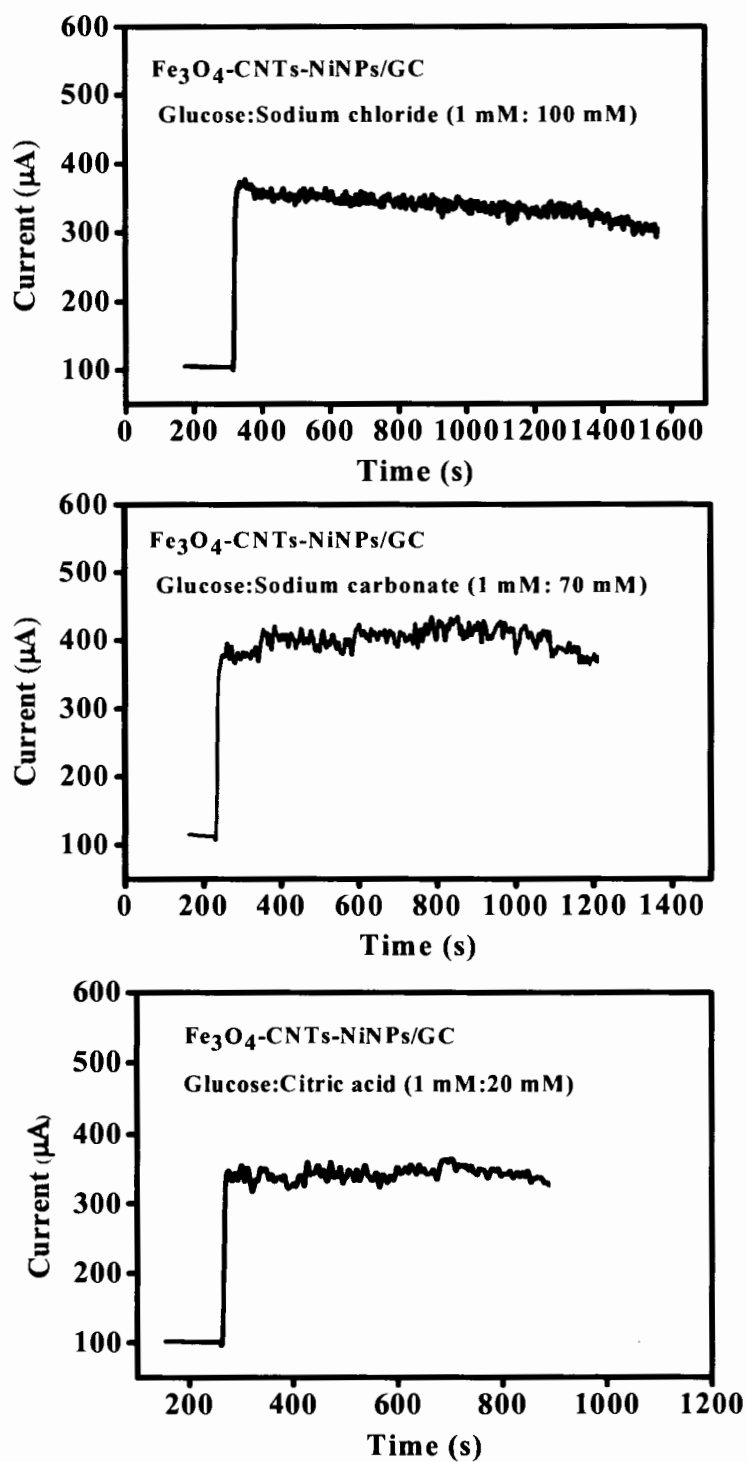


Figure B.3 Amperograms of the interference on the glucose sensor.

Sample determination: Sponsor active (D-1)

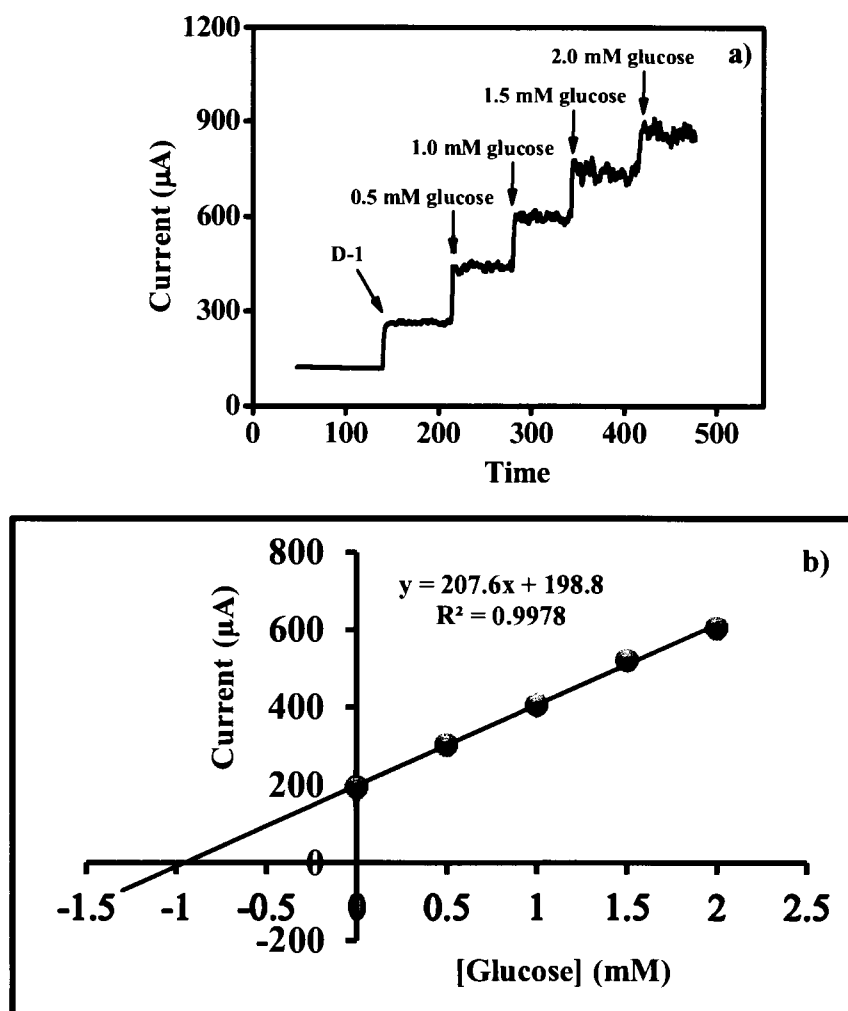


Figure B.4 a) Amperograms of the D-1 sample on the glucose sensor and b) linear calibration plot of anodic peak current versus glucose concentration and regression equation from standard addition method.

$$y = 207.60x + 198.80$$

$$y = 0; x = 0.958$$

$$\text{Dilute 500 fold; } x = 0.958 \times 500 = 479 \text{ mM}$$

$$n = g/MW; g = n \cdot MW$$

$$g = (0.479 \text{ mol}) \times (180.16 \text{ g mol}^{-1}) = 86.30 \text{ g}$$

$$\text{Solution 1000 mL} = 86.30 \text{ g}$$

$$100 \text{ mL} = ((86.30 \text{ g} \times 100 \text{ mL})/1000 \text{ mL}) = 8.63 \text{ \%w/v}$$

Concentration of glucose in Sponsor active is 8.63 %w/v.

Sample determination: Vejpong (H-2)

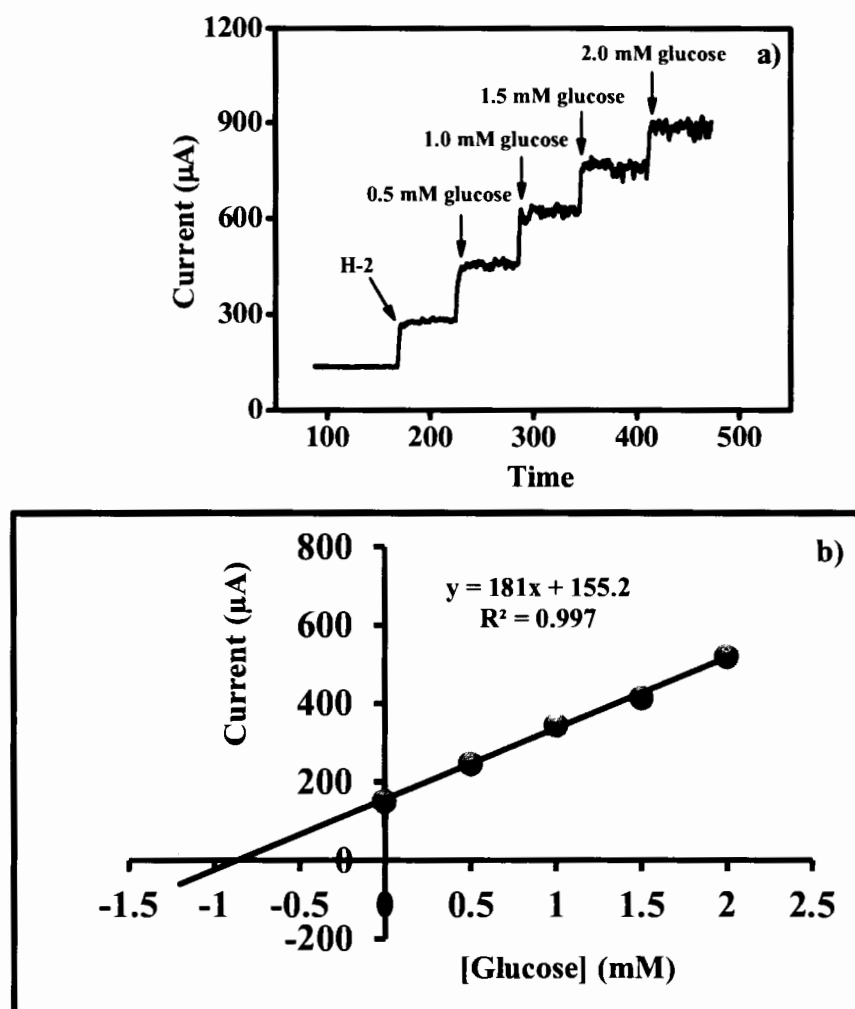


Figure B.5 a) Amperogram of the H-2 sample on the glucose sensor and b) linear calibration plot of anodic peak current versus glucose concentration and regression equation from standard addition method.

$$y = 181x + 155.20$$

$$y = 0; x = 0.857$$

$$\text{Dilute 1,000 fold; } x = 0.857 \times 1,000 = 0.857 \text{ M}$$

$$n = g/MW; g = n \cdot MW$$

$$g = (0.857 \text{ mol}) \times (180.16 \text{ g mol}^{-1}) = 154.40 \text{ g}$$

$$\text{Solution 1000 mL} = 154.40 \text{ g}$$

$$100 \text{ mL} = ((154.40 \text{ g} \times 100 \text{ mL})/1000 \text{ mL}) = 15.44 \text{ \%w/v}$$

Concentration of glucose in Vejpong honey is 15.44 %w/v.

APPENDIX C

Development of sulfite sensor based on GC/ Fe₃O₄-CNTs-NiNPs

Effect of $\text{Fe}_3\text{O}_4\text{-CNTs-NiNPs}$ modified amount on the detection of sulfite (raw data for Figure 4.14)

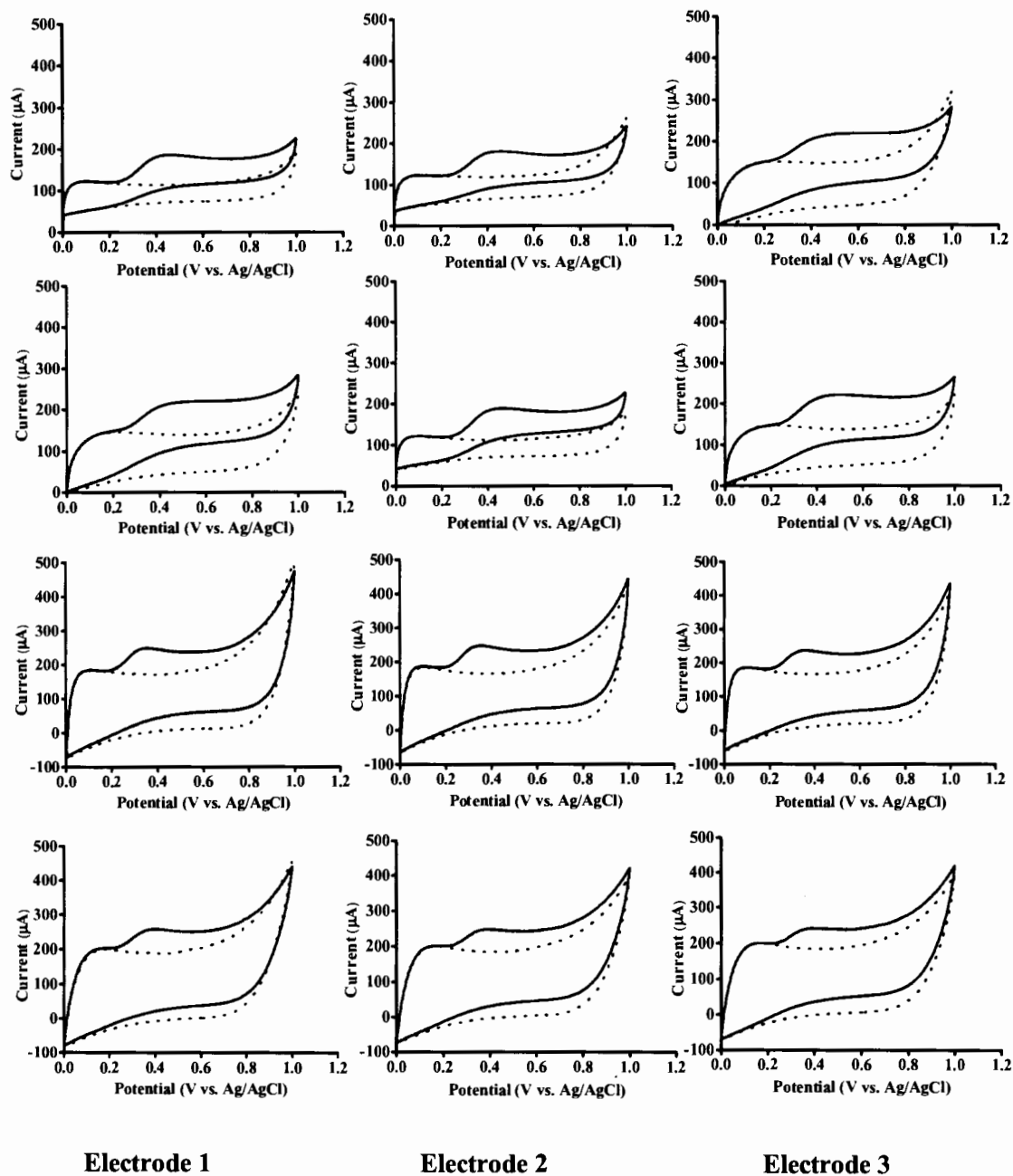


Figure C.1 Cyclic voltammograms of concentration of $\text{Fe}_3\text{O}_4\text{-CNTs-NiNPs}$ (mg mL^{-1}).

Interference study (raw data for Table 4.5)

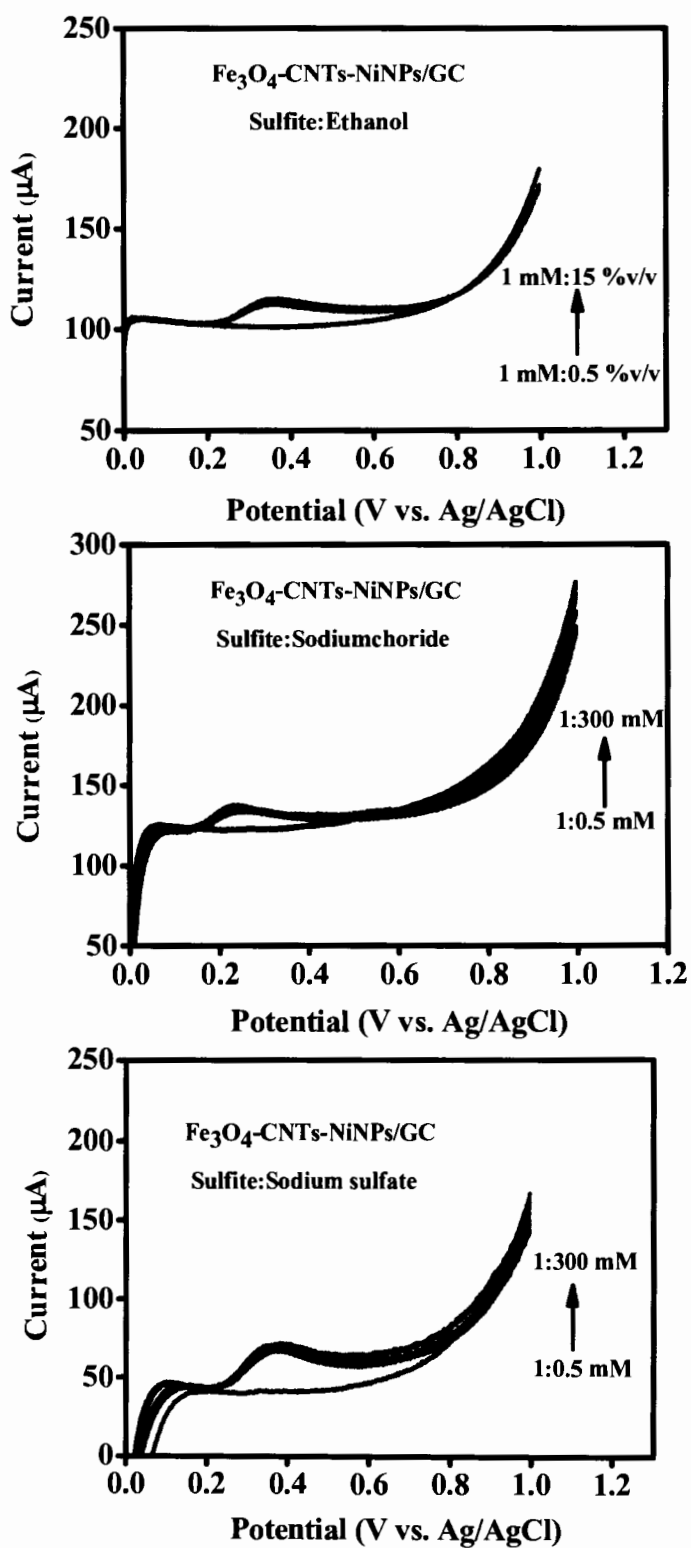


Figure C.2 Linear sweep voltammograms of the interference on the $\text{Fe}_3\text{O}_4\text{-CNTs-NiNPs/GC}$.

Interference study (raw data for Table 4.5) (Continued)

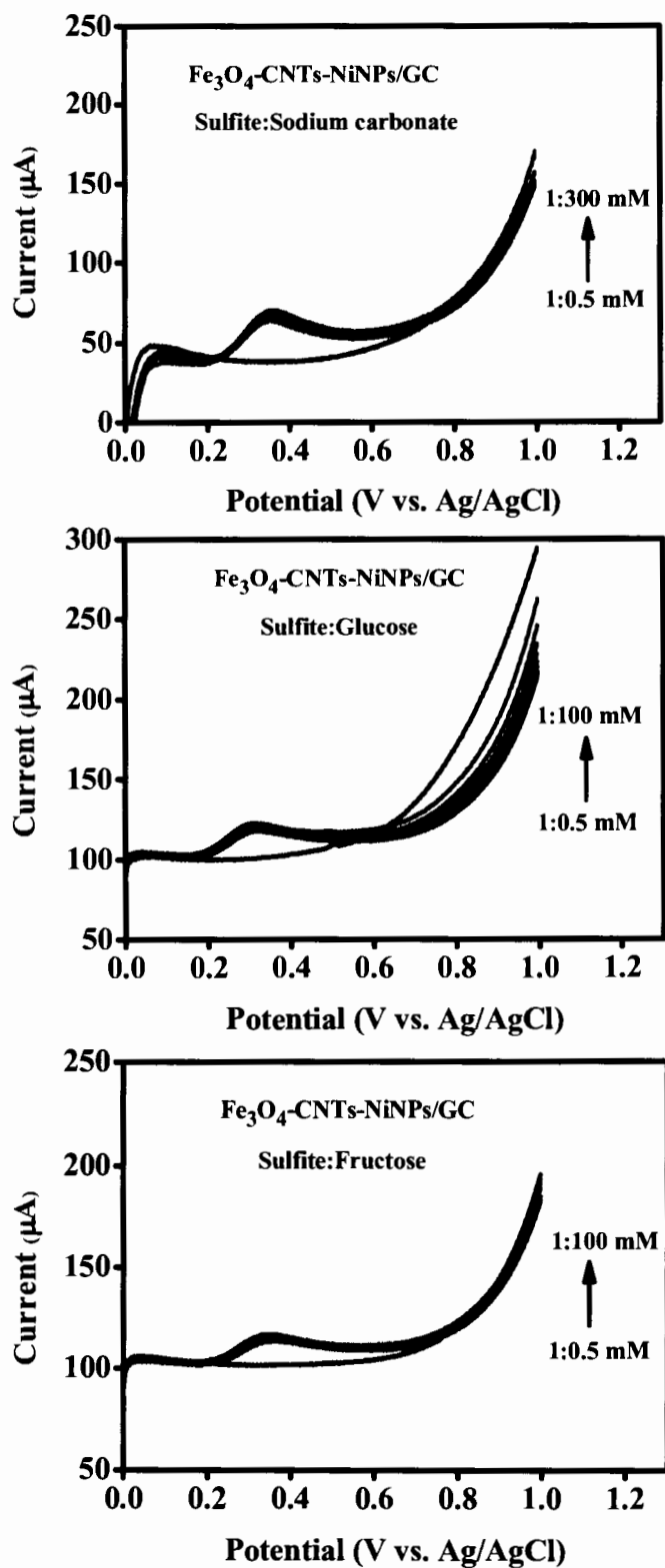


Figure C.2 Linear sweep voltammograms of the interference on the $\text{Fe}_3\text{O}_4\text{-CNTs-NiNPs/GC}$.

Interference study (raw data for Table 4.5) (Continued)

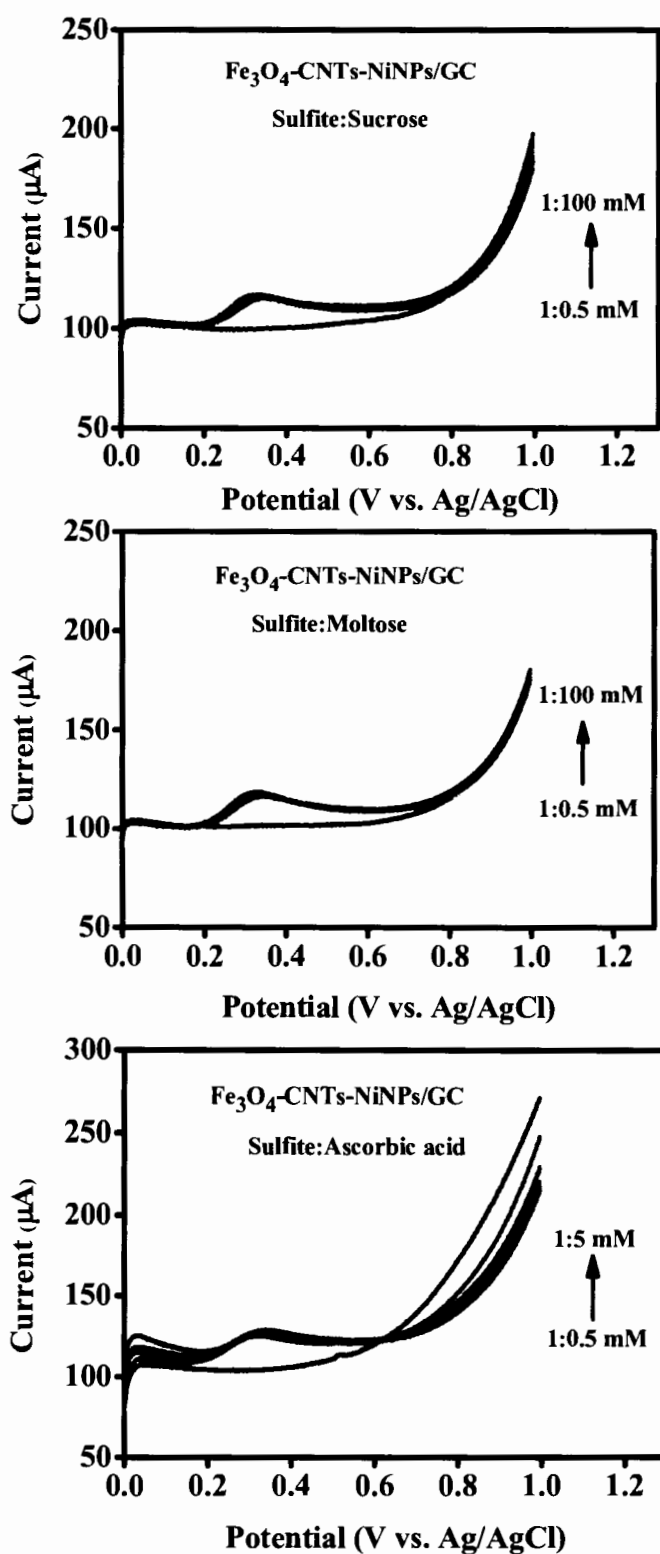


Figure C.2 Linear sweep voltammograms of the interference on the $\text{Fe}_3\text{O}_4\text{-CNTs-NiNPs/GC}$.

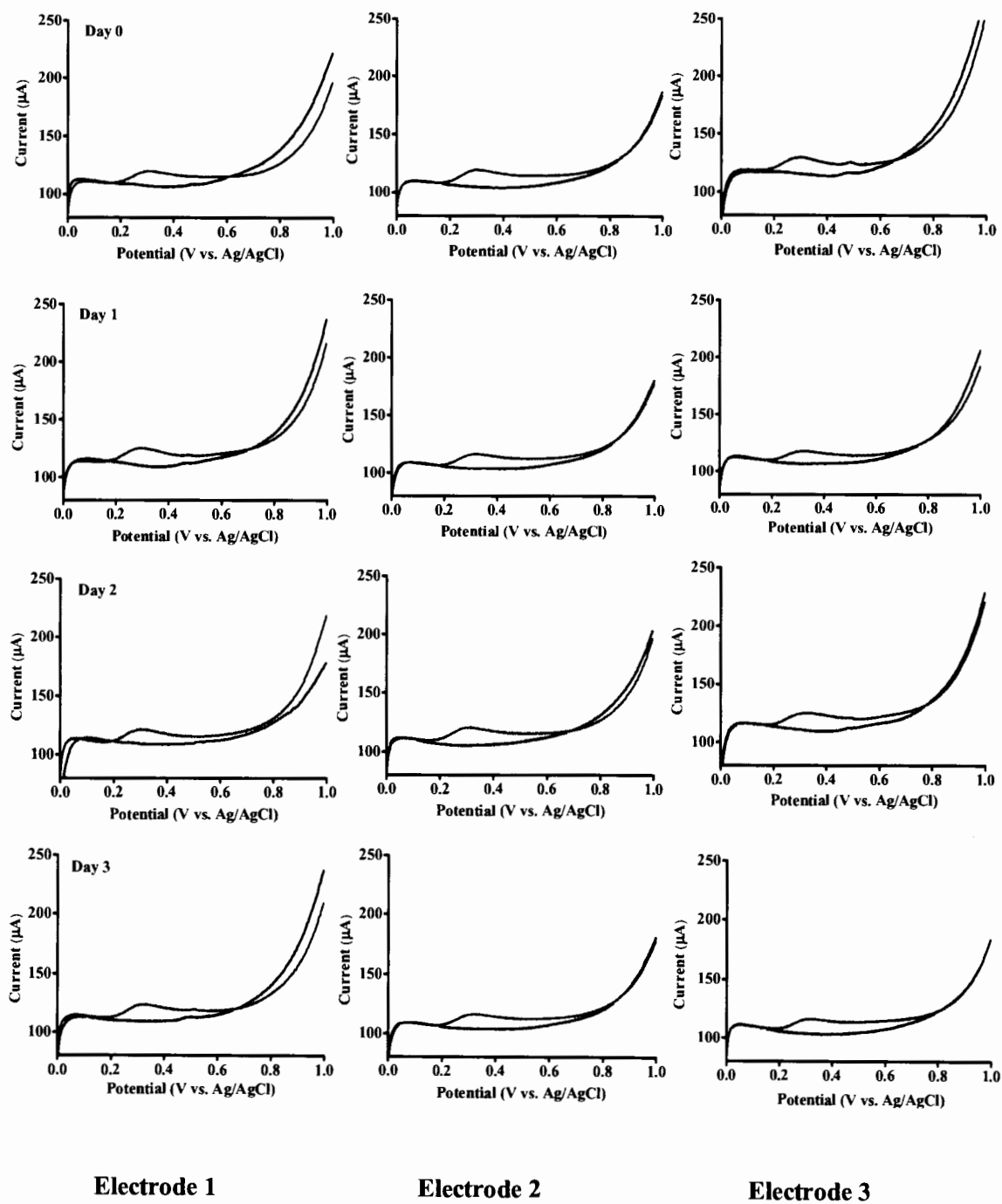
Stability of sulfite chemical sensor (raw data for Figure 4.19)

Figure C.3 The storage stability of the developed sulfite sensor calculated from response of 1 mM sulfite in 0.1 M phosphate buffer solution, (pH 7.0).

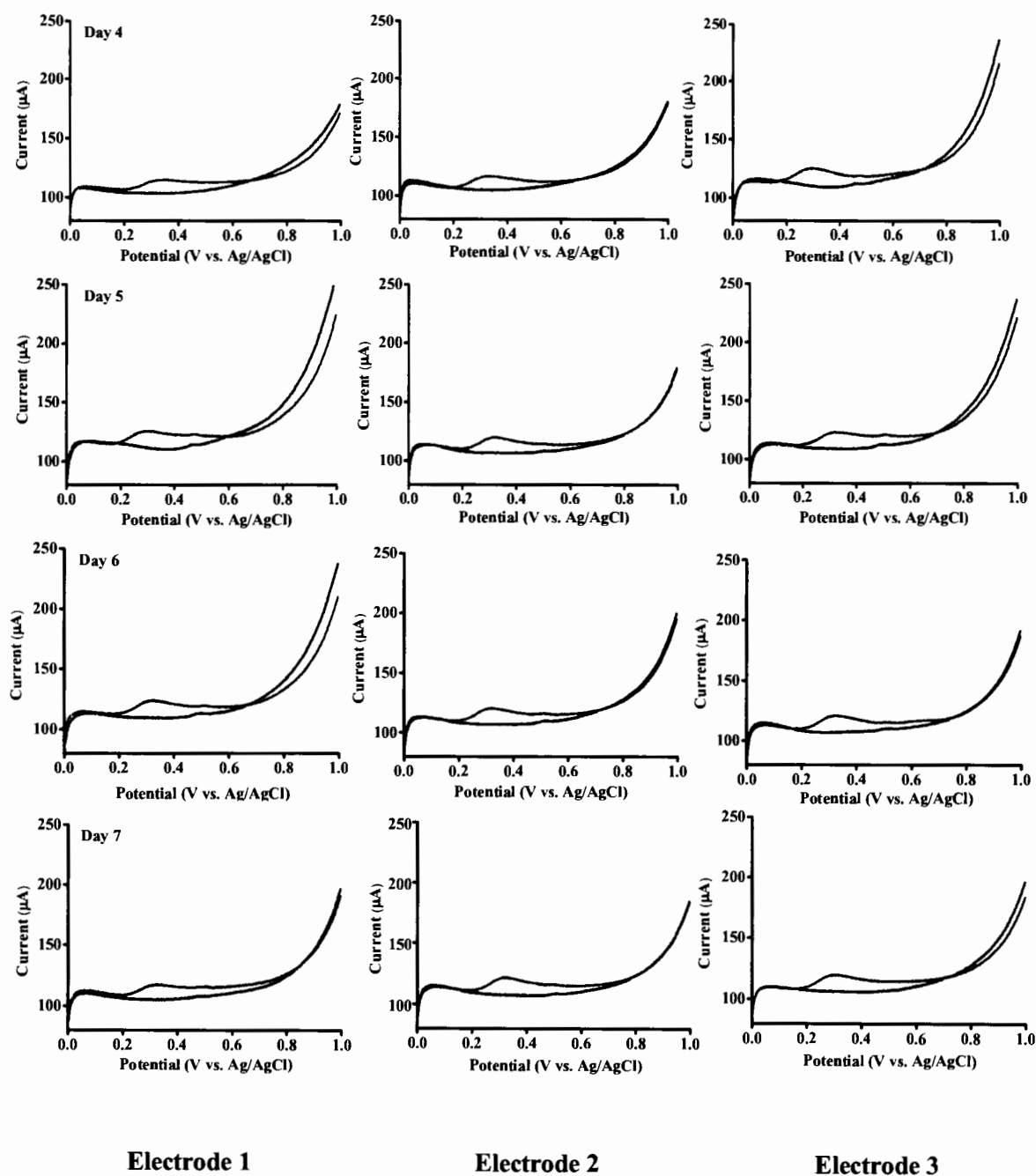
Stability of sulfite chemical sensor (raw data for Figure 4.19) (Continued)

Figure C.3 The storage stability of the developed sulfite sensor calculated from response of 1 mM sulfite in 0.1 M phosphate buffer solution, (pH 7.0).

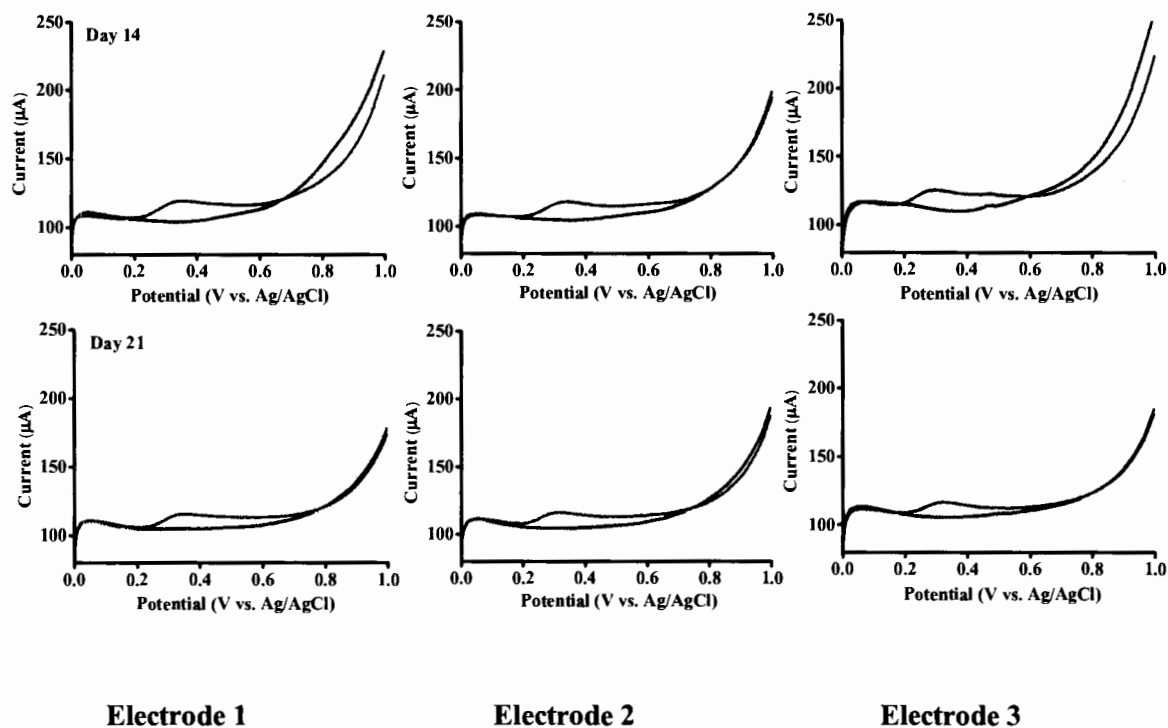
Stability of sulfite chemical sensor (raw data for Figure 4.19) (Continued)

Figure C.3 The storage stability of the developed sulfite sensor calculated from response of 1 mM sulfite in 0.1 M phosphate buffer solution, (pH 7.0).

Sample determination: Boones cheek berry (W-2)

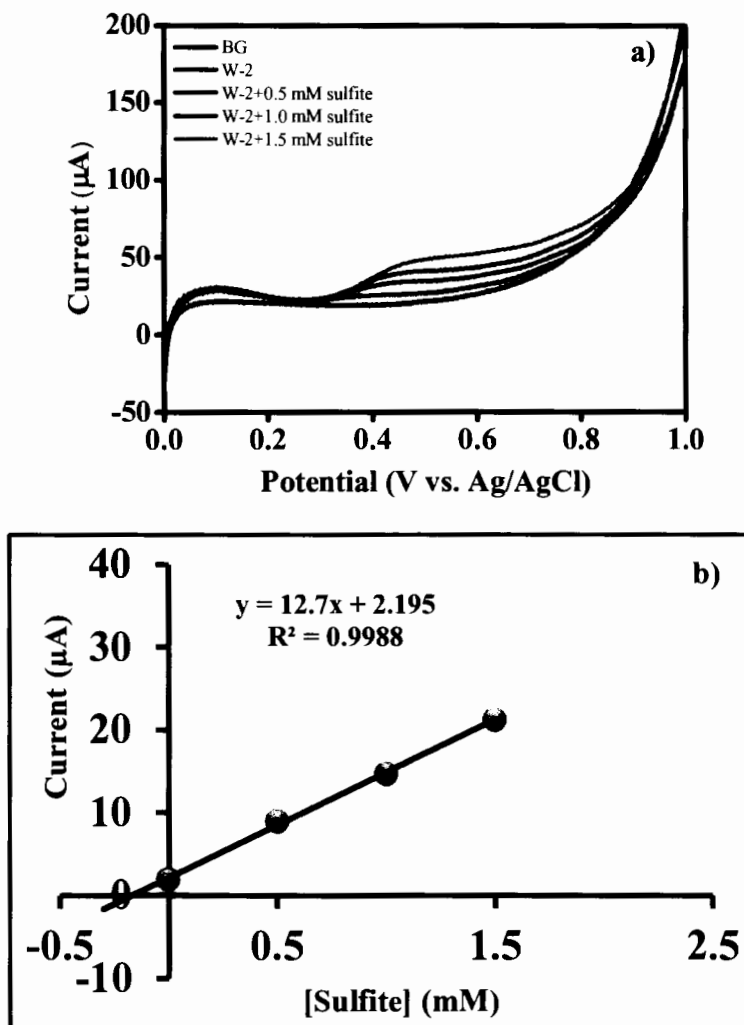


Figure C.4 a) Linear sweep voltammogram of the W-2 sample on the sulfite sensor and b) linear calibration plot of anodic peak current versus sulfite concentration and regression equation from standard addition method.

$$y = 12.70x + 2.195$$

$$y = 0; x = 0.173$$

$$\text{Dilute 1.05 fold } x = 0.173 \times 1.05$$

$$= 0.181 \text{ mM}$$

$$n = g/MW; g = n \cdot MW$$

$$g = (0.181 \times 10^{-3} \text{ mol}) \times (80.08 \text{ g mol}^{-1}) = 14.50 \times 10^{-3} \text{ g or } 14.50 \text{ mg}$$

Concentration of sulfite in Boones cheek berry wine is 14.50 ppm.

Sample determination: House wife (M-1)

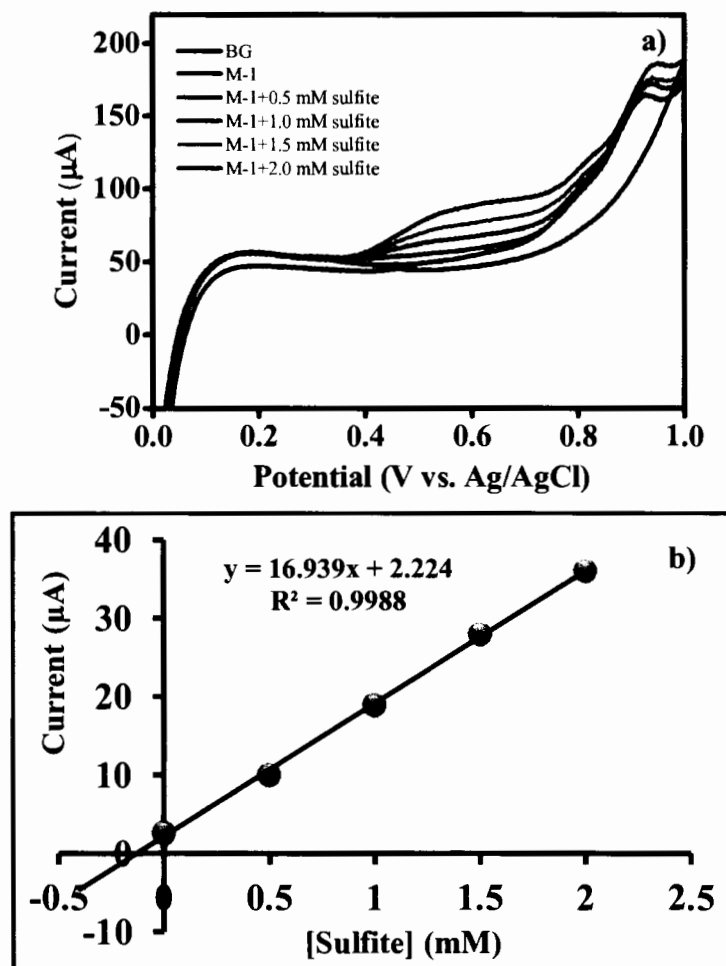


Figure C.5 a) Linear sweep voltammogram of the M-1 sample on the sulfite sensor and b) linear calibration plot of anodic peak current versus sulfite concentration and regression equation from standard addition method.

$$y = 16.939x + 2.224$$

$$y = 0; x = 0.131$$

$$\text{Dilute 2 fold } x = 0.173 \times 1.05$$

$$= 0.262 \text{ mM}$$

$$n = g/MW; g = n \cdot MW$$

$$g = (0.262 \times 10^{-3} \text{ mol}) \times (80.08 \text{ g mol}^{-1}) = 21.03 \times 10^{-3} \text{ g or } 21.03 \text{ mg}$$

Concentration of sulfite in House wife is 21.03 ppm.

APPENDIX D
CONFERENCES

CONFERENCES

Poster presentation

1. Nongyao Nontawong, Sanoë Chairam and Maliwan Amatatongchai. Development of non-enzymatic glucose sensor based on nickel and magnetic nanoparticles decorated multi-walled carbon nanotubes. Pure and Applied Chemistry International Conference 2016 (PACCON 2016), Bitec, Bangkok, Thailand.

Publication

1. Nongyao Nontawong, Maliwan Amatatongchai, Purim Jarujamrus, Suparb Tamuang and Sanoë Chairam. Non-Enzymatic Glucose Sensors for Sensitive Amperometric Detection Based on Simple Method of Nickel Nanoparticles Decorated on Magnetite Carbon Nanotubes Modified Glassy Carbon Electrode. International Journal of ELECTROCHEMICAL SCIENCE, Ubon Ratchathani University, volume: 12, Issue: 2 Pages: 1362 – 1376, 2017.



PACCON
PURE AND APPLIED CHEMISTRY
INTERNATIONAL CONFERENCE 2016

'THAILAND: One Hundred Years of **100**
Advancement in Chemistry' **Years**

9 - 11 February 2016
BITEC, Bangkok, Thailand

Development of non-enzymatic glucose sensor based on nickel and magnetic nanoparticles decorated multi-walled carbon nanotubes

Nongyoa Nontavong, Sanoe Chairam and Maliwan Amatongchai*

Department of Chemistry and Center of Excellent for Innovation in Chemistry, Faculty of Science,
Ubon Ratchathani University, Ubon Ratchathani, 34190, Thailand
*E-mail: amalivana@gmail.com

ABSTRACT

The sensitive and selective non-enzymatic glucose sensor was developed based on nickel and magnetite (Fe_3O_4) nanoparticles decorated carbon nanotubes (Fe_3O_4 -CNTs-NiNPs). Fe_3O_4 nanoparticles were in situ loaded on the surface of carboxylated multi-walled carbon nanotubes (MWCNTs-COOH) by a chemical co-precipitation procedure. Nickel nanoparticles (NiNPs) were prepared through reducing nickel chloride by hydrazine hydrate. Fe_3O_4 -CNTs-NiNPs composites were then prepared under ultra-sonication and characterized using transmission electron microscopy (TEM). The glucose sensor was fabricated using glassy carbon (GC) coated with Fe_3O_4 -CNTs-NiNPs composites film. Electrochemical investigations indicated that the Fe_3O_4 -CNTs-NiNPs/GC electrode exhibits excellent performance in the electrochemical oxidation of glucose at an applied potential of +0.55 V (vs. Ag/AgCl) in 0.1 M NaOH solution. Amperometry ($E_{\text{app}} = +0.55$ V) exhibits a linear dynamic range for glucose from 1.0×10^{-5} – 1.8×10^{-2} M ($r^2 = 0.998$) with the sensitivity of $335.25 \mu\text{A mM}^{-1}$; and a low detection limit of 6.7×10^{-6} M ($S/N = 3$). In addition, the fabricated sensor was applied to determine glucose in real samples with good results.

Experimental

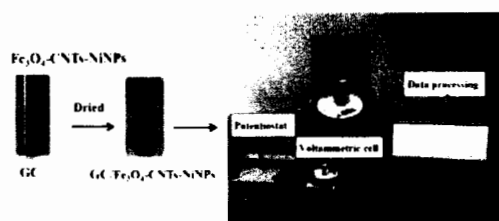


Fig. 1 Preparation procedure of the GC/ Fe_3O_4 -CNTs-NiNPs chemical sensor and Experimental set up for cyclic voltammetry

Results

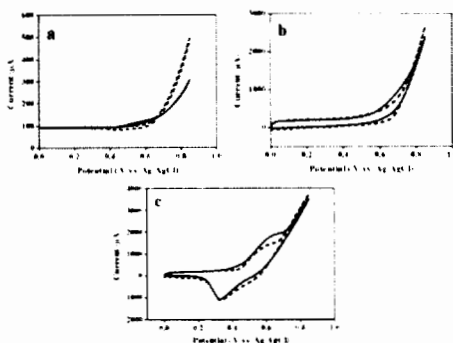


Fig. 2 CVs of a) GCE/ Fe_3O_4 -NiNPs, b) GCE/ Fe_3O_4 -MWCNTs and c) GCE/ Fe_3O_4 -MWCNTs-NiNPs of 4 mM Glucose in a 0.1 M NaOH pH 13.0

Conclusion

In summary, using a simple coprecipitation method, MWCNTs were decorated with iron oxide magnetic nanoparticles and was prepared under sonicated with NiNPs. The Fe_3O_4 -MWCNTs-NiNPs modified GC electrode, a pair of well-defined peaks with low potential and high peak current. The electrochemical behavior of modified electrode has been investigated by cyclic voltammetry. It was found that glucose can be oxidized by the nickel and magnetite (Fe_3O_4) nanoparticles decorated carbon nanotubes (Fe_3O_4 -CNTs-NiNPs) with significantly lowering the over potential in 0.1 M NaOH (pH 13.0) solution. Amperometric detection at +0.55 V exhibits a linear dependency on the glucose concentration, with a detection limit of 6.7×10^{-6} M at linear range from 1.0×10^{-5} – 1.8×10^{-2} M glucose.

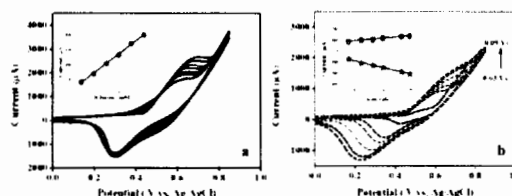


Fig. 3 CVs of a Different concentrations of glucose internal to external 0, 1, 2, 3, 4, 5 and 6 mM. Inset is the plot of catalytic current versus glucose concentration. b) 0.5 mM Glucose at GCE/ Fe_3O_4 -MWCNTs-NiNPs in 0.1 M NaOH pH 13.0 shows with scan rate ranging from 30 to 90 mV/s internal to external. The inset plot of the anodic i_a and cathodic current i_c versus $v^{1/2}$.

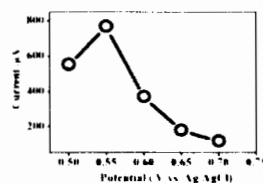


Fig. 4 Influence of the applied potential on the GCE/ Fe_3O_4 -MWCNTs-NiNPs response for 2 mM glucose.

Analytical features

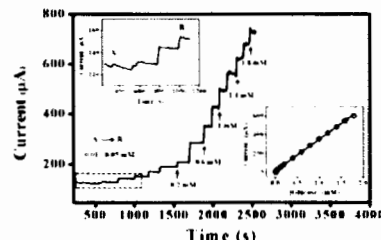


Fig. 5 Amperometric response of GCE/ Fe_3O_4 -MWCNTs-NiNPs in 0.1 M NaOH pH 13.0 at an applied potential of +0.55 V. The inset are low concentration of glucose.



Non-Enzymatic Glucose Sensors for Sensitive Amperometric Detection Based on Simple Method of Nickel Nanoparticles Decorated on Magnetite Carbon Nanotubes Modified Glassy Carbon Electrode

Nongyao Nontawong, Maliwan Amatatongchai*, Purim Jarujamrus, Suparb Tamuang and Sanoee Chairam

Department of Chemistry and Center of Excellence for Innovation in Chemistry,
Faculty of Science, Ubon Ratchathani University, Ubon Ratchathani, 34190, Thailand.
*E-mail: maliwan.a@ubu.ac.th, amaliwan@gmail.com

Received: 29 November 2016 / Accepted: 19 December 2016 / Published: 30 December 2016

A sensitive and selective non-enzymatic glucose sensor was developed based on magnetite (Fe_3O_4) and nickel nanoparticles decorated carbon nanotubes (Fe_3O_4 -CNTs-NiNPs). Fe_3O_4 nanoparticles were in situ loaded on the surface of carboxylated multi-walled carbon nanotubes (CNTs-COOH) by a chemical co-precipitation procedure. Nickel nanoparticles (NiNPs) were prepared through reducing nickel chloride by hydrazine hydrate and then decorated on Fe_3O_4 -CNTs using ultra-sonication. The as-prepared Fe_3O_4 -CNTs-NiNPs was characterized using transmission electron microscopy (TEM) and X-Ray Diffraction (XRD). Glucose sensor was fabricated using glassy carbon (GC) coated with Fe_3O_4 -CNTs-NiNPs composites film. Electrochemical investigations indicate that the Fe_3O_4 -CNTs-NiNPs/GC electrode possesses excellent performance in the electrochemical oxidation of glucose at an applied potential of +0.55 V (vs. Ag/AgCl) in 0.1 M NaOH solution. The linear dynamic range for glucose amperometric detection ($E_{\text{app}} = +0.55$ V) was observed from 10 μM to 1.8 mM ($r^2 = 0.998$) with the sensitivity of 335.25 $\mu\text{A mM}^{-1}$; and a low detection limit of 6.7 μM (S/N = 3). In addition, the fabricated sensor was successfully applied to determine glucose in honey and energy drinks with good results.

Keywords: Amperometric sensor; carbon nanotubes; magnetite, nickel nanoparticles; glucose

1. INTRODUCTION

Recently, methods for monitoring glucose levels in body fluids for clinical applications, pharmaceutical products and beverages for industrial quality control have received considerable attention. In the previous reports, efforts to develop selective and sensitive methods for the analysis of

glucose include colorimetric [1-5], chemiluminescent [6, 7], and electrochemical approaches [8-15]. These approaches all rely on glucose oxidation reaction catalyzed by enzyme glucose oxidase (GOx). Among these methods, electrochemical detection by a biosensor [8-15] is one of the most commonly used because of inherent high sensitivity and simplicity of instrumentation. Most of the electrochemical glucose biosensors are based on GOx immobilized on a material to prepare glucose sensor. Typically, GOx catalyzes the oxidation of glucose into gluconolactone in the presence of dissolved O_2 with O_2 being reduced to H_2O_2 . Therefore, electrochemical detection of glucose is accomplished by monitoring either O_2 consumption or H_2O_2 production. Another approach has been developed based on direct electrochemistry of GOx using nanomaterials [10, 14, 16]. Although GOx is relatively more stable than other enzymes, use of the biosensor is limited by relatively high cost, inherent stability, complicated immobilization procedures, and certain critical operational and storage conditions e.g. temperature, pH and ionic strength [8, 10, 11, 15].

In contrast, non-enzyme glucose sensors are based on nanostructured metal (Ni) [17, 18], metal alloy (Pt-Pb, Pt-Au) [19, 20] or metal oxides (NiO, MnO_2) [21, 22] as inorganic electrocatalysts using carbon materials such as carbon nanotubes (CNTs) [21, 22] and graphene as scaffolds [18]. This enzyme-free based sensor is an attractive alternative technique to solve the disadvantages of enzymatic biosensors. Quantification of glucose is achieved via directly electrochemical oxidation of glucose at the surface of developed sensors. However, the direct oxidation of glucose based on the mentioned electrodes has a key problem, which is the low sensitivity due to the sluggish kinetics of glucose electro-oxidation [19, 20]. Higher performance for glucose detection has been obtained by using several kind of electrodes contained Ni, NiO or $Ni(OH)_2$ nanocomposites [22-26] compared to the other electrodes. For examples, Lu et al. [23] synthesized Ni nanowire arrays using template-directed electropolymerization strategy with nanopore polycarbonate membrane as a template. $Ni(OH)_2$ nanoflowers for non-enzymatic glucose sensor were synthesized under harsh conditions and high temperature [24]. Sun et al. [25] combined Ni with CNTs to fabricate nanohybrid films on glassy carbon electrode using electrodeposition of $NiCl_2$ and CNTs in ionic liquids. Recently, Choi et al. reported strategy to fabricated CNTs-Ni nanocomposites through atomic layer deposition of Ni followed by chemical vapor deposition of functionalized CNTs [27]. These electrodes showed highly sensitive, selective and satisfactorily stable response towards glucose at low over potential under alkaline condition. However, the methods for synthesized Ni nanostructured or Ni-hybrid materials are somehow relatively complicated. In practice, the high cost of the electrode due to the sophisticated method and expensive instruments may limit their real applications.

This paper describes a simple and effective method for constructing a glucose non-enzymatic sensor using hybrid materials of magnetite (Fe_3O_4) and nickel nanoparticles decorated carbon nanotubes (Fe_3O_4 -CNTs-NiNPs). The combination of CNTs with magnetite and nickel nanoparticles is expected to be an effective electrocatalyst to make glucose sensor. It is well known that CNTs are very hydrophobic and cannot be wetted by liquids possessing a surface tension greater than approximately 100 or 200 $mN\ m^{-1}$ [28, 29]. Thus, most metals nanoparticles or metal oxide nanoparticles, including Fe_3O_4 and NiNPs, are unable to adhere to the CNTs surface. Our simple and effective strategy to solve this problem is loading Fe_3O_4 nanoparticles in situ on the surface of carboxylated multi-walled carbon nanotubes (CNTs-COOH) via a chemical co-precipitation procedure. After that, NiNPs were decorated

on Fe₃O₄-CNTs using ultra-sonication. Our simple and effective method enables the uniformly deposition of Fe₃O₄ and NiNPs onto the surface of CNTs. We constructed a glucose sensor using the Fe₃O₄-CNTs-NiNPs nanocomposites coated on the surface of glassy carbon electrode. The Fe₃O₄-CNTs-NiNPs/GC electrode shows an excellent activity for the electrocatalysis of glucose oxidation. The fabricated electrode was applied for amperometric detection of glucose in honey and energy drinks with good sensitivity and acceptable selectivity. The developed electrode is found to be a promising enzyme-free glucose sensor.

2. EXPERIMENTAL

2.1 Reagent and Chemical

Carboxylated functionalized multiwall carbon nanotubes (CNTs-COOH), diameter: 15 ± 5 nm, with purity of 95%, were purchased from Nanolab Inc (MA, USA). Iron (II) chloride tetrahydrate (FeCl₂·4H₂O), iron (III) chloride hexahydrate (FeCl₃·6H₂O), uric acid (UA), D (+) glucose, ascorbic acid (AA) and dopamine (DA) were purchased from Sigma-Aldrich (St. Louis, USA). Sodium hydroxide (NaOH) and hydrazine hydrate (N₂H₂·N₂H₂·H₂O, 98%) were purchased from Carlo Erba (Val-de-Reuil, France). Ethylene glycol (99.8%, anhydrous) was purchased from Acros organic (Geel, Belgium). All chemicals were of analytical reagent grade and were used without further purification. All solutions were prepared in deionized-distilled water (Water Pro PS, USA).

2.2 Apparatus

Cyclic voltammetric measurements were carried out using an eDAQ potentiostat (model EA 161, Australia) equipped with an e-corder 210 and e-chem v 2.0.13 software. The active surface area of glassy carbon electrode, (diameter 3 mm, CH Instrument, USA) was approximately 0.07 cm². An in house three-electrode cell, comprising a working electrode (Fe₃O₄-CNTs-NiNPs/GC electrode), a reference electrode (Ag/AgCl) and a counter electrode (stainless steel) was employed. Measurements were performed using 0.1 M sodium hydroxide (pH 13.0) as supporting-electrolyte solution and all electrochemical measurements were performed at room temperature. The morphology of nanoparticles and nanocomposites were observed by JEM-1230 transmission electron microscope (TEM; JEOL, Japan). X-ray Diffraction (XRD) analysis of the samples was carried out using a Siemens D5000 diffractometer with Cu K_α monochromatized radiation source, operated at 40 kV and 100 mA.

2.3 Preparation of NiNPs

A method for synthesis of nickel nanoparticles (NiNPs) through reducing nickel chloride by hydrazine hydrate as described by Wu's method [30, 31] was adopted. The reaction mechanism can be described by the following reaction equation,



In brief, 0.952 g of nickel chloride and 5.0 g of hydrazine hydrate were dissolved in 395.0 mL ethylene glycol. Then, 4.0 mL of 1.0 M sodium hydroxide solution was added to the solution. The solution was further stirred in a capped flask for 1 h at 60°C. The obtained black Ni nanoparticles (NiNPs) was washed thoroughly with ethanol and dried at 60°C for 24 h. NiNPs were obtained as a black powder.

2.3 Preparation of Fe₃O₄-CNTs nanocomposites

Fe₃O₄-CNTs nanocomposite was prepared according to a method described previously by Teymourian *et al.* [32] with a slight modification. The nanocomposite was synthesized under N₂ atmosphere. Briefly, 20 mg of carboxylated carbon nanotubes (CNTs-COOH) were dispersed in 20 mL of distilled water in an ultrasonic bath for 20 min. Then 30 mg of FeCl₃·6H₂O was added under vigorous stirring. After the mixture was stirred for 30 min, 40 mg of FeCl₂·4H₂O was added and continued stirring for 30 min. 2 mL of concentrated NH₃ diluted with 10 mL of deionized water was slowly added into the mixture. The solution was then heated at 60°C for another 2 h. Fe₃O₄-CNTs nanoparticles were separated using an external magnetic field, then washed with ethanol and deionized water. After drying in a desiccator, Fe₃O₄-CNTs nanoparticles were obtained as a powder.

2.4 Preparation of the Fe₃O₄-CNTs-NiNPs

Simple method for preparation of Fe₃O₄-CNTs-NiNPs dispersion was firstly proposed in this work. The dispersion was prepared by only dispersing 2 mg of Fe₃O₄-CNTs into 1.0 mL of aqueous solution containing 1% DMF and ultrasonicated for 30 min. After that, 2 mg NiNPs was added into the resulting dispersion and ultrasonicated for 30 min. Finally, homogeneous Fe₃O₄-CNTs-NiNPs dispersion was obtained and the resulting solution was sonicated for 5 min before use.

2.5 Preparation of the Fe₃O₄-CNTs-NiNPs modified GC electrode

Prior to the electrochemical experiments, glassy carbon (GC) electrode was polished using 1.0 and 0.03 μm alumina slurry, successively. The electrode was rinsed with distilled water and sonicated in deionized water of 5 min to remove residual abrasive particles. Fe₃O₄-CNTs-NiNPs/GC electrode was prepared by casting 40 μL of the Fe₃O₄-CNTs-NiNPs dispersion (2 mg mL⁻¹), mentioned above, on the surface of the polished glassy carbon (GC) electrode, and then left to dry at room temperature.

3. RESULTS AND DISCUSSION

3.1 Characterization of the nanomaterials

The morphology and structure of the different composites were studied by TEM and XRD. The TEM samples were prepared by dispersing the nanocomposites in de-ionized water with ultrasonicator and then drying a drop of the suspension on a copper grid. Fig. 1 (A-C) shows TEM

images of (A) the fine nanotubular morphology of CNTs-COOH, (B) a homogenous dispersion of NiNPs and (C) synthesized Fe_3O_4 -CNTs-NiNPs. In our work, NiNPs were prepared by reduction of Ni^{2+} by hydrazine in the presence of ethylene glycol, as a stabilizing agent [29]. The average diameter of synthesized NiNPs was 21.6 ± 3.2 nm (count = 50). The TEM image of Fe_3O_4 -CNTs-NiNPs (Fig. 1C) shows a typical deposition of Fe_3O_4 and NiNPs on the surface of CNTs' nanotubular structure. The average diameter of the nanoparticles synthesized on CNTs surface was estimated to be 20.3 ± 1.6 nm (count = 50), and the nanoparticles tends to homogeneously dispersed all over the CNTs tubes. Fig. 1D shows the X-ray diffraction patterns of NiNPs, Fe_3O_4 -CNTs and Fe_3O_4 -CNTs-NiNPs obtained under our synthesis conditions.

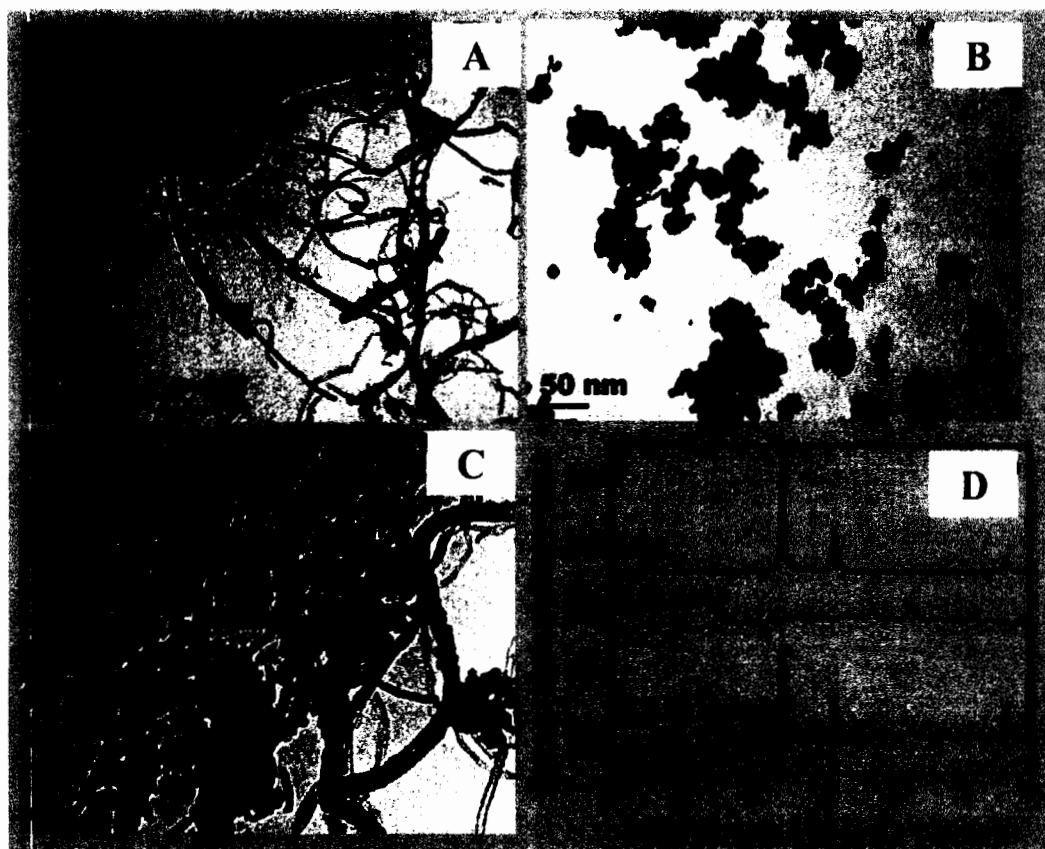


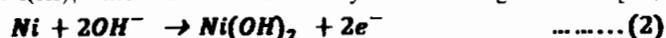
Figure 1. TEM images of (A) CNTs, (B) NiNPs, (C) Fe_3O_4 -CNTs-NiNPs and (D) XRD patterns of NiNPs, Fe_3O_4 -CNTs and Fe_3O_4 -CNTs-NiNPs nanocomposites.

The three well-resolved peaks at 2θ of approximately 44.7° , 52.1° and 76.6° can be assigned to the (111), (200) and (220) planes of pure fcc nickel, which accorded to previous report [30, 31]. This suggests that the as-prepared nanoparticles are nickel nanoparticles. XRD patterns for the Fe_3O_4 -CNTs show the peaks at 2θ of approximately 30.4° , 35.7° , 43.6° , 57.8° and 63.4° which were marked by their indices (220), (311), (400), (511) and (440), correspond to the spinel structure of magnetite phase [5,

33, 34], (JCPDS No. 82-15330). The XRD pattern of Fe₃O₄-CNTs-NiNPs displays indices corresponding peaks for both NiNPs and Fe₃O₄ which is indicated the formation of Fe₃O₄ and NiNPs decorated on the CNTs.

3.2. Electrochemical behavior of Fe₃O₄-CNTs-NiNPs/GC electrode

Cyclic voltammetry was used to compare and investigate the catalytic activity of the Fe₃O₄-CNTs/GC, NiNPs-CNTs/GC and Fe₃O₄-CNTs-NiNPs/GC electrodes. Fig. 2 shows the cyclic voltammograms (CVs) for different electrodes in 0.1 M NaOH (dash line) with containing 1 mM glucose (solid line). As shown in Fig. 2, no peak was observed on the Fe₃O₄-CNTs/GC while NiNPs-CNTs/GC and Fe₃O₄-CNTs-NiNPs/GC displayed a pair of well-defined redox peak in the potential range of 0-0.8 V, which can be assigned to the electrochemical redox reaction of Ni(II)/Ni(III) couple on the electrode surface in the alkaline medium [27, 35]. However, the electrode modified with only NiNPs produced very small current. The Fe₃O₄-CNTs-NiNPs/GC electrode shows much larger peak currents than that of NiNPs-CNTs/GC electrode. This result reveals that electrochemical performance of the hybrid nanocomposites is greatly enhanced compared to its individual counterparts. Fig. 2C (dotted line), a pair of well-defined redox peaks, an anodic peak at +0.54 V and a cathodic peak at +0.32 V are observed in the absence of glucose. The couple of peaks are corresponding to the Ni(II)/Ni(III), which can be described by the following reactions [27, 35]:



Glucose oxidation is an electrochemically irreversible process. In the presence of glucose, notable enhancement of the oxidation peak current was observed as shown in Fig. 2C (solid line). This enhancement of anodic current is attributed to the electro-oxidation of glucose with the participation of Ni (III), the process may be as following:



The electro-catalytic in glucose oxidation by NiNPs in Fe₃O₄-CNTs-NiNPs/GC electrode is accordance to the previous reports of non-enzymatic glucose sensing fabricated from three-dimension porous nickel nanostructure [36], CNTs-nickel nanocomposites [27] and ultrathin Ni(OH)₂ nanoplates [36] synthesized by hydrogen-evolution-assisted electro-deposition [35], atomic layer deposition [27] and pyrolysis melamine foam followed by the microwave process [36].

Herein, we proposed the good electrochemical performance of Fe₃O₄-CNTs-NiNPs nanocomposites, such as large surface area and electrical conductivity, with the electrocatalytic activity of the hybrid nanocomposites towards glucose oxidation. Our method for the preparation of Fe₃O₄-CNTs-NiNPs nanocomposites is very simple using uncomplicated precipitation method and common laboratory equipment. The fabricating process was cost-effective, time-saving and easy to prepare under ultrasonication.

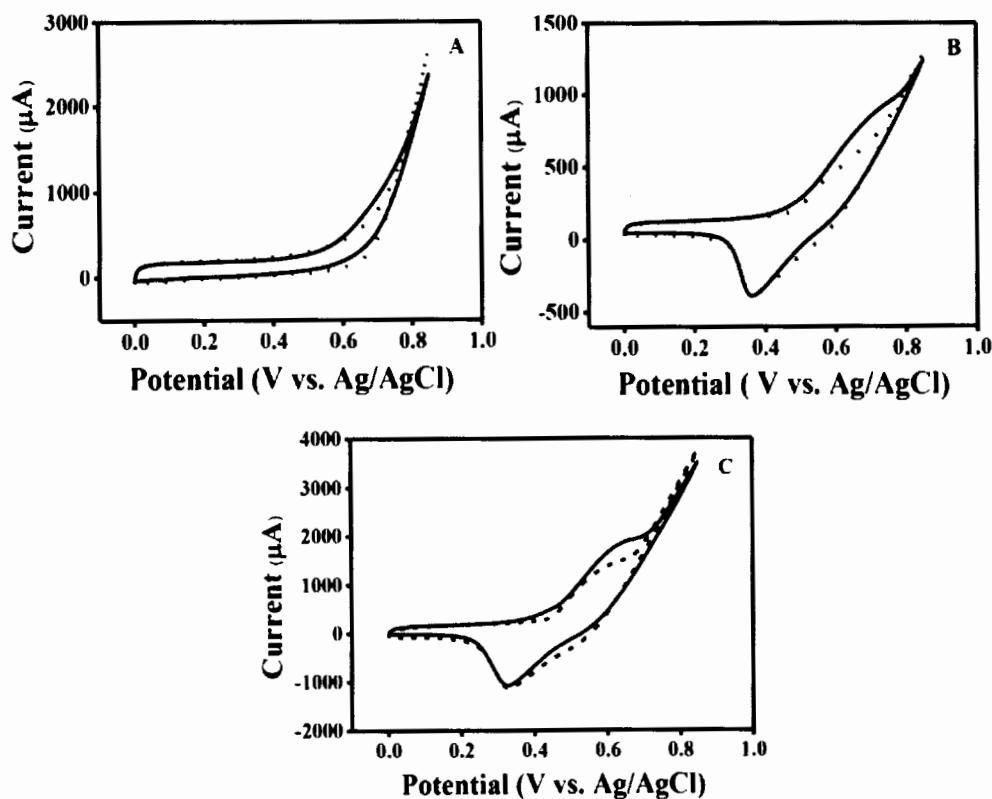


Figure 2. CVs of (A) $\text{Fe}_3\text{O}_4\text{-CNTs/GC}$, (B) NiNPs-CNTs/GC and (C) $\text{Fe}_3\text{O}_4\text{-CNTs-NiNPs/GC}$ electrodes in 0.1 M NaOH, pH 13.0 (dashed line) and in the present of 4 mM glucose (solid line), scan rate 0.05 V s^{-1} .

3.3 Scan rate and concentration dependence study

The influence of scan rate at $\text{Fe}_3\text{O}_4\text{-CNTs-NiNPs/GC}$ electrode was investigated in 0.1 M NaOH solution containing 0.5 mM glucose, the results are displayed in Fig. 3A. As seen in the inset of Fig. 3A, peak currents (μA) for both the oxidation and the reduction were linearly proportional to the square root of scan rate ($\text{V}^{1/2} \text{ s}^{-1/2}$) in the range of $0.03\text{-}0.09 \text{ V s}^{-1}$. The linear regression equations were $I_{p,a} = 2327.55 v^{1/2} + 1.60$ ($r^2 = 0.994$) and $I_{p,c} = -6625.05 v^{1/2} + 487.13$ ($r^2 = 0.993$), respectively. This result indicated a diffusion-controlled process at the $\text{Fe}_3\text{O}_4\text{-CNTs-NiNPs/GC}$ electrode.

Fig. 3B displayed CVs of $\text{Fe}_3\text{O}_4\text{-CNTs-NiNPs/GC}$ electrode with various concentrations of glucose in 0.1 M NaOH solution. It can be observed that by increasing the glucose concentration, the oxidation peak current increased and the potential shifted to a more positive value, demonstrating the good catalytic effect of the Ni(II)/Ni(III) redox couple in glucose oxidation [27, 36]. The relationship between oxidation peak current (μA) and glucose concentration was examined from 1 to 6 mM. Linear calibration ($r^2 = 0.999$) was obtained with the slope of $128.31 \mu\text{A.mM}^{-1}$. These results have demonstrated that the $\text{Fe}_3\text{O}_4\text{-CNTs-NiNPs/GC}$ electrode is appropriate for the quantitation of glucose.

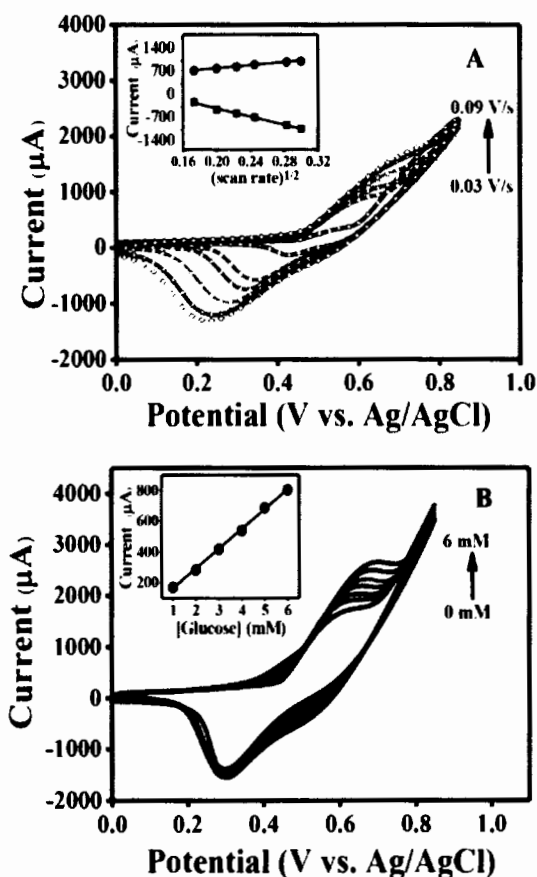


Figure 3. (A) CVs of $\text{Fe}_3\text{O}_4\text{-CNTs-NiNPs/GC}$ electrode for 0.5 mM glucose in 0.1 M NaOH (pH 13) with the variation of scan rate ranging from 0.03 to 0.09 V/s (internal to external). Inset is the plot of the anodic (i_a) and cathodic current (i_c) versus $v^{1/2}$. (B) CVs of glucose in 0.1 M NaOH with the variation of glucose concentration from 0 to 6 mM (internal to external). Inset is the plot of anodic peak currents versus glucose concentration.

3.4 Optimum potential for amperometric detection

The applied potential is an important parameter in amperometry because it strongly affects the size of the current signal from glucose. The proposed amperometric method for detection of glucose was based on the electrochemical monitoring of the oxidation signal from glucose at the $\text{Fe}_3\text{O}_4\text{-CNTs-NiNPs/GC}$ electrode. In this study, we investigated the optimal potential for amperometric detection at the electrode over the potential range from 0.4 to 0.6 V. As shown in Fig. 4, the anodic current response increases rapidly from 0.45 to 0.55 V, and then decreased from 5.5 to 0.7 V. Maximum sensitivity occurred at an operating potential of 0.55 V (versus Ag/AgCl), and thus, we use this optimal voltage for amperometric detection.

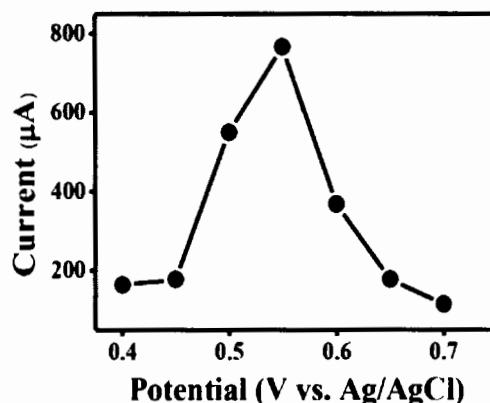


Figure 4. Anodic current of $\text{Fe}_3\text{O}_4\text{-CNTs-NiNPs/GC}$ electrode at different potentials from 0.40 V to 0.70 V upon addition of 1 mM glucose to 0.1 M NaOH.

3.5 Amperometric response of the $\text{Fe}_3\text{O}_4\text{-CNTs-NiNPs/GC}$ electrode to glucose

The amperometric response of the $\text{Fe}_3\text{O}_4\text{-CNTs-NiNPs/GC}$ electrode was investigated by successively addition of glucose standard in a continuous stirring 10 mL of 0.1 M NaOH. Figure 5 displays the amperometric signals corresponding to its calibration plot at optimal potential of +0.55 V. As shown in Fig. 5A, the anodic current increases with increasing the concentration of glucose ranging from 10 μA to 3.0 mM. The $\text{Fe}_3\text{O}_4\text{-CNTs-NiNPs/GC}$ electrode shows very fast current response ($\sim 5\text{s}$) indicated that the electrode is very sensitive to glucose. As shown in Fig. 5B, the linear response range of the developed sensor for glucose concentration was from 10 μM to 1.8 mM with a sensitivity of $335.25 \mu\text{A mM}^{-1}$ and correlation coefficient (r^2) of 0.998. The detection limit estimated based on the signal-to-noise ratio ($S/N=3$) was 6.7 μM .

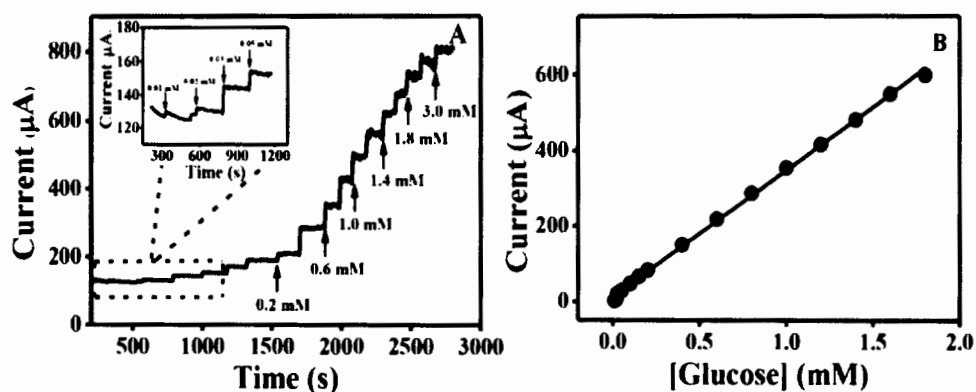


Figure 5. (A) Typical amperometric $i-t$ curve of $\text{Fe}_3\text{O}_4\text{-CNTs-NiNPs/GC}$ electrode to successive additions of glucose solution into a stirred system of 0.1 M NaOH (pH 13.0) at +0.55 V. (B) The linear calibration plot of the corresponding current versus glucose concentration.

Table 1. Response characteristics of the Fe₃O₄-CNTs-NiNPs/GC electrode and other non-enzymatic glucose sensors.

MnO ₂ /CNTs ^a	0.30	33.19	0.01-28	-	[22]
RGO-Ni(OH) ₂ ^b	0.54	11.43	0.002-3.1	0.6	[25]
CS-RGO-NiNPs ^c	0.60	318.4	0.2-9	4.1	[18]
Ni/NiO-GP ^c	0.55	1997	0.029-6.4	1.8	[37]
NiO-GP ^b	0.35	7.57	0.02-4.5	5	[38]
Ni(OH) ₂ /TiO ₂ ^d	0.50	192	0.03-14	8	[39]
Ni nanowires ^b	0.55	131.1	0.0005 – 7	0.1	[23]
Ni(OH) ₂ nanoflowers ^b	0.49	265.3	0.1-1.1	0.5	[24]
Cu nanoclusters/CNTs ^b	0.65	17.8	0.0007 – 3.5	0.21	[40]
Ni-CNTs ^b	0.60	67.2	0.003 – 17.5	0.89	[26]
Ni/Cu/CNTs ^b	0.58	186.2	0.00003 –0.8	0.03	[41]
Fe ₃ O ₄ -CNTs-Ni ^b	0.55	335.3	0.01-1.8	6.7	This work

RGO-Ni(OH)₂ = reduced graphene oxide assembled with Ni(OH)₂ nanoplates, CS = chitosan, RGO = reduced graphene oxide, NiNPs= nickel nanoparticles, GP = Graphene, E_{pp}= applied potential, ^aCarbon nanotubes electrode (CNTsE), ^bGlassy Carbon Electrode (GCE), ^cScreen Printed Electrode (SPE), ^dNiTi alloy sheet

Table 1 provides a comparison of the analytical characteristics of our non-enzymatic glucose sensor with related modified electrodes from the literature. The analytical characteristics of our sensor are comparable to, or better than, those reported for other nanomaterial based-glucose sensor designs. Additionally, the applied potential for our sensor is lower [18, 26, 40], or comparable to, those in previous reports [23, 25, 37, 39, 41]. Moreover, the use of the Fe₃O₄-CNTs-NiNPs/GC electrode offers a higher sensitivity [22-26, 38-41], or comparable [18] to those previously reported values for other modified electrodes. The developed electrode provides a satisfactory wide range of linearity and low detection limit. Our approach to fabricate a sensitive and selective non-enzymatic glucose sensor using glassy carbon (GC) electrode coated with Fe₃O₄-CNTs-NiNPs composites film resulted in high electrocatalytic activity and improved sensor performance toward glucose detection. The synthesis of

signal alteration of greater than $\pm 5\%$. Tolerance limit for fructose, maltose, sucrose, sodium carbonate, citric acid and sodium chloride was found to be 20, 5, 15, 70, 20 and 100 mM, respectively. Our results demonstrated that different sugars (fructose, maltose and sucrose) and anions (CO_3^{2-} , $\text{C}_6\text{H}_5\text{O}_7^{3-}$ and Cl^-) produce very low interference signals at molar concentration of 5 mM or greater (100 mM) with respect to glucose. However, because samples were diluted between 100 and 1,000 times prior to analysis, the presence of these foreign species is assumed not to be problematic. Thus the selectivity of $\text{Fe}_3\text{O}_4\text{-CNTs-NiNPs/GC}$ electrode for glucose detection was satisfied in the presence of possible interfering reagents and sample ingredients.

Reproducibility and stability experiments were also performed to evaluate the performance of the developed electrode. The electrode-to-electrode reproducibility of $\text{Fe}_3\text{O}_4\text{-CNTs-NiNPs/GC}$ was investigated from the sensitivity or slope of the calibration curve (0.5 to 2.0 mM) of five sensors. As shown in Fig.7, the sensitivity obtained from five electrodes was acquired with a relative standard deviation (RSD) less than 5.0%. The repeatability of the electrode was estimated from six amperometric measurements of 0.5 mM glucose. The sensor shows RSD of 4.13% which indicates that the modified electrode possesses a good stability. This good reproducibility and stability make the developed electrode feasible for practical applications.

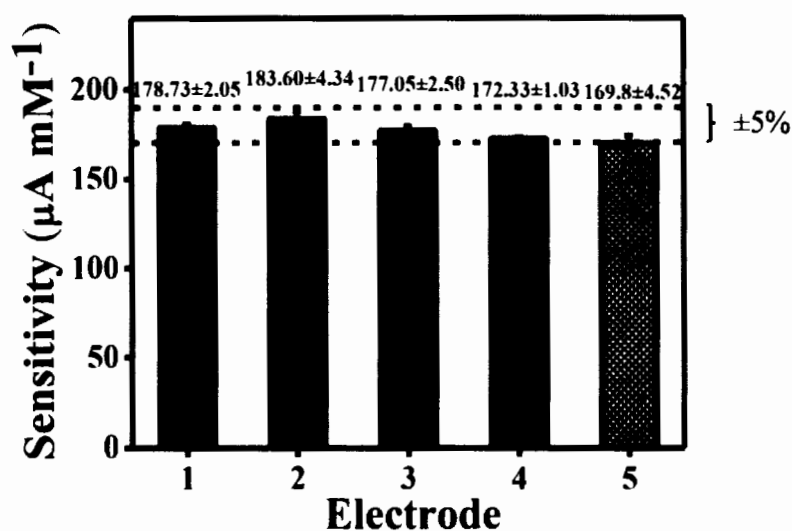


Figure 7 Sensitivity of the calibration curves obtained from five electrodes fabricated independently, concentration of glucose from 0.5 to 2.0 mM.

3.7 Application to energy drinks and honey

In order to test the usefulness of the developed method, $\text{Fe}_3\text{O}_4\text{/CNTs/NiNPs/GC}$ electrode was applied to the determination of glucose in energy drinks and honey. Three different brands of energy drinks (D-1 to D-3) and honey (H-1 to H-3) were analyzed in triplicate by amperometry (Table 2). The samples were diluted appropriately using deionized water prior to the analysis to ensure that the glucose concentrations were within the linear working range and to reduce possible matrix effects.

Glucose content found in D-1 to D-3 by our method is comparable to the label values. Additionally, the results in H-1 to H-3 compare well with measurements obtained from a commercially available glucose meter. The differences between our method and the reference values range from 0.63% to 3.96%, indicating that our test results are in good agreement with those obtained from the drink manufacturers and the glucose meter. These results indicate that our developed method is sufficiently accurate and suitable for the determination of glucose in these samples.

Table 2. Glucose contents found in energy drinks (D-1 to D-3) and honey (H-1 to H-3), which were obtained by the developed method ($\text{Fe}_3\text{O}_4/\text{CNTs}/\text{NiNPs}$ electrode) and comparative values from labeled value and glucose meter. Determination by each method was carried out in triplicate for a sample.

Samples	Glucose content (%w/v)		Developed method (%w/v)	Relative Difference (%)
	Label	Glucose meter		
D-1	8.50		8.63 ± 0.11	+1.53
D-2	8.00		7.91 ± 0.11	-2.38
D-3	4.80		4.83 ± 0.12	+0.63
H-1		20.10	19.27 ± 0.76	+3.96
H-2		15.00	15.46 ± 0.14	+1.95
H-3		8.20	8.35 ± 0.10	+1.83

4. CONCLUSION

A simply new route for the fabrication of sensitive and selective non-enzymatic glucose sensor based on Fe_3O_4 and NiNPs decorated carbon nanotubes ($\text{Fe}_3\text{O}_4\text{-CNTs-NiNPs}$) was proposed. The surface of CNTs-COOH was loaded with Fe_3O_4 nanoparticle via a chemical co-precipitation procedure followed by decorated with NiNPs that prepared through reducing nickel chloride by hydrazine hydrate via ultrasonication. The resulting $\text{Fe}_3\text{O}_4\text{-CNTs-NiNPs}$ nanocomposites were coated on the surface of GC electrode displaying high electrocatalytic activity towards the oxidation of glucose. Thus, the proposed procedure enables simple preparation of non-enzymatic glucose sensor and exhibits high sensitivity, selectivity, stability and reliability using amperometry. Results of glucose measurements in honey and energy drinks using our developed sensor correlated well with those obtained by manufacturer' label and glucose meter.

ACKNOWLEDGEMENTS

The authors gratefully acknowledge financial support received from the National Research Council of Thailand (NRCT, 2560A11702005), the Center of Excellence for Innovation in Chemistry (PERCH-CIC), the Commission on Higher Education, the Ministry of Education, the instrumental facility of the Department of Chemistry, and the Faculty of Science at Ubon Ratchathani University. We also gratefully acknowledge a Scholarship from the Science Achievement Scholarship of Thailand (SAST) that was awarded to N. Nontawong.

References

1. H. Wei and E. Wang, *Anal. Chem.*, 80 (2008) 2250.
2. L. Caseli, D.S. dos Santos Jr, R.F. Aroca and O. N. Oliveira Jr, *Mater. Sci. Eng. C*, 29 (2009) 1687.
3. G. Palazzo, L. Facchini and A. Mallardi, *Sens. Actuators B*, 161 (2012) 366.
4. W. Zhang, D. Ma and J. Du, *Talanta*, 120 (2014) 362.
5. K. Ponlakhet, M. Amatatongchai, W. Sroysee, P. Jarujamrus and S. Chairam, *Anal. Methods*, 8 (2016) 8288.
6. L. Qingwen, L. Guoan, W. Yiming and Z. Xingrong, *Mater. Sci. Eng., C* 11 (2000) 67.
7. C. Wang and H. Huang, *Anal. Chim. Acta*, 498 (2003) 61.
8. J. Wang, S. Li, J.-W. Mo, J. Porter, M. M. Musameh and P. K. Dasgupta, *Biosens Bioelectron.*, 17 (2002) 999.
9. I. Willner and E. Katz, *Angew. Chem. Int. Ed.*, 39 (2000) 1180.
10. V. Mazeiko, A. K. Minkstimiene, A. Ramanaviciene, Z. Belevicius and A. Ramanavicius, *Sens. Actuators, B* 189 (2013) 187.
11. V. Mani, R. Devasenathipathy, S.-M. Chen, B. Subramani and M. Govindasamy, *Int. J. Electrochem. Sci.*, 10 (2015) 691.
12. B. Unnikrishnan, S. Palanisamy and S.-M. Chen, *Biosens Bioelectron.*, 39 (2013) 70.
13. P. Rattanarat, P. Teengam, W. Siangproh, R. Ishimatsu, K. Nakano, O. Chailapakul and T. Imato, *Electroanalysis*, 27 (2015) 703.
14. M. L. Mena, P. Yez-Sedeo and J. M. Pingarrn, *Anal. Biochem.*, 336 (2005) 20.
15. A. Fatoni, A. Numnuam, P. Kanatharana, W. Limbut, C. Thammakhet and P. Thavarungkul, *Sens. Actuators B*, 185 (2013) 725.
16. M. Amatatongchai, W. Sroysee, S. Chairam and D. Nacapricha, *Talanta*, (2016), <http://dx.doi.org/10.1016/j.talanta.2015.11.072>
17. K. E. Toghill, L. Xiao, M. A. Phillips and R. G. Compton, *Sensors. Actuators, B* 147 (2010) 642.
18. J. Yang, J. H. Yu, J. R. Strickler, W. J. Chang and S. Gunasekaran, *Biosens Bioelectron.*, 47 (2013) 530.
19. J. Wang, D. F. Thomas and A. Chen, *Anal. Chem.*, 80 (2008) 997.
20. X. Zhu, C. Li, X. Zhu and M. Xu, *Int. J. Electrochem. Sci.*, 7 (2012) 8522.
21. Y. Mu, D. Jia, Y. He, Y. Miao and H.-L. Wu, *Biosens Bioelectron.*, 26 (2011) 2948.
22. J. Chen, W.-D. Zhang and J.-S. Ye, *Electrochem. Commun.*, 10 (2008) 1268.
23. L. M. Lu, L. Zhang, F. L. Qu, H. X. Lu, X. B. Zhang, Z. S. Wu, S. Y. Huan, Q. A. Wang, G. L. Shen and R. Q. Yu, *Biosens Bioelectron*, 25 (2009) 218.
24. H. Yang, G. Gao, F. Teng, W. Liu, S. Chen and Z. Ge, *J. Electrochem. Soc.*, 161 (2014) B216.
25. Y. Zhang, F. Xu, Y. Sun, Y. Shi, Z. Wen and Z. Li, *J. Mater. Chem.*, 21 (2011) 16949.
26. A. Sun, J. Zheng and Q. Sheng, *Electrochim. Acta*, 65 (2012) 64.
27. T. Choi, S. H. Kim, C. W. Lee, H. Kim, S.-K. Choi, S.-H. Kim, E. Kim, J. Park and H. Kim, *Biosens Bioelectron.*, 63 (2015) 325.
28. S. Hrapovic, Y. Liu, K. B. Male and J. H. T. Luong, *Anal. Chem.*, 76 (2004) 1083.
29. M. Tominaga, T. Shimazoe, M. Nagashima and I. Taniguchi, *Electrochem. Commun.*, 7 (2005) 189.
30. S. H. Wu and D. H. Chen, *J. Colloid Interface Sci.*, 259 (2003) 282.
31. X. Wu, W. Xing, L. Zhang, S. Zhuo, J. Zhou, G. Wang and S. Qiao, *Powder Technol.*, 224 (2012) 162.
32. H. Teymourian, A. Salimi and R. Hallaj, *Biosens Bioelectron.*, 33 (2012) 60.
33. S. Karamipour, M. S. Sadjadi and N. Farhadyar, *Spectrochim. Acta, Part A*, 148 (2015) 146.
34. W. Sroysee, K. Ponlakhet, S. Chairam, P. Jarujamrus and M. Amatatongchai, *Talanta*, 156-157 (2016) 154.
35. X. Niu, M. Lan, H. Zhao and C. Chen, *Anal. Chem.* 85 (2013) 3561.

36. Q. Guo, M. Zhang, S. Liu, G. Zhou, X. Li, H. Hou and L. Wang, *Anal. Methods*, 8 (2016) 8227.
37. X. Zhang, Z. Zhang, Q. Liao, S. Liu, Z. Kanga and Y. Zhang, *Sensors*, 16 (2016) 1791.
38. X. Zhu, Q. Jiao, C. Zhang, X. Zuo, X. Xiao, Y. Liang and J. Nan, *Microchim Acta*, 180 (2013) 477.
39. A. Gao, X. Zhang, X. Peng, H. Wu, L. Bai, W. Jin, G. Wu, R. Hang and P. K. Chu, *Sens. Actuators, B*, 232 (2016) 150.
40. X. Kang, Z. Mai, X. Zou, P. Cai and J. Mo, *Anal. Biochem.*, 363 (2007) 143.
41. K.-C. Lin, Y.-C. Lin and S.-M. Chen, *Electrochim. Acta*, 96 (2013) 164.
42. J. Wang, *Chem. Rev.*, 108 (2008) 814.
43. S. Canivell and R. Gomis, *Autoimmun. Rev.*, 13 (2014) 403.

© 2017 The Authors. Published by ESG (www.electrochemsci.org). This article is an open access article distributed under the terms and conditions of the Creative Commons Attribution license (<http://creativecommons.org/licenses/by/4.0/>).

VITAE

NAME Miss. Nongyao Nontawong

BIRTH DATE 25 April 1992

EDUCATION Bachelor of Science (Chimistry), Department of chemistry,
Faculty of science, Ubon Ratchathani University, Ubon
Ratchathani, Thailand. 2011-2014.
Master of Science (Analytical Chemistry), Department of
chemistry, Faculty of science, Ubon Ratchathani University,
Ubon Ratchathani, Thailand, 2015-2016

SCHOLASHIPS Research Price from Faculty of science, Ubon Ratchathani
University, Ubon Ratchathani, Thailand. Recipient of the
Science Achievement Scholarship of Thailand (SAST) In the
Academic Years of 2015-2016

